MOLECULAR ANALYSIS OF PLACODAL DEVELOPMENT IN ZEBRAFISH

A Dissertation

by

BRYAN T. PHILLIPS

Submitted to the Office of Graduate Studies of
Texas A&M University
in partial fulfillment of the requirements for the degree of

DOCTOR OF PHILOSOPHY

December 2004

Major Subject: Biology

MOLECULAR ANALYSIS OF PLACODAL DEVELOPMENT IN ZEBRAFISH

A Dissertation

by

BRYAN T. PHILLIPS

Submitted to Texas A&M University
in partial fulfillment of the requirements
for the degree of

DOCTOR OF PHILOSOPHY

Approved as to style and content by:

Bruce Riley (Chair of Committee)	Sumana Datta (Member)
Arne Lekven (Member)	Luis R. Garcia (Member)
Vincent Cassone (Head of Department)	

December 2004

Major Subject: Biology

ABSTRACT

Molecular Analysis of Placodal Development in Zebrafish.

(December 2004)

Bryan T. Phillips, B.S, University of Illinois at Urbana-Champaign

Chair of Advisory Committee: Dr. Bruce B. Riley

Vertebrates have evolved a unique way to sense their environment: placodally-derived sense organs. These sensory structures emerge from a crescent-shaped domain, the preplacodal domain, which surrounds the anterior neural plate and generates the paired sense organs as well as the cranial ganglia. For decades, embryologists have attempted to determine the tissue interactions required for induction of various placodal tissues. More recently, technological advances have allowed investigators to ask probing questions about the molecular nature of placodal development. In this dissertation I largely focus on development of the otic placode. I utilize loss-of-function techniques available in the zebrafish model system to demonstrate that two members of the fibroblast growth factors family of secreted ligands, Fgf3 and Fgf8, are redundantly required for otic placode induction. I go on to show that these factors are expressed in periotic tissues from the beginning of gastrulation. These findings are consistent with a model where Fgf3 and Fgf8 signal to preotic tissue to induce otic-specific gene expression. This model does not address other potential inducers in otic induction. A study using chick explant cultures suggests that a member of the Wnt family of secreted

ligands also has a role in otic induction. I therefore test the relative roles of Wnt and Fgf in otic placode induction. The results demonstrate that Wnt functions primarily to correctly position the Fgf expression domain and that it is these Fgf factors which are directly received by future otic cells. Lastly, I examine the function of the muscle segment homeobox (*msx*) gene family expressed in the preplacodal domain. This study demonstrates that Msx proteins refine the boundary between the preplacodal domain and the neural plate. Further, *msx* genes function in the differentiation and survival of posterior placodal tissues (including the otic field), neural crest and dorsal neural cell types. Loss of Msx function results in precocious cell death and morphogenesis defects which may reflect perturbed BMP signaling.

I dedicate this dissertation to my wife, Dr. Lori Adams-Phillips, for all of her unwavering support and her devoted love. See Dear, fish really do have ears.

ACKNOWLEDGEMENTS

I'm very grateful to my committee members, Drs. Sumana Datta, Arne Lekven and Rene Garcia, for leading excellent classes on developmental biology and helpful discussions about my project. I especially want to thank my advisor, Dr. Bruce Riley, who undertook the gargantuan task of teaching me developmental genetics. He has been a great mentor and a good friend. His easygoing but enthusiastic leadership made working in the lab, both exciting and rewarding.

My labmates were also instrumental in my graduate career. Thanks to undergraduate researchers Colt Melton, who worked tirelessly on the Msx project, and Kevin Bolding for all of his efforts on the Fgf project. The graduate students in the lab were also exceptionally influential. I'm appreciative to Elly Mae Storch for great times in the lab and her impeccable work on the Fgf-Wnt project. Thanks to Su Jin Kwak and Ming-Yung Chiang for all the molecular biology assistance, great advice on experiments and enjoyable years in the lab. Thanks to Bonnie Butler, a new grad student in the lab, who was helpful in several experiments. Finally, I thank Dr. Hye-Joo Kwon for all her advice and help on the Msx project. They have all been great colleagues and good friends over the years.

The members of the Lekven lab, Gerri Buckles, Marie-Christine Ramel and Kevin Baker, were always a source of assistance. They provided marvelous advice on experiments, let me pilfer desperately needed reagents and made for fun times in the lab.

Thanks to all the Department of Biology graduate students and friends. They helped me gain perspective on my work, bounce ideas around and were party to many valuable ideas sketched out on barroom napkins.

I want to thank my father, Terry Philips, and my mother, Janyce Eviston, for teaching me perseverance in the face of adversity, for their valued love and support and for always being there for me. Finally, I want to thank both of my parents for providing me their best genes. They've really come in handy.

TABLE OF CONTENTS

CHAPTER Page

LIST OF FIGURES

FIGURE Page

LIST OF TABLES

CHAPTER I

INTRODUCTION

BACKGROUND

General description of vertebrate ectodermal patterning

During vertebrate embryonic gastrulation, the ectoderm is subdivided into three distinct domains: the ventral epidermal ectoderm, the dorsal neurectoderm, and, located between these two domains, the preplacodal ectoderm (Fig. 1). The preplacodal field is so named because it is a continuous domain around the anterior neural plate which gives rise to all of the cranial placodes. Placodes are columnar epithelial thickenings which make important contributions to the paired sense organs including the nose, eyes and ears, as well as cranial ganglia such as the trigeminal (cranial nerve V) and the vagal ganglia (cranial nerve X, a derivative of the nodose placode; Fig. 2). The preplacodal field wraps around the anterior CNS in a crescent-shaped domain in close proximity to the lateral edge of the neural plate. The neural plate border gives rise to the cranial neural crest, another important vertebrate-specific tissue. Neural crest is a migratory population of dorsal neurectodermal cells which move to various destinations in the embryo. Upon arrival, they differentiate into a wide variety of cell types, including pigment cells and cranial cartilage and bone. Cranial neural crest and cranial placodes share several features: they develop in immediately adjacent positions within the head, they go on to develop into an overlapping array of cell types, and together they

---

This dissertation follows the style of the journal *Development.*

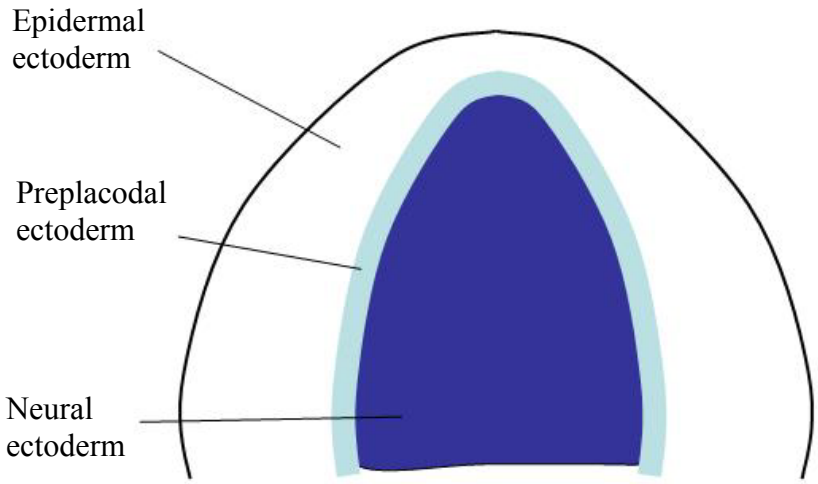

Figure 1. Head ectoderm of a vertebrate gastrula. The three ectodermal domains are indicated. Dorsal view.

constitute the peripheral nervous system. They have also been linked evolutionarily, as they are thought to have simultaneously arisen during vertebrate evolution and may share a common ancestral cell population.

The preplacodal domain

The existence of a general preplacodal field is still a topic of debate, though much of the data supports the presence of such a domain. The dispute revolves around whether all placodally-derived tissues must first pass through a common pre-placodal state (the "preplacodal field hypothesis") or whether each individual placode is specified independently (the "independent placode hypothesis").

The independent placode hypothesis maintains that each individual placode is specified directly by its own particular inducing tissue without progressing through a general preplacodal stage. This general idea disagrees with decades of experimental

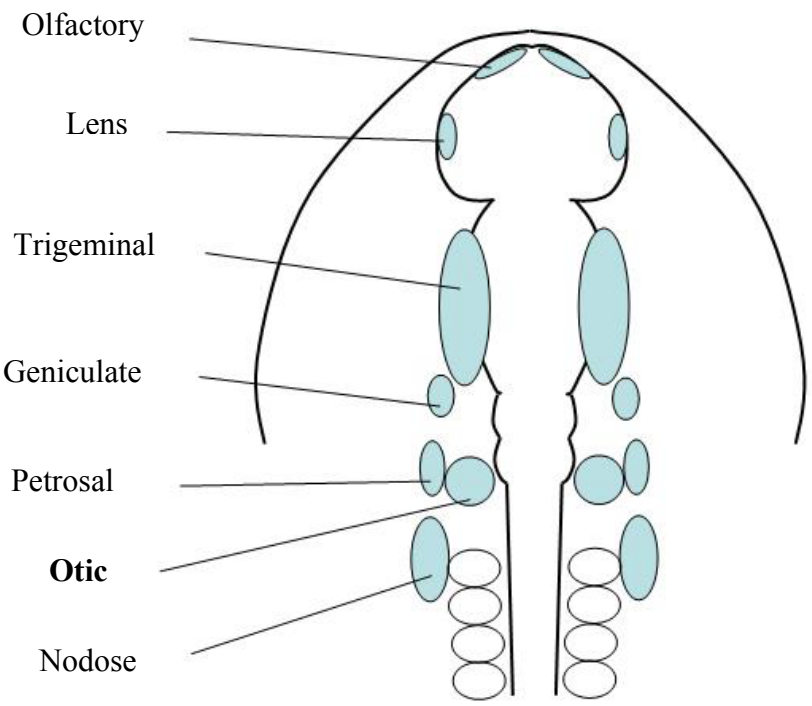

Figure 2. Schematic of cranial placodes. A dorsal view of a generalized vertebrate head showing the cranial placodes (shaded ovals). The individual placodes are indicated. Adapted from Baker and Bronner-Fraser (2001).

embryology, particularly with respect to the otic placode, which indicates that placode induction is a gradual, stepwise process (Yntema, 1950; Baker and Bronner-Fraser, 2001). The observation that each placode has its own specific inducer and therefore can be thought of as separate entities has been used to challenge to the preplacodal field hypothesis. For example, Bone Mophogenetic Protein 7 (BMP7) from the pharyngeal endoderm specifically induces only the epibranchial placodes (Graham and Begbie, 2000; Begbie and Graham, 2001). However, the fact that each placode may have its own specific inducer does not preclude the possibility that they went through a common

preplacodal state. In fact, the presence of a preplacodal state would prime the prospective placodal tissue, ensuring competence to respond to local inducers of specific placodes. Furthermore, Fibroblast growth factor (Fgf) misexpression in chick and zebrafish can respecify other preplacodal tissues (such as lens or nasal epithelium) as otic but not trunk/tail ectoderm, for example (Vendrell et al., 2000; Phillips et al., 2004). Further discussions of the effects of Fgf continue below.

The recent finding that some protochordates possess structures analagous to the olfactory and otic placodes while they lack other cranial placodes has also been cited by Begbie and Graham to challenge the preplacodal field hypothesis. They suggest that these evolutionary data indicate that not all placodes evolved simultaneously and therefore may not share a common evolutionary or developmental origin. However, the observation that non-vertebrate chordates possess some, but not all, placodal tissues does not disprove the notion that placodes of modern vertebrates do not pass through a common preplacodal state. One possible explanation for these observations is the enlargement of a smaller ancestral preplacodal domain. This new preplacodal tissue could then be co-opted as new placodal tissues when new inducers were introduced.

There are several lines of evidence indicating that all placodes originate from a common domain. First, fate mapping studies show that different placodal derivatives originate from overlapping regions that later separate into specific placodes, suggesting plasticity in the potential of preplacodal tissues. Also, the entire preplacodal domain can be seen in some vertebrates as a morphologically visible ectodermal thickening (Knouff, 1935; van Oostrom and Verwoed, 1972).

Molecular and genetic data also support the existence of a preplacodal domain. Members of the Distal-less (Dlx), Sine oculis (Six), and Eyes absent (Eya) families of transcription factors are expressed in a crescent-shaped pattern throughout the preplacodal domain (Baker and Bronner-Fraser, 2001). This observation suggests two general ideas: that the preplacodal domain has a distinct molecular identity from the surrounding ectoderm and that this identity is shared by the precursors of all placodes. Mutant analysis of these preplacodal-specific factors also supports the preplacodal hypothesis. Six is a transcriptional repressor which can be converted into an activator when it interacts with Eya (Li et al., 2003). Loss of Eya1 function in mice leads to severe inner ear defects such as loss of the cochlea and the statoacoustic ganglion (Xu et al., 1999). Six1 knockout mice exhibit similar otic phenotypes (Zheng et al., 2003; Ozaki et al., 2004). Importantly, cranial ganglia VII and IX (derived from the geniculate and petrosal placodes) are also missing. Developmental control of multiple placodal fates by an Eya-Six interaction is consistent with a molecular identity common to all placodes. Another example of a common preplacodal identity comes from analysis of the *distalless* family of transcription factors. *dlx3b* and *dlx4b* are both expressed in the zebrafish preplacodal domain (Solomon and Fritz, 2002). Dlx3b and Dlx4b are redundantly required for both otic and olfactory placode development, consistent with a pan-placodal role for these proteins. Several muscle segment homeobox (Msx) family members are coexpressed in the posterior preplacodal domain with *dlx3b* and *dlx4b.* Msx homeodomain proteins repress Dlx function both at the level of transcription and through protein-protein interactions (Zhang et al., 1997). Functional analysis of these

Msx genes and potential interactions with Dlx family members is examined later in this dissertation (See Chapter IV).

Specification of the neural plate

Since placodes form at the neural plate border, it has been hypothesized that neural induction and development of the preplacodal domain are linked. The most widely-accepted model of neural induction suggests that the spatial arrangement of the three ectodermal domains results from the concerted action of dorsal-ventral signals (reviewed by Schier, 2001). Of primary importance are the ventralizing pathways, BMP and Wingless (Wnt), as well as antagonists of these pathways which act as dorsalizers and are secreted from the organizer or its derivatives. The combined action of axial signaling events gives rise to a concentration gradient of BMP and Wnt such that these secreted factors are at a high concentration ventrally and are in low abundance dorsally. Genetic studies in zebrafish have been instrumental in elucidating the effect early dorsal-ventral axis formation has on placodal development. *swirl (swr, BMP2b)* mutants have a radialized neural plate which expands to wrap around the circumference of the embryo (Nguyen et al., 1998). Hence, these mutants have no placodal or epidermal fates. Moderately dorsalized mutants such as *snailhouse (snh, BMP7)* and the deficiency mutant which removes the *wnt8* locus have ventrally displaced placodal domains (Nguyen et al., 1998; Phillips et al., 2004). The emerging consensus, therefore, is that the preplacodal domain is specified by an intermediate concentration of axial signals such as BMP present at the neural-nonneural interface.

The naïve ectoderm responds to these early axial specifiers by expressing appropriate transcription factors in spatially restricted domains (i.e. Nguyen et al., 1998). Ventrally located epidermal markers abut dorsal neural marker expression domains. Fate mapping studies reveal that placodal tissues initially overlap these two early ectodermal domains (Kozlowski et al., 1997). Later, however, the preplacodal domain is refined and begins to express regional markers such as *dlx, msx*, *six* and *eya*. It seems likely that one function of these early preplacodal genes is to respond to a specific concentration of dorsal-ventral signals and then to refine this rough pattern into the three distinct ectodermal domains. A combinatorial code of different transcription factors may mediate axial signals and help specify various ectodermal domains, providing these domains with a unique molecular identity.

Derivatives of cranial placodes

The preplacodal domain encompasses a crescent-shaped field surrounding the lateral neural plate. This can be best visualized by examining the expression of pan-placodal markers including members of the *dlx*, *sox* and *six* families of transcription factors. This domain is then subdivided into various cranial placodes (Fig. 2). The olfactory placodes give rise to the sensory apparatus of the nasal epithelium and its associated neurons. The hypophyseal placode forms portions of the pituitary gland of the neurendocrine system. The lens placode is unique among all placodal tissues as it gives rise not to neural cells but instead to the lenses of the eyes. The trigeminal placode forms cranial nerve V, a ganglion consisting of mechanosenory neurons which innervate the facial region. The epibranchial placodes give rise to cranial nerves VII, IX, and X

which relay information from the taste buds and visceral organs. Finally, the otic placode forms the vestibuloacoustic apparatus of the inner ear including the statoacousitic ganglion (cranial nerve VIII) which relays information from the inner ear to the CNS. Development of the otic placode is the focus of this dissertation.

Inner ear anatomy

The vertebrate inner ear is a complex organ consisting of several chambers able to provide the CNS with both vestibular and auditory information. Each chamber of the inner ear contains a sensory epithelium, either maculae or cristae depending on the chamber. These epithelia consist of ciliated hair cells and associated supporting cells. Deflection of the ciliary bundles by either accelerational forces (such as gravity or inertia) or acoustic vibrations triggers hair cell mediated activation of its associated neurons. The auditory or posterior portion of the inner ear shows considerable divergence amongst different phylogenies of vertebrates, ranging from the lagenar chamber and the saccular macula in fishes to the cochlea in birds and mammals. The anterior vestibular system, however, is well conserved in all vertebrates and consists of the utricle and the semicircular canals.

The otic placode: potential inducing tissues

Despite the complexity of the inner ear at adult stages, all otic tissues are derived from the comparatively simple otic placode. The otic placode is an ectodermal thickening located just lateral to the neural plate at the level of the hindbrain. It undergoes a striking series of morphogenetic cell rearrangements which results in formation of the various chambers of the adult inner ear. Classic embryological

experiments in amphibians and avians have demonstrated that otic placode development is an inductive process, i.e. other nearby tissues are required to signal to the naïve preotic ectoderm to instruct it to undergo the otic developmental program. Determining the nature of the otic inducing tissue(s) has been the focus of many of the studies into otic induction over the last century. These studies have been recently reviewed (Riley and Phillips, 2003; Whitfield et al., 2002; Baker and Bronner-Fraser, 2001) and I will briefly discuss only those studies pertinent to this work.

The neural tube, specifically hindbrain tissue, has been the most intensely studied potential otic-inducing tissue. The otic placode develops immediately adjacent to the developing hindbrain in all vertebrates. Transplanting hindbrain tissue to the ventral side of the embryo results in ectopic otic tissue near the graft, suggesting hindbrain emits a factor sufficient for otic induction (Woo and Fraser, 1998). Consistent with this hypothesis, mutations in genes expressed solely in the hindbrain result in varied otic defects both in mammals and zebrafish (Deol, 1964; Deol, 1966; Wilkinson et al., 1988; Goulding et al., 1991; Mansour et al., 1993; Cordes and Barsh, 1994; Whitfield et al., 1996; Phillips et al., 2001). These genetic studies support the hypothesis that the hindbrain is an important source for otic inducing signals.

The subjacent mesendoderm is another potential otic inducing tissue. The evidence for this relies upon both experimental embryology as well as mutant analysis. Transplants of germring, the site of mesoderm formation, to anterior locations can induce ectopic otic tissue (Woo and Fraser, 1997). Moreover, hindbrain transplantation is most effective in inducing ear tissue when grafted to regions near the germring (Woo

and Fraser, 1998). Specific mesodermal tissues have not been exhaustively examined, but the notochord has been proposed based on its proximity to the inner ear and its reported ability to induce ectopic otic placodes (Kohan, 1944). Genetic studies in zebrafish also reveal possible roles for mesendoderm in otic development. Nodal is a member of the transforming growth factor β family of secreted ligands required for mesoderm induction. Zebrafish *cyclops (cyc)* encodes a secreted Nodal-related protein. *cyc* mutants have a partial loss of prechordal mesoderm and show a moderate (up to one hour) delay in otic induction. *one-eyed pinhead (oep)*encodes a coreceptor absolutely required for reception of the zebrafish Nodal-related ligands. Zygotic *oep* mutants have a more severe deficiency in prechordal mesoderm and, correspondingly, show a more extensive delay (1.5 hr) in otic induction and display a small otic vesicle (Mendonsa and Riley, 1999). Maternal-zygotic *oep* (*MZoep*) mutants lack all mesoderm and show the most severe delay (2 hr) in otic induction, while *no tail* mutants, which lack only notochord, have no ear defects (Mendonsa and Riley, 1999; Phillips et al., 2001). These data suggest that paraxial cephalic mesoderm and/or prechordal mesoderm emit an otic-inducing factor(s) necessary for timely inner ear formation while notochord is unlikely to be an otic-inducing tissue. However, ectodermal factors can compensate for the loss of mesoderm and otic induction eventually occurs in MZ*oep* embryos. Taken together, both the embryologic and the genetic studies are consistent with the hypothesis that otic-inducing signals are emitted by both the hindbrain and the underlying mesoderm in a partially redundant fashion.

Candidate otic-inducing factors

Considerable effort has gone into identifying otic-inducing signals. Members of the FGF family of secreted ligands are the most likely candidates. Fgf3 is expressed in the hindbrains of zebrafish, Xenopus, chick and mouse adjacent to the otic domain as well as zebrafish periotic mesendoderm. In *Fgf3* mutant mice, the ear forms but displays gross malformations. It is reduced in size and lacks the endolymphatic duct (Mansour et al., 1993). These mutants often die shortly after birth, but the survivors display deafness and vestibular defects consistent with inner ear defects. In zebrafish Fgf3 is also expressed in the hindbrain between the otic primordia. Knockdown of zebrafish Fgf3 results in a small ear phenotype (Phillips et al. 2001). In chick, retroviral misexpression of Fgf3, but not Fgf2, results in ectopic otic placodes and vesicles (Vendrell et al., 2000), while antibody- or antisense RNA-mediated knockdown of Fgf3 inhibits otic development (Represa et al., 1991). However, otic induction still occurs in the Fgf3 knockout mouse (Mansour et al., 1993), suggesting other redundant inductive signals could be involved. In zebrafish a potential candidate for a redundant factor is Fgf8. Fgf8 is mutated in the zebrafish mutant *acerebellar (ace)* and these mutants also have a small ear phenotype, often lacking the saccular macula (Whitfield, et al., 1996). Fgf8 is coexpressed in the hindbrain with Fgf3. These data suggests the hypothesis that Fgf3 and Fgf8 may be acting redundantly to induce otic tissue, whereby loss of either one can be partially compensated by presence of the other. In mouse, Fgf8 is not expressed near the ear and therefore cannot participate in placode formation in this species. However, another Fgf, Fgf10, is expressed in subjacent mesoderm at the time of otic induction and

may cooperate with Fgf3 emanating from the hindbrain (Wright and Mansour, 2003). In both these model systems, a synergistic loss of otic tissue would be predicted to result from the loss of multiple Fgfs, for example Fgf3 and Fgf8 in the zebrafish.

Evidence also exists that multiple families of secreted factors may cooperatively participate in otic induction. In chick a member of the Wnt family of secreted factors, Wnt8c, was postulated to act in concert with Fgf19 in inducing otic tissue. Wnt8c is a homolog of mouse/fish Wnt8, a signaling factor that acts through the Wnt/β-catenin signal transduction pathway (Schubert et al, 2000; Lekven et al., 2001). In chick, Fgf19 is normally coexpressed with Fgf3 in the hindbrain and mesoderm while Wnt8c is expressed in the hindbrain (Ladher et al., 2000a). When chick explants of uncommitted ectoderm are cultured in the presence of both Fgf19 and Wnt8c a number of otic markers are induced. Importantly, explants exposed to either Fgf19 or Wnt8c induce only low levels of a subset of otic markers. The authors conclude that naïve ectoderm is instructed to initiate otic development by the combined activities of both the Fgf and the Wnt pathways. Interestingly, Wnt8c was observed to induce high levels of Fgf3 expression in this experiment, raising the possibility that Wnt is acting indirectly through Fgf3 to induce otic fate.

Dissertation objectives

Chapters II-IV address different phases of otic development and are outlined below. For all of these studies I utilized the zebrafish as a model system for vertebrate developmental genetics. Zebrafish is an excellent system for these studies because of is rapid development, optical clarity and short generation time. For loss-of-function

studies there are many mutants available from the fish community as well as antisense morpholino technology for targeted gene knockdown. Gain-of-function data are also obtainable since microinjection of DNA or RNA can be accomplished with little difficulty. Finally, the zebrafish genome project is nearing completion, providing investigators with easily accessible sequence information.

Chapter II readdresses the long-standing issue of determining the molecular nature of the otic-inducing signals. I utilize loss-of-function techniques to demonstrate that Fgf3 and Fgf8 emanating from the hindbrain and subjacent mesendoderm are required redundantly for otic induction. I go on to show that posteriorization of the neural tube with retinoic acid enlarges the hindbrain domains of Fgf3 and Fgf8. This results in ectopic otic placodes and vesicles which are abolished in Fgf loss-of-function embryos.

Chapter III deals with the relative roles of the Fgf and Wnt pathway. Here I use both gain- and loss-of-function techniques to demonstrate that Wnt8 serves to correctly position the temporal and spatial expression domains of Fgf3 and Fgf8. I go on to show that the preotic domain expresses Fgf reporter genes, but not a Wnt-inducible transgene. These data indicate that Fgf and Wnt are not in parallel pathways but instead a linear pathway where Fgf is directly received by the preotic domain.

Chapter IV addresses the function of the muscle segment homeobox (Msx) family of transcription factors in placodal and hindbrain development. Three family members, *msxB*, *msxC* and *msxE* are expressed in the preplacodal domain and the neural plate from the trigeminal on back. As development proceeds expression shifts solely

into the lateral neural plate, the site of neural crest formation and is retained in the dorsal neural tube. Msx proteins are thought to be repressors which mediate the effects of the BMP and/or Wnt pathways. This study offers insight to how these *msx* genes regulate feedback with signaling interactions at the neural-nonneural boundary by restraining Dlx activity. I go on to show that Msx is required for normal development of placodal and neural tissues.

The appendix is a publication consisting primarily of the work of my colleague, S.J. Kwak. It deals with later roles of Fgf3 in patterning the otic vesicle. I include it in this dissertation as a record of my work and describe my relative contributions in the overview.

CHAPTER II

ZEBRAFISH FGF3 AND FGF8 ENCODE REDUNDANT FUNCTIONS REQUIRED FOR OTIC PLACODE INDUCTION*

OVERVIEW

This chapter is a published work (Phillips et al., 2001). It assesses the role of fibroblast growth factors in otic induction and represents the first genetic data implicating signaling molecules required for inner ear specification. K. Bolding was an undergraduate researcher working under my direction and contributed to this work.

SUMMARY

Members of the fibroblast growth factor (FGF) family of peptide ligands have been implicated in otic placode induction in several vertebrate species. Here we have functionally analyzed the roles of *fgf3* and *fgf8* in zebrafish otic development. The role of *fgf8* was assessed by analyzing *acerebellar* (*ace*) mutants. *fgf3* function was disrupted by injecting embryos with antisense morpholino oligomers (MO) specifically designed to block translation of *fgf3* transcripts. Disruption of either *fgf3* or *fgf8* causes moderate reduction in the size of the otic vesicle. Injection of fgf3-MO into *ace/ace* mutants causes much more severe reduction or complete loss of otic tissue. Moreover, pre-placode cells fail to express *pax8* and *pax2.1*, indicating disruption of early stages of otic induction in fgf3-depleted *ace/ace* mutants. Both *fgf3* and *fgf8* are normally

---

*Reprinted from *Developmental Biology*, Vol. 235, Phillips, et al., Zebrafish *fgf3* and *fgf8* encode redundant functions required for otic placode induction, pp 351-365, Copyright (2001), with permission from Elsevier.

expressed in the germring by 50% epiboly and are induced in the primordium of rhombomere 4 by 80% epibloy. In addition, *fgf3* is expressed during the latter half of gastrulation in the prechordal plate and paraxial cephalic mesendoderm, tissues that either pass beneath or persist near the prospective otic ectoderm. Conditions that alter the pattern of expression of *fgf3* and/or *fgf8* cause corresponding changes in otic induction. Loss of maternal and zygotic *one-eyed pinhead* (*oep*) does not alter expression of *fgf3* or *fgf8* in the hindbrain but ablates mesendodermal sources of fgf signaling and delays otic induction by several hours. Conversely, treatment of wild-type embryos with retinoic acid greatly expands the periotic domains of expression of *fgf3*, *fgf8*, and *pax8* and leads to formation of supernumerary and ectopic otic vesicles. These data support the hypothesis that fgf3 and fgf8 cooperate during the latter half of gastrulation to induce differentiation of otic placodes.

INTRODUCTION

The vertebrate inner ear develops from a simple columnar epithelial structure, the otic placode. The otic placode differentiates gradually from naïve ectoderm in response to localized inductive signals (Yntema, 1933, 1950; Waddington, 1937; Jacobson, 1963; Gallagher et al., 1996; Groves and Bronner-Fraser, 2000). Analysis of early markers of otic differentiation indicates that induction of the otic placode begins much earlier than previously thought, perhaps by mid-gastrulation (Pfeffer et al., 1998; Heller and Brandli, 1999). A longstanding goal has been to identify the tissue-sources of otic inducing signals. Transplantation studies indicate that prospective hindbrain tissue is sufficient to induce ectopic otic placodes (Stone, 1931; Harrison, 1935; Waddington, 1937; Woo and

Fraser, 1998). In addition, mutations in several genes expressed in the developing hindbrain lead indirectly to patterning defects in the inner ear, presumably by disrupting hindbrain-derived signals (Epstein et al., 1991; Lufkin et al., 1991; Chisaka et al., 1992; Cordes and Barsh, 1994; Moens et al., 1998). Subjacent mesendodermal tissues also appear to play a role in otic induction (Jacobson, 1963). Mutations in zebrafish that disrupt formation of the prechordal plate and paraxial cephalic mesendoderm significantly delay the onset of otic induction (Mendonsa and Riley, 1999). In contrast, mutations that ablate chordamesoderm cause no detectable changes in the timing or patterning of inner ear development. These findings suggest that the first mesodermal cells to involute during gastrulation deliver inductive signals to the prospective otic tissue. However, it is not yet clear whether this event precedes the onset of signaling from the prospective hindbrain. In addition to the above signaling sources, the lateral and ventral germring of the zebrafish gastrula can induce ectopic otic vesicles when transplanted to the prospective forebrain region (Woo and Fraser, 1997). Although such grafts also induce ectopic hindbrain tissue, which could emit its own otic-inducing factors, direct transplantation of hindbrain tissue to the forebrain region is not sufficient to induce ectopic otic vesicles (Woo and Fraser, 1998). Thus, additional signals from the germring appear to be necessary for otic induction in this region.

A number of signaling molecules have been implicated in otic placode induction, and members of the fibroblast growth factor (FGF) family appear to play especially prominent roles. In the chick, *FGF19* is expressed in paraxial cephalic mesoderm adjacent to the prospective otic placode and is later expressed in the adjacent hindbrain

(Ladher et al., 2000a). Transplants of *FGF19*-expressing mesoderm are sufficient to induce expression of otic markers in anterior ectoderm. FGF19 alone is not sufficient to induce otic differentiation unless prospective neural tissue is also present, in which case numerous otic markers are induced in uncommitted ectoderm. This interaction led to the discovery that FGF19 induces expression of *Wnt-8c* in prospective neural tissue, and together these two signaling molecules induce high level expression of a wide range of otic markers.

Another strong candidate for an otic inducing factor is FGF3. In the chick, the pattern of *FGF3* expression is strikingly similar to that of *FGF19* (Mahmood et al., 1995). In addition to being expressed in paraxial mesoderm and hindbrain tissue adjacent to the otic anlagen, *FGF3* is also expressed later in the developing otic placode and vesicle. Importantly, misexpression of *FGF3* leads to formation of ectopic otic vesicles (Vendrell et al., 2000). Depletion of FGF3 in explants of presumptive otic tissue prevents formation of otic vesicles (Represa et al., 1991). In contrast, targeted disruption of *FGF3* in the mouse does not prevent placode induction, although otic vesicles produced in *FGF3* mutants are small and malformed. While this apparent contradiction could reflect species differences in the requirement for FGF3, it is more likely that the different methodologies used can explain the different results. For example, the effects of disrupting *FGF3* in the mouse could be ameliorated by the presence of redundant functions, possibly including FGF19 and Wnt-8. Differentiation of chick explants may be more dependent on endogenous *FGF3* function since the explanted tissue is separated from other potential sources of inducing factors. Together,

these data suggest that FGF3 plays an important role in otic induction, but that redundant functions can partially compensate for its loss.

Mutational studies in zebrafish have identified yet another FGF homolog required for early otic development. A null mutation in the zebrafish *fgf8* gene, termed *acerebellar* (*ace*), causes embryos to produce small malformed otic vesicles (Whitfield et al., 1996; Reifers et al., 1998). Although placode induction has not been previously examined in *ace* mutants, *fgf8* is expressed in the hindbrain anlagen during gastrulation, suggesting that it could play an early role in otic induction. If so, the ability to produce small otic vesicles in *ace* mutants could reflect functional redundancy in the induction pathway.

Here we have tested whether fgf3 and fgf8 cooperate to induce otic placodes in the zebrafish. Mutant loci of *fgf3* are not yet available in zebrafish, but we injected anti-sense "morpholino" oligomers (Nasevicius and Ekker, 2000) into 1- to 2-celled embryos to specifically knockdown *fgf3* function. Knockdown of *fgf3* in wild-type embryos results in the formation of small otic vesicles, whereas knockdown of *fgf3* in *ace/ace* mutant embryos results in complete loss of otic tissue. Both *fgf3* and *fgf8* are expressed in close proximity to prospective otic tissues through much of gastrulation. The first inductive signals appear to emanate from subjacent mesendoderm, followed closely by signaling from the hindbrain. Ablation of mesendoderm by disrupting *one-eyed pinhead* (*oep*) specifically delays otic differentiation by several hours, despite normal expression of *fgf3* and *fgf8* in adjacent hindbrain primordium. In contrast, treatment of wild-type embryos with retinoic acid (RA) expands the domains of *fgf3* and *fgf8*

expression in the hindbrain and leads to a dramatic increase in the amount of otic tissue induced. These data indicate that *fgf3* and *fgf8* provide redundant functions required for otic induction, and that the cumulative effects of signaling from a variety of sources over a prolonged period of development are required for normal otic induction.

MATERIALS AND METHODS

Strains and developmental conditions

The wild-type strain was derived from the AB line (Eugene, OR). The functionally null *ace*^{ti282a} mutation was induced with ENU in the Tu wild-type strain (Brand et al., 1996). Embryos were developed in an incubator at 28.5°C in water containing 0.008% Instant Ocean salts.

In situ hybridization

Embryos were fixed in MEMFA (0.1 M MOPS at pH 7.4, 2 mM EGTA, 1 mM $MgSO_4$, 3.7% formaldehyde). In situ hybridizations (Stachel et al., 1993) were performed at 67°C using probes for pax2.1 (Krauss et al., 1991), fgf8 (Reifers et al., 1998), fgf3 (Kiefer et al., 1996), and pax8 transcripts (Pfeffer et al., 1998). Two-color in situ hybridization was performed essentially as described by Jowett (1996), with several modifications. Rnase inhibitor (Promega, 100 units/ml) was added to the solution during antibody incubation steps to help stabilize mRNA. NBT-BCIP (Gibco-BRL) was used in the first alkaline phosphatase reaction to give a blue color. Afterwards, alkaline phosphatase from the first color reaction was inactivated by re-fixing embryos in MEMFA for 2 hours at room temperature. Fast Red (Sigma) was used for the second alkaline phosphatase reaction to give red color and fluorescence. For sectioning,

embryos were embedded in Immunobed resin (Polysciences No. 17324) and cut into 4 μm sections.

Immunofluorescence

Antibody staining was performed essentially as described by Riley et al., (1999). Embryos were incubated with the polyclonal primary antibody directed against mouse Pax2 (Berkeley Antibody Company, diluted 1:100) or the monoclonal primary antibody directed against acetylated tubulin (Sigma T-6793, diluted 1:100). Embryos were then washed and incubated with one of the following secondary antibodies: Alexa 546 goat anti-rabbit IgG (Molecular Probes A-11010, diluted 1:50) or Alexa 488 goat anti-mouse IgG (molecular Probes A-11001, diluted 1:50).

Morpholino oligomer injections

Morpholino oligomers obtained from Gene Tools Inc. were diluted in Danieaux solution (58mM NaCl, 0.7mM KCl, 0.4mM $MgSO_4$, 0.6mM $Ca(NO_3)_2$, 5.0mM N-[2-Hydroxyethyl] piperazine-N'-[2-ethanesulfonic acid] (HEPES) pH 7.6) to a concentration of 5μg/μl. Filtered green food coloring was added to a concentration of 3% to visualize fluid during injections. Approximately 1 nl (5ng MO) was injected into the yolk of one- to two-cell stage embryos. Embryos were injected and allowed to briefly recover in Holtfreter's solution (60 mM NaCl, 0.6 mM KCl, 0.9 mM $CaCl_2$, 5 mM HEPES pH 7.4) with 50 units/ml penicillin and 50 ug/ml streptomycin. Morpholino sequences were as follows: fgf3-MO: 5' CAT TGTGGCATG GCGGGATGTCGGC 3'; oep-MO: 5' GCCAATAAACTCCAAAACAACT CGA 3'.

Retinoic Acid Treatment

At the shield stage (6h), embryos were incubated for 1 hour at 28.5°C in a solution of 10^{-6} M retinoic acid in 0.5% DMSO, produced by diluting a stock solution of 10^{-3}M RA in DMSO. Chorions were perforated using a glass needle to facilitate retinoic acid exposure. Control embryos were incubated for 1 hr in 0.5% DMSO. After incubation, embryos were rinsed and raised under standard conditions.

RESULTS

***fgf3* and *fgf8* are required for formation of otic vesicles**

It has been previously noted that disruption of *fgf8* perturbs otic development (Whitfield at al., 1996; Reifers et al., 1998). Otic vesicles in *ace/ace* mutant embryos are smaller than normal and frequently contain only a single sensory patch and otolith (Fig. 3D). Timing of otic vesicle formation is normal in *ace/ace* embryos (data not shown), suggesting that the reduced size is caused by deficient induction or growth of otic placodes. If so, then there must be (an) additional factor(s) able to induce otic tissue in the absence of fgf8 to account for the ability of *ace/ace* embryos to produce any otic tissue.

Studies in other vertebrate species support a role for *FGF3* in otic induction (Represa et al., 1991; Mansour et al., 1993; Vendrell et al., 2000). Although zebrafish *fgf3* has been partially analyzed (Kiefer et al., 1996a,b), no mutant alleles have yet been identified. To test the consequences of *fgf3* dysfunction, we effected an *fgf3* knockdown by injecting antisense "morpholino" oligomers into wild-type blastulae. Morpholino oligomers (MO) are non-hydrolyzable polynucleotides that can form stable

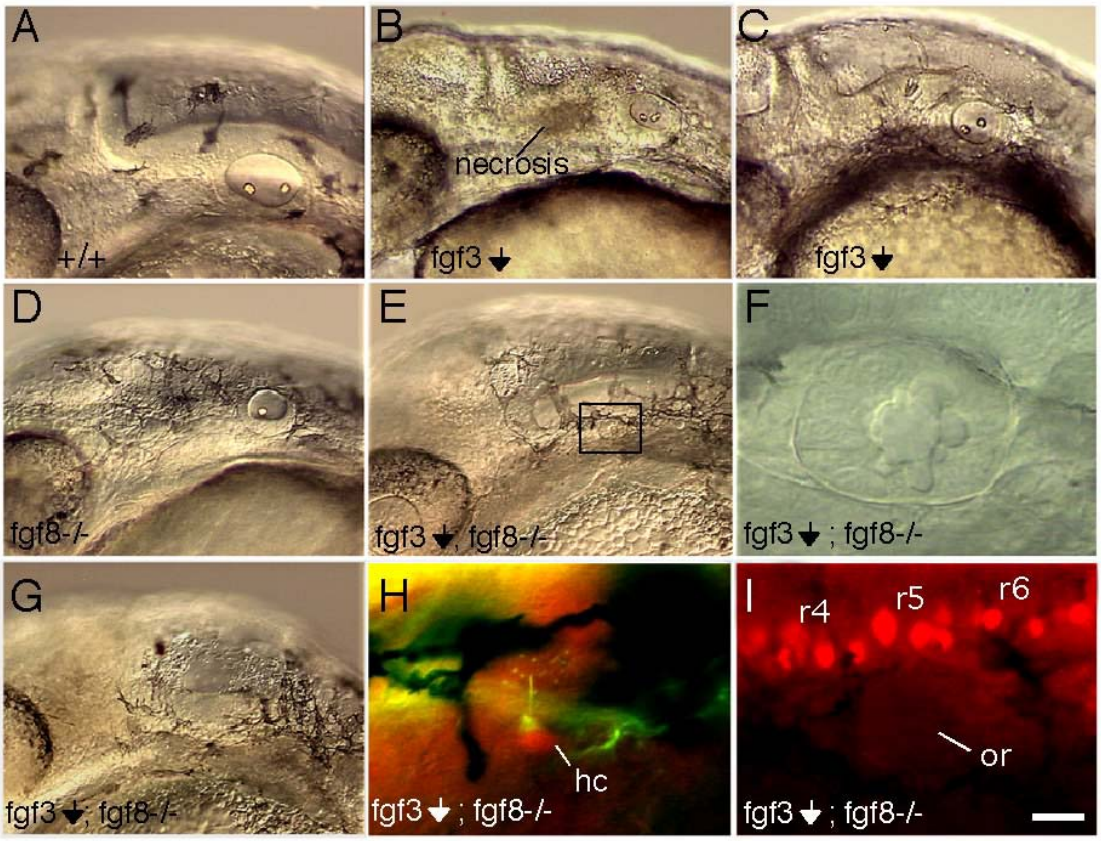

Figure 3. Formation of otic vesicles. (A-G) Lateral views of live embryos at 32h. (A) Wild-type, (B) fgf3-MO injected wild-type embryo with moderate necrosis, (C) fgf3-MO injected wild-type embryo with little or no necrosis and (D) *ace/ace* mutant. (E) fgf3-MO injected *ace/ace* mutant with a minute otic vesicle (boxed region). (F) Enlargement of minute otic vesicle of specimen shown in (E). (G) fgf3-MO injected *ace/ace* mutant with no visible otic vesicle. (H and I) Immunolocalization of hair cell markers in fgf3-MO injected *ace/ace* mutant at 32h. (H) Nuclear pax2.1 (red) and ciliary acetylated tubulin (green) in a specimen with a minute otic vesicle containing a single hair cell (hc). (I) Nuclear pax2.1 in a specimen with no visible otic vesicles. Note lack of pax2.1 in the otic region (or) while staining is retained in neurons of the hindbrain. Positions of rhombomeres 4, 5, and 6 (r4, r5, and r6) are indicated. In all specimens, anterior is to the left and dorsal is upward. Scale bar, 5 µm (F), 10µm (H), 15µm (I), 55µm (A-E, G).

duplexes with complementary regions of endogenous mRNA molecules. Upon hybridizing to 5' sequences near the translation initiation codon, morpholinos specifically inhibit translation of target transcripts by up to 99%. In zebrafish, morpholino-mediated knockdowns of several embryonic genes have been shown to cause developmental defects that closely mimic phenotypes caused by null mutations in the same genes (Nasivecius and Ekker, 2000).

Injection of fgf3-MO into wild-type embryos results in a range of developmental defects, including moderate perturbation of otic development. Otic vesicles are significantly smaller than normal in 80-90% (195/237) of injected embryos (Fig. 3B, C). Two sensory patches and associated otoliths are present in each vesicle. Moderate necrosis is observed in the brain and spinal cord in most (166/237) injected embryos (Fig. 3B), but even embryos with no discernable necrosis often have reduced otic vesicles (in one experiment, of 67 embryos with small ears, 18 had little or no necrosis, Fig 3C).

Much more severe disruption of otic development is observed when fgf3-MO is injected into intercross progeny of *ace/+* adults. About 85% (34/40) of the injected *ace/ace* homozygotes form either extremely small otic vesicles or none at all (Fig. 3E-G). In specimens with minute otic vesicles, no otoliths are produced (Fig. 3F). To determine whether these embryos produce any differentiated hair cells, they were stained with an antibody generated against mouse Pax2. This antibody strongly cross-reacts with zebrafish pax2.1. Although *pax2.1* is initially expressed throughout the otic placode, it later becomes restricted to sensory hair cells (Riley et al., 1999). In fgf3-

depleted *ace/ace* embryos, often only one or two hair cells are evident, with scarcely enough room within the lumen to accommodate their ciliary bundles (Fig. 3H). In specimens with no visible otic vesicles, no anti-pax2 staining is detected in the otic region (Fig. 3I). The ability of MO injection to disrupt otic development in *ace/ace* embryos is specific to fgf3-MO, as injection of control MO, or MO directed against other gene products (including *pax2.2*, *msxB*, and *lef-1*), has no effect on otic development (data not shown). Thus, loss of both fgf3 and fgf8 causes a synergistic loss of otic tissue, indicating that these genes encode redundant functions required for induction or completion of otic development.

Induction of otic placodes

We sought to determine the effects of disrupting *fgf3* and *fgf8* on otic induction. The earliest known marker of otic placode induction is *pax8* (Pfeffer et al., 1998; Heller and Brandli, 1999). Because early expression of *pax8* has not been described in detail, expression was examined in wild-type embryos at multiple stages during gastrulation and early segmentation. Weak expression is detected in the shield at 60% epiboly (data not shown). By 75% epiboly (8 h), staining is induced along the ventral and lateral margin in cells that eventually gives rise to the pronephros. Expression in the otic anlagen first appears at 85-90% epiboly (9 h) as longitudinal stripes extending from the margin along the lateral edges of the neural plate (Fig. 4A). Between 95% epiboly and the tailbud stage (10 h), the preotic domain moves away from the margin to form isolated patches in which *pax8* expression is strongly upregulated (Fig. 4B). High level

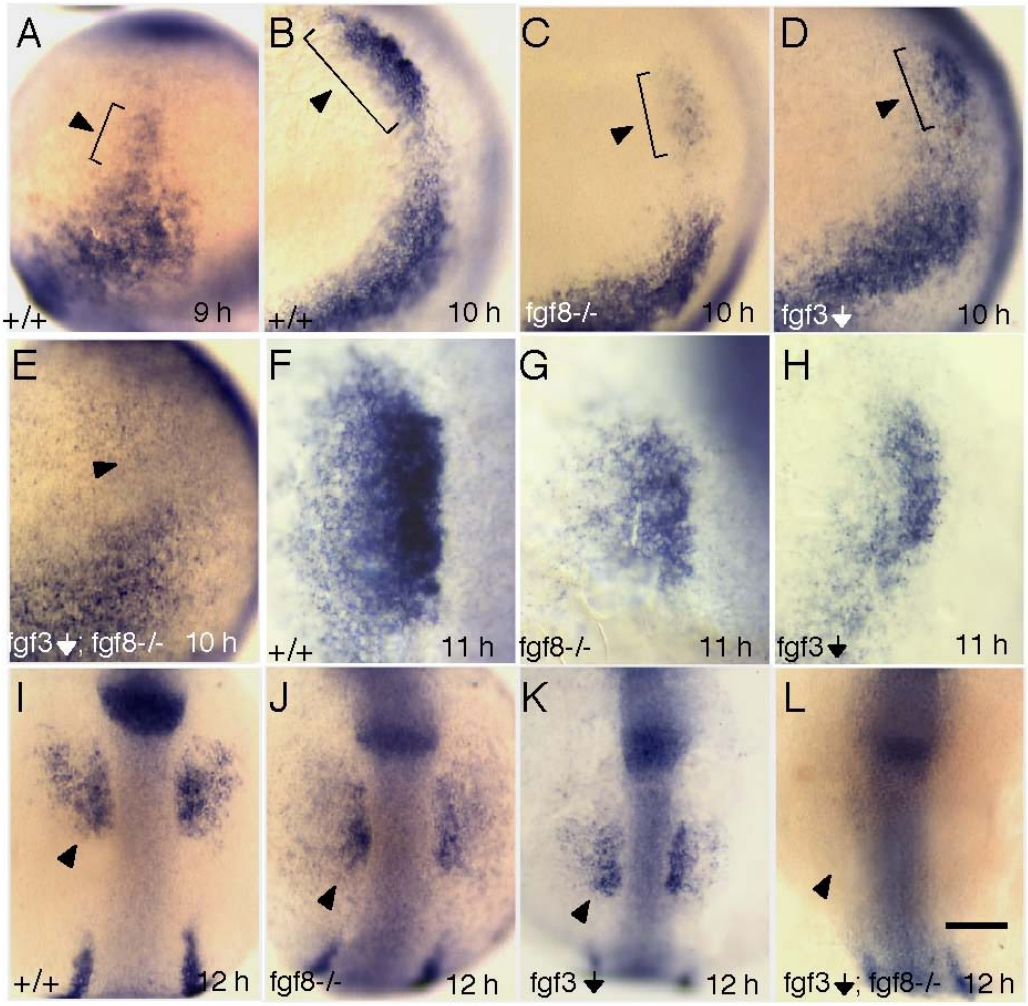

Figure 4. Induction of *pax8* expression in the pre-placode. Expression of *pax8* in wild-type embryos at (A) 90% epiboly and (B) tailbud stage. *pax8* expression at tailbud stage in (C) *ace/ace* mutant, (D) fgf3-MO injected wild-type embryo and (E) fgf3-MO injected *ace/ace* mutant. Enlarged view of placodal *pax8* expression at 3 somite stage in (F) wild-type embryo, (G) *ace/ace* mutant and (H) fgf3-MO injected wild-type embryos. *pax8* expression at 6 somite stage in (I) wild-type embryo, (J) *ace/ace* mutant, (K) fgf3-MO injected wild-type embryo, and (L) fgf3-MO injected *ace/ace* mutant. Note the lack of otic expression in injected *ace/ace* mutants. A-H are lateral views with dorsal to the right and anterior upward. I-L are dorsal views with anterior upward. Scale bar, 60µm (F-H), 125µm (B-E, I-L), 150µm (A).

expression is still evident at 6-7 somites (Fig. 4I). Expression in this domain subsequently declines until formation of the otic vesicles at the 18 somites stage, after which expression is lost (Pfeffer et al., 1998). Another preotic marker, *pax2.1*, is induced in the otic anlagen by the 3 somite stage (11 h) and is strongly upregulated as the placode develops (Ekker et al., 1992; Mendonsa and Riley, 1999; Fig. 5A).

Expression of *pax8* in presumptive *ace/ace* embryos shows normal timing, but the size of the otic anlagen is significantly reduced at the tailbud stage (Fig. 4C) and at the 3 somites stage (compare Figs. 4F and G). Although the otic anlagen expands dramatically by 6-7 somites, the number of *pax8*-expressing cells remains lower than in the wild type (Fig. 4J). Similarly, *pax2.1* is initially expressed in only a small fraction of the normal number of cells at 3 somites (not shown). The number of otic cells expressing *pax2.1* increases by 10 somites but remains lower than in the wild type (Fig. 5B). Thus, otic induction begins at approximately the normal time in *ace/ace* embryos, but the number of preotic and otic cells expands slowly and remains lower than normal throughout otic development.

We next examined the effects of *fgf3* knockdown on otic induction. Injection of fgf3-MO into wild-type embryos reduces the number of *pax8*-expressing cells in the otic anlagen to an extent similar to that seen in *ace/ace* embryos (Fig. 4D, H, K). Expression of *pax2.1* in preotic cells is strongly reduced at 3 somites (not shown), but only moderately reduced by 10 somites (Fig. 5C). fgf3-MO caused more variability than did the *ace* mutation, possibly reflecting residual fgf3 activity in morpholino-injected embryos. Nonetheless, these data suggest that fgf3 and fgf8 play similar roles in

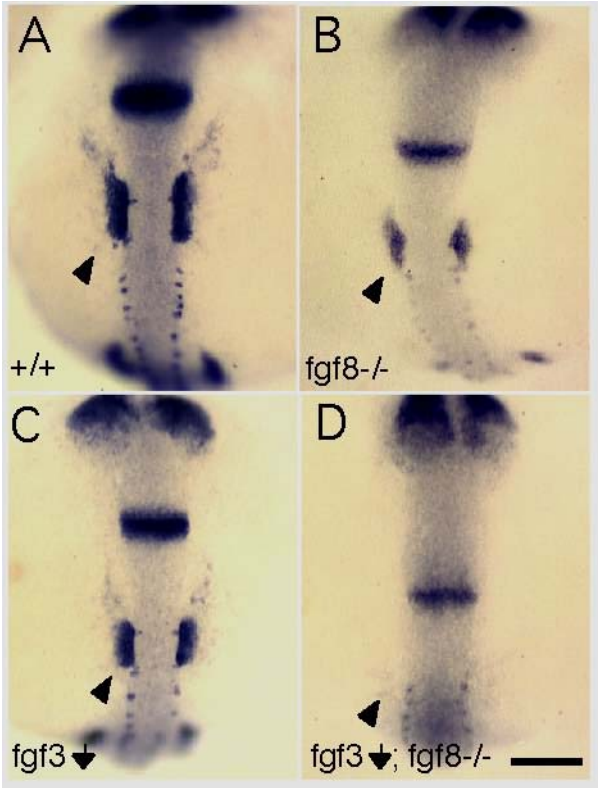

Figure 5. Expression of *pax2.1* in the otic placode. Dorsal views of embryos at the 10 somite stage showing expression of *pax2.1* in (A) wild-type, (B) *ace/ace*, (C) wild-type injected with fgf3-MO and (D) *ace/ace* embryo injected with fgf3-MO. Arrows indicate placodes. Note the lack of otic expression in injected mutant. Scale bar, 25µm.

regulating early otic development.

Injection of fgf3-MO into intercross progeny of *ace/+* parents gave quite different results. Approximately one quarter (13/50) of these embryos show no *pax8* staining in the otic region at the tailbud stage (Fig. 4E). We infer that loss of preotic staining occurs only in *ace/ace* homozygotes since this phenotype is never observed in wild-type embryos injected with fgf3-MO. *ace/ace* homozygotes can be identified at 6-7 somites stage by virtue of their low level of *pax8* expression in the midbrain-hindbrain border. At this time, about two thirds (15/23) of fgf3-depleted *ace/ace* embryos show little or no *pax8* expression in the otic region (Fig. 4L). Similarly, expression of *pax2.1* is greatly reduced or absent in most (11/13) fgf3-depleted *ace/ace* embryos (Fig. 5D). These data support the hypothesis that fgf3 and fgf8 are both required for normal otic induction.

Expression patterns of *fgf3* and *fgf8*

To localize potential signaling interactions required for otic induction, expression patterns of *fgf3* and *fgf8* were visualized in wild-type embryos at various stages of gastrulation and early segmentation. At 50% epiboly, *fgf8* is expressed throughout the margin, with maximal expression in the shield (Fürthauer et al., 1997; and Fig. 6A). *fgf8* expression is not maintained in hypoblast cells after they migrate away from the margin. Between 75% and 80% epiboly, *fgf8* is expressed in bilateral transverse stripes in the epiblast, a domain corresponding to the anlagen of rhombomere 4 (r4) in the hindbrain (Fig. 6B). Expression within this domain is initially weak and variable but upregulates rapidly such that, by 90% epiboly, all embryos show strong uniform expression (Fig.

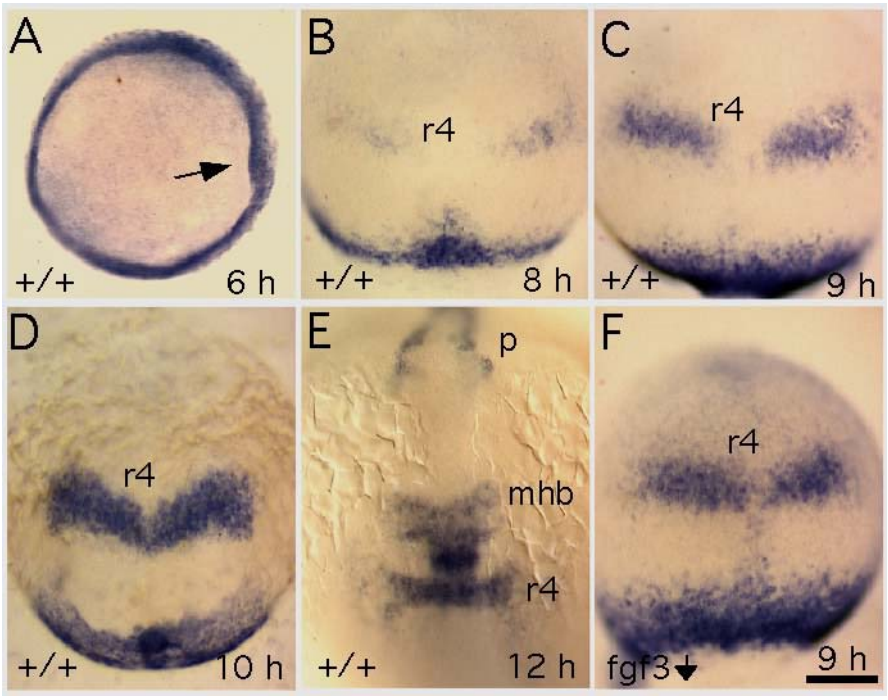

Figure 6. Expression of *fgf8*. Expression of *fgf8* in wild-type embryos at (A) shield stage (arrow indicates shield), (B) 75% epiboly, (C) 90% epiboly, (D) tailbud stage, and (E) 6 somite stage. (F) Expression of *fgf8* at 90% epiboly in a fgf3-MO injected wild-type embryo. Abbreviations: r4, rhombomere 4; mhb, midbrain-hindbrain border; p, prechordal plate. (A) An animal pole view with dorsal to the right. (B-F) Dorsal views with anterior upwards. Scale bar, 125µm (E), 150µm (B,C,D,F), 215µm (A).

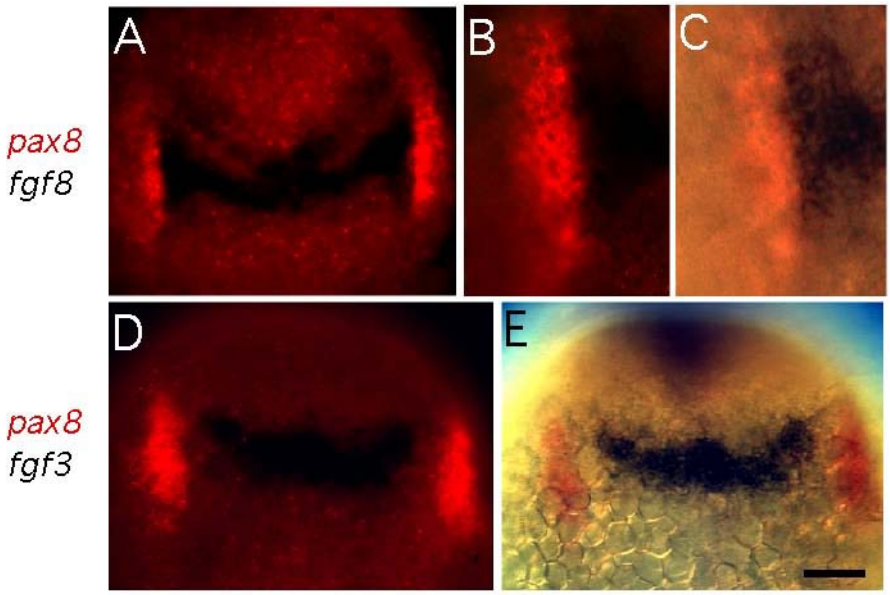

Figure 7. Relationship between expression of *pax8* and *fgf8* or *fgf3*. (A-C) Two color in situ hybridization of tailbud stage wild-type embryos showing *fgf8* (blue) and *pax8* expression (red). (A) Fluorescence image showing fgf8 in the hindbrain and pax8 in the preotic placodes. (B and C) Enlargement of the left otic region viewed under fluorescence (B) or transmitted light plus fluorescence (C). (D and E) Two color in situ hybridization of wild-type embryos showing *fgf3* (blue) and *pax8* (red) expression viewed under fluorescence (D) or transmitted light plus fluorescence. Scale bar, 50µm (B,C), 100µm (A,D,E).

6C). The lateral edges of the r4 stripe appose the medial edges of the otic anlage. By the tailbud stage, expression in the r4 domain meets at the midline to form a single chevron-shaped stripe (Fig. 6D). In addition, expression near the lateral edges of the chevron begins to spread posteriorly along the medial edges of the otic anlage. Two-color in situ hybridization reveals that the domains of *fgf8* and *pax8* in and around the otic anlagen are complementary, with little or no overlap in expression (Fig. 7 A-C). This periotic domain of *fgf8* persists in earless mutants (ace/ace mutants injected with fgf3-MO; data not shown), suggesting that it marks the lateral edges of the hindbrain. Between 3 and 10 somites, expression of *fgf8* is maintained in r4 and several additional domains, corresponding to the anterior hindbrain, the midbrain-hindbrain border, and the prechordal plate, become evident (Reifers et al., 1998; and Fig. 6E).

fgf3 is expressed in a dorsal-ventral gradient along the margin at 50% epiboly, with maximal expression in dorsal cells (Fig. 8A). As gastrulation proceeds, *fgf3* strongly upregulates in the shield and is maintained at high levels in the prechordal hypoblast as it migrates away from the margin. The prechordal domain passes between the otic anlage by 75% epiboly (Fig. 8B). At this time, weak diffuse staining is also observed in anterior cells surrounding the lateral and posterior edges of the prechordal domain. Between 80% and 90% epiboly, *fgf3* is expressed in bilateral transverse stripes corresponding to the r4 anlagen (Fig. 8C). Prechordal staining has progressed to a region anterior to r4, but a broad arc of diffuse staining curves around the anterior edge of the prechordal domain back to the lateral edges of the r4 stripes. Expression in the r4 domain intensifies by 95% epiboly and forms a single chevron by the tailbud stage (Fig.

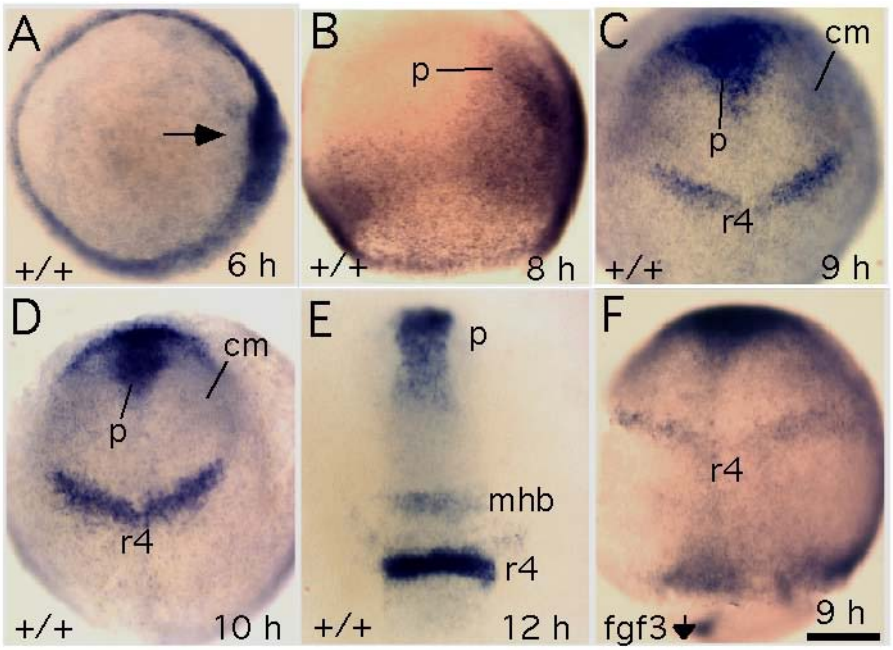

Figure 8. Expression of *fgf3*. Expression of *fgf3* in wild-type embryos at (A) shield stage (arrow indicates shield), (B) 75% epiboly, (C) 90% epiboly, (D) tailbud stage, and (E) 6 somite stage. (F) Expression of *fgf3* at 90% epiboly in a fgf3-MO injected wild-type embryo. (A) Animal pole view with dorsal to the right. (B-F) Dorsal views with anterior upward. Abbreviations: r4, rhombomere 4; mhb, midbrain-hindbrain border; p, prechordal plate; cm, cephalic mesendoderm. Scale bar, 125µm (E), 150µm (B,C,D,F), 215µm (A).

8D). Expression in r4 is maintained at high levels through 6 somites stage (Fig. 8E), and well past the 10 somites stage when the otic placodes become morphologically visible (data not shown). In contrast to *fgf8*, the r4 domain of *fgf3* expression does not directly abut the *pax8*-expressing cells in the otic anlagen (Fig. 7D, E).

The complexity of *fgf3* expression led us to section stained specimens to establish which germ layers express the gene. As expected, staining within the r4 domain is restricted to the epiblast (Fig. 9D). Expression in the prechordal domain is more complex. Most cells in the prechordal hypoblast express moderate levels of *fgf3*. However, maximal expression in the prechordal domain occurs in cells at the interface between hypoblast and epiblast and includes some cells in the epiblast (Fig. 9B). Analysis of parasagittal sections shows that the broad arcs of staining sweeping from the prechordal plate to the lateral r4 region is primarily localized to the hypoblast (Fig. 9C).

In summary, *fgf3* and *fgf8* are expressed in close proximity to the future otic placode throughout the latter half of gastrulation. Notably, all domains of expression are tissues previously implicated in otic induction, including the germring, nascent prechordal plate and paraxial cephalic mesendoderm, and r4 in the hindbrain. Thus, fgf3 and fgf8 could cooperate to induce and maintain otic placode differentiation over a prolonged period of development. Expression patterns of both genes are normal in all *ace*/+ intercross progeny, as well as in fgf3 depleted embryos (Fig. 6F, Fig 8F, and data not shown). This confirms that, when one gene function is lost, the other continues to be expressed normally, consistent with the notion that the two genes play redundant roles in otic induction.

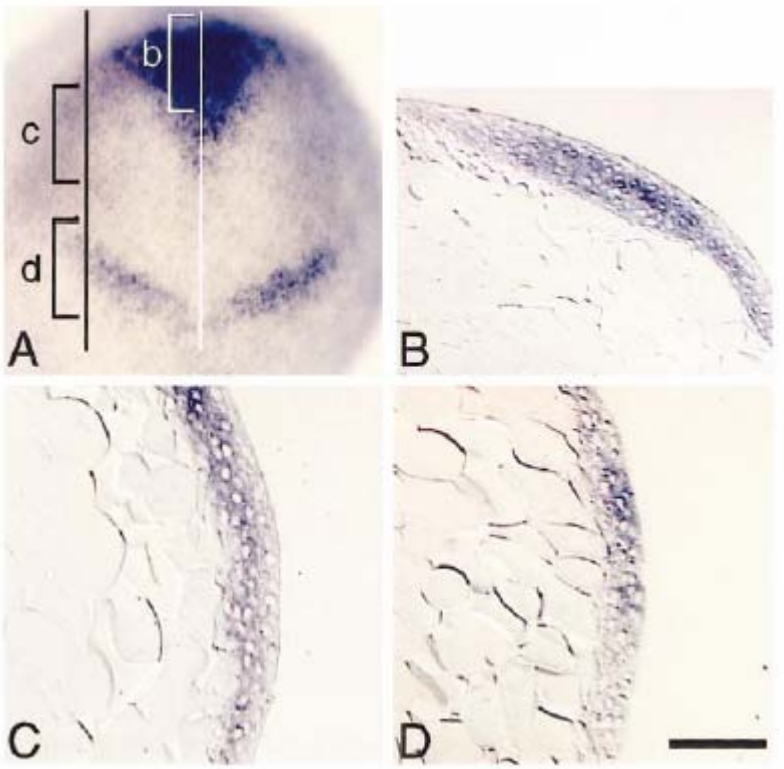

Figure 9. Sections of *fgf3* wholemount in situs. (A) Wild-type embryo stained for *fgf3* expression at 95% epiboly showing sectioning planes for B-D. (B-D) Sections of wild-type embryos stained for *fgf3* expression at 95% epiboly. (B) Midsagittal section through the prechordal domain. (C) Parasagittal section through cephalic mesendoderm domain. (D) Parasagittal section through r4 domain. (A) Dorsal view with anterior upward. (B-D) Dorsal is to the right and anterior is upward. Scale bar, 40µm (C,D), 55µm (B), 150µm (A).

Delayed otic induction in the absence of mesendoderm

We previously examined the effects of mesendoderm ablation on otic induction by analyzing *one-eyed pinhead* (*oep*) mutants (Mendonsa and Riley, 1999). The *oep* gene encodes a EGF-CFC protein that serves as a cofactor required for nodal signaling (Gritsman et al., 1999). Mutant embryos lacking zygotic *oep* function fail to form prechordal mesendoderm and show a 30-60 minute delay in otic placode induction, as judged by delayed expression of *dlx3* and *pax2.1*. Simultaneous loss of zygotic *oep* and *no-tail* (*ntl*) causes a more extensive depletion of mesendoderm (Schier et al., 1997) and leads to a 2-3 hour delay in otic development. Although *oep-ntl* double mutants also lack chordamesoderm, analysis of other compound mutants shows that loss of chordamesoderm does not contribute to the delay in otic differentiation. Importantly, a number of hindbrain markers (*eng-3*, *krox20*, *msxB*, and *pax2.1*) are induced normally in *oep-ntl* double mutants, indicating that the developmental delay is specific for otic tissue. This delay does not reflect a general deficit in establishing dorsolateral fates near the neural/non-neural border since expression of *msxB* and *dlx3* along the lateral edges of the neural plate (excluding the otic domain) occurs normally in such mutants (Mendonsa and Riley, 1999). These data support the hypothesis that it is the loss of mesendoderm that causes the delay in otic induction.

Here we have used a more efficient technique to ablate mesendoderm to examine how early inductive signaling is altered. It was recently shown that disruption of both maternal and zygotic *oep* function ablates nearly all mesendoderm, with only a few somites forming in the tail (Zhang et al., 1998). This phenotype is effectively

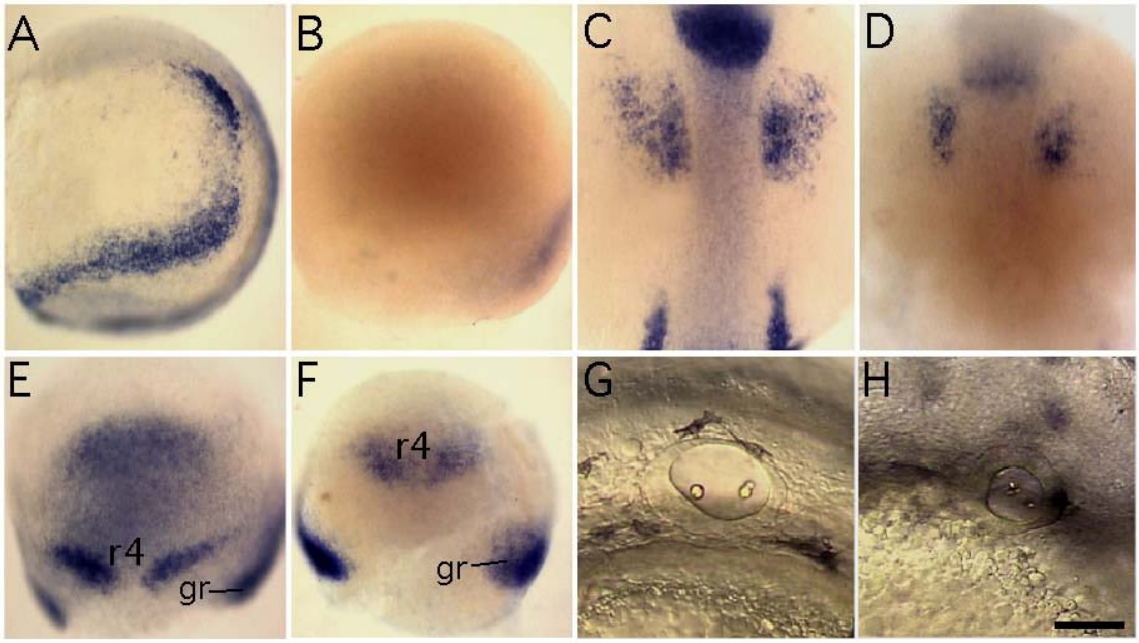

Figure 10. Effects of oep knockdown. (A, B) *pax8* expression at tailbud stage in (A) wild-type embryo and (B) wild-type embryo injected with oep-MO. (C, D) *pax8* expression at 6 somite stage in (C) wild-type embryo and (D) wild-type embryo injected with oep-MO. (E) *fgf3* and (F) *fgf8* expression at 90% epiboly in wild-type embryos injected with oep-MO. (G, H) lateral views of otic vesicles at 32h in (G) wild-type and (H) oep-MO injected wild-type embryos. Abbreviations: r4, rhombomere 4; gr, germ ring. (A and B) Lateral views with dorsal to the right and anterior upward. (C-F) Dorsal views with anterior upward. (G and H) Lateral views with anterior to the left and dorsal upward. Scale bar, 55µm (G,H), 150µm (A-F).

phenocopied by injecting oep-MO into wild-type blastulae (Nasevicius and Ekker, 2000). Though the efficiency of oep-MO in knocking down *oep* function varies between strains, it is highly efficient in our wild-type background. Injection of oep-MO produces varying degrees of the *oep* mutant phenotype in 80-90% (129/147) of injected embryos, and about a third (53/147) resemble severely affected mutants lacking both maternal and zygotic *oep* function. Severely affected embryos show reduced expression of *fgf3* and *fgf8* in the germring (not shown), and expression is totally ablated in the shield (Fig. 10E, F). About 75% (59/79) of oep-MO injected embryos fail to show high level *fgf3* expression in the prechordal domain, although weak diffuse expression persists in the anterior neural plate (Fig. 10E). In contrast to the above changes, *fgf3* and *fgf8* are expressed on time in the r4 domain in all embryos (Fig. 10E, n = 79; Fig. 10F, n = 85). Nevertheless, early expression of *pax8* is strongly inhibited. At the tailbud stage, about a third (12/32) of oep-depleted embryos show little or no *pax8* expression in either the pronephric or otic primordia (Fig. 10B). Expression in the otic domain is first detected at the 6 somites stage, although the size of the domain and the level of expression are significantly reduced in about half (17/37) of oep-depleted embryos (Fig. 10D). Later in development, severely affected embryos produce otic vesicles that are significantly smaller than normal (Fig. 10H). Thus, otic induction is delayed by several hours in *oep*-depleted embryos, even though *fgf3* and *fgf8* are expressed on time in the r4 domain. This indicates that, in the absence of mesendodermal signals, normal expression of hindbrain signals is not sufficient to induce otic differentiation on time.

Expanded otic induction following retinoic acid treatment

Treatment of vertebrate embryos with retinoic acid (RA) posteriorizes the neural plate such that forebrain and midbrain structures are reduced or lost and the hindbrain is expanded (Papalopulu et al., 1991; Marshall et al., 1993; Simeone et al., 1995; Alexandre et al., 1996). Accordingly, when zebrafish embryos are treated briefly with RA at the shield stage, the r4 domain of *fgf3* expression is greatly expanded along the anterior-posterior axis (Fig. 11D). Concomitant loss of midbrain and hindbrain tissue brings the r4 and prechordal domains into close proximity, thereby forming a nearly contiguous domain that covers much of the head region. The domain of *fgf8* expression is similarly expanded (Fig. 11E). The size and position of the otic anlage are altered accordingly. By 3 somites stage, the anterior limit of the placode domain of *pax8* expression extends forward to completely encircle the head (Fig. 11F). Later in development, most RA-treated embryos produce enlarged or supernumerary otic vesicles (Fig. 11J). In addition, 20-30% (33/129) of these embryos produce ectopic otic vesicles at the anterior limit of the head (Fig. 11K).

To determine whether the RA-induced expansion of otic differentiation requires *fgf3* and *fgf8*, the effects of RA treatment were examined in embryos deficient in either or both of these gene functions. The domain of *pax8* expression was notably reduced in about a quarter (9/32) of RA-treated progeny of *ace*/+ parents. Both the size of the *pax8* domain and the level of expression were greatly reduced in over half (25/41) of wild-type embryos that were injected with fgf3-MO and then RA-treated. When progeny of

Figure 11. Retinoic acid treatment. Embryos were incubated for 1 hr, beginning at the shield stage, in 10^{-6} M RA and 0.5% DMSO. Control embryos were incubated in 0.5% DMSO alone. Control embryos stained for (A) *fgf3*, (B) *fgf8*, and (C) *pax8* expression at the 3 somite stage. RA treated embryos stained for (D) *fgf3*, (E) *fgf8*, and(F) *pax8* expression at the 3 somite stage. *Pax8* expression at 3 somites in RA treated (G) presumptive *ace/ace* mutant, (H) fgf3-MO injected wild-type embryo, and (I) fgf3-MO injected presumptive *ace/ace* mutant. (J-L) Live RA-treated embryos at 32 h. (J) Lateral view of a specimen showing a cluster of 3 otic vesicles (arrows). (K) An anterio-lateral view of a specimen with ectopic otic vesicles at the anterior limit of the head (arrows), which formed in addition to enlarged bilateral otic vesicles further caudally (not shown). (L) Lateral view of an embryo injected with fgf3-MO prior to RA treatment. No otic vesicles are discernable. (A-I) Dorsal views with anterior upward. (J-L) Anterior is to the left and dorsal is upward. Scale bar, 70µm (J, K); 125 µm (A-I); 140µm (L).

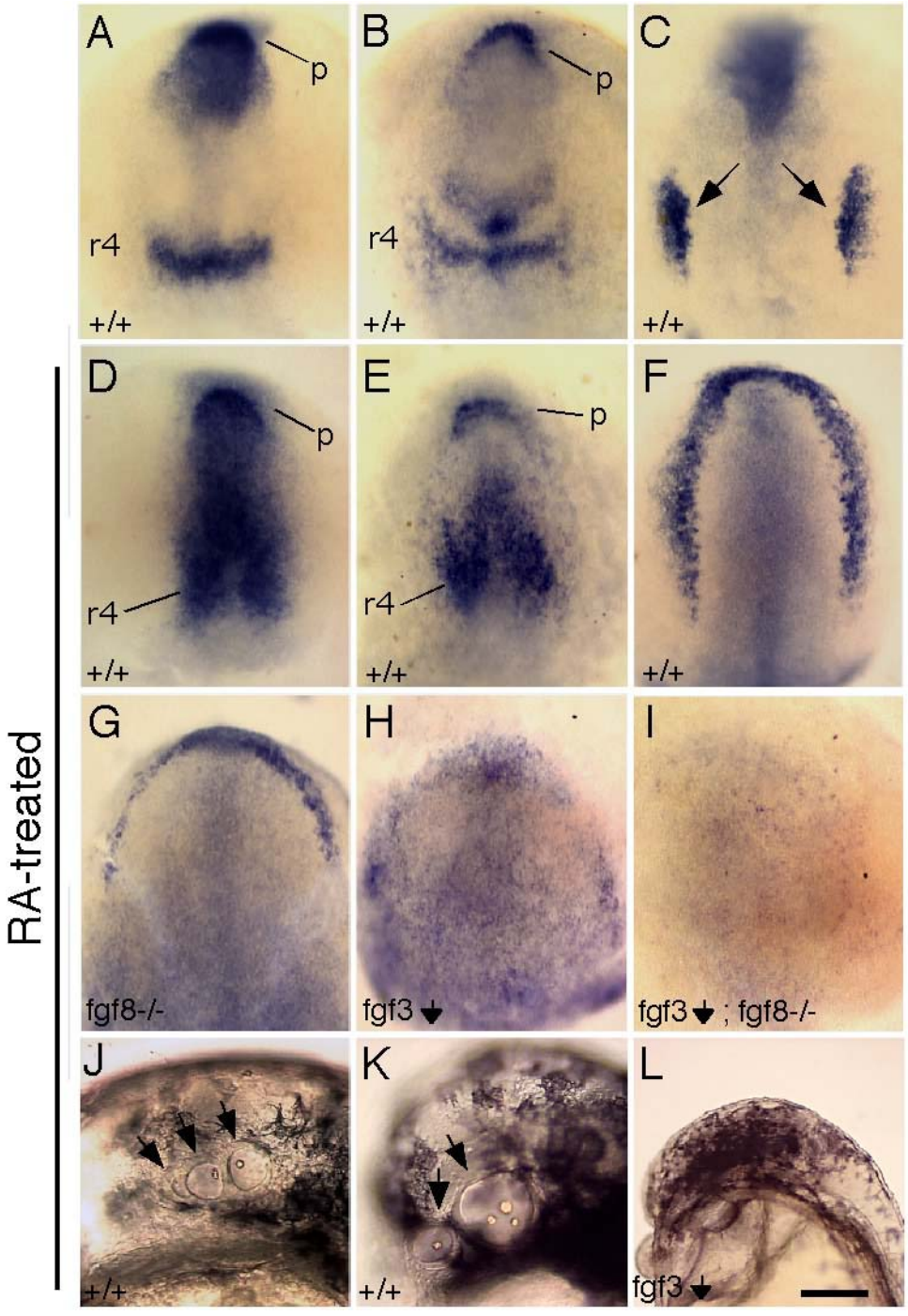
A
p
r4
+/+
B
p
r4
+/+
C
+/+
D
p
r4
+/+
E
p
r4
+/+
F
+/+
G
fgf8-/-
H
fgf3
I
fgf3 ; fgf8-/-
J
+/+
K
+/+
L
fgf3
RA-treated

ace/+ parents were injected with fgf3-MO and then RA-treated, nearly a fifth (8/45) show almost no detectable *pax8* expression. Similarly, depletion of fgf3 in wild-type embryos is sufficient to block the RA-induced formation of ectopic and supernumerary otic vesicles in virtually all cases (59/59, data not shown). Moreover, most (44/59) of these embryos failed to form any otic vesicles at all (Fig. 11L). When the progeny of *ace*/+ parents were RA-treated, 19/100 failed to form otic vesicles. Thus, the stimulatory effect of RA treatment on otic induction requires *fgf3* and *fgf8* function. These data support the hypothesis that expansion of the domains of *fgf3* and *fgf8* leads to an expanded domain of otic induction.

DISCUSSION

The role of FGF signaling

FGF3 has been implicated in otic induction in mouse and chick (Represa et al., 1991; Mansour et al., 1993; Vendrell et al., 2000), and here we provide evidence that *fgf3* plays a similar role in zebrafish. Moreover, the data presented here extend previous studies by elucidating key aspects of the timing and nature of inductive interactions. First, *fgf3* is expressed in several tissues that have the potential to interact with prospective otic ectoderm throughout the latter half of gastrulation (Fig. 12). Second, removal of mesendodermal sources of fgf3 (Fig. 10), or expansion of the domain of *fgf3* expression (Fig. 11), correlate with inhibition or enhancement of otic induction, respectively. Third, *fgf8* is expressed in an overlapping domain with *fgf3* (Fig. 12) and plays a redundant role in otic induction. Specifically, loss of both fgf3 and fgf8 completely blocks otic induction. It is not yet known whether FGF8 plays a similar role

in other vertebrates. Targeted knockouts of *FGF8* in the mouse disrupt development during early gastrulation, thereby preventing assessment of its role in otic induction (Sun et al., 1999). However, since targeted disruption of *FGF3* does not prevent otic induction, *FGF8* or some other *FGF* family member could provide a redundant function. Analysis of tissue-specific alleles of *FGF8* generated in the mouse could address this possibility (Meyers et al., 1998).

Another candidate for a redundant function is FGF19, which was recently shown to play a role in otic induction in the chick (Ladher et al., 2000a). In chick embryos, *FGF3* and *FGF19* are coexpressed in paraxial cephalic mesoderm around the time of otic induction. Thus, these two ligands could cooperate as otic inducers, either additively by stimulating the same receptors, or synergistically by activating distinct receptor isoforms (see below). In this context, it is interesting that, in zebrafish, loss of mesendoderm caused by *oep* dysfunction leads to a significant delay in otic induction, whereas depletion of fgf3 does not. This suggests that mesendoderm expresses other otic-inducing factors in addition to fgf3, possibly including fgf19. Neither zebrafish nor mouse homologs of *FGF19* have yet been identified, but an important future goal will be to analyze the effects of disrupting *FGF19* in these species, particularly in embryos also lacking *FGF3* function.

Compared to the effects of fgf3-depletion in zebrafish, the *ace* mutant phenotype is generally more severe and usually results in total ablation of the posterior (saccular) sensory epithelium. In contrast, even the most severely affected fgf3-depleted embryos form both anterior and posterior sensory epithelia. A possible explanation for this

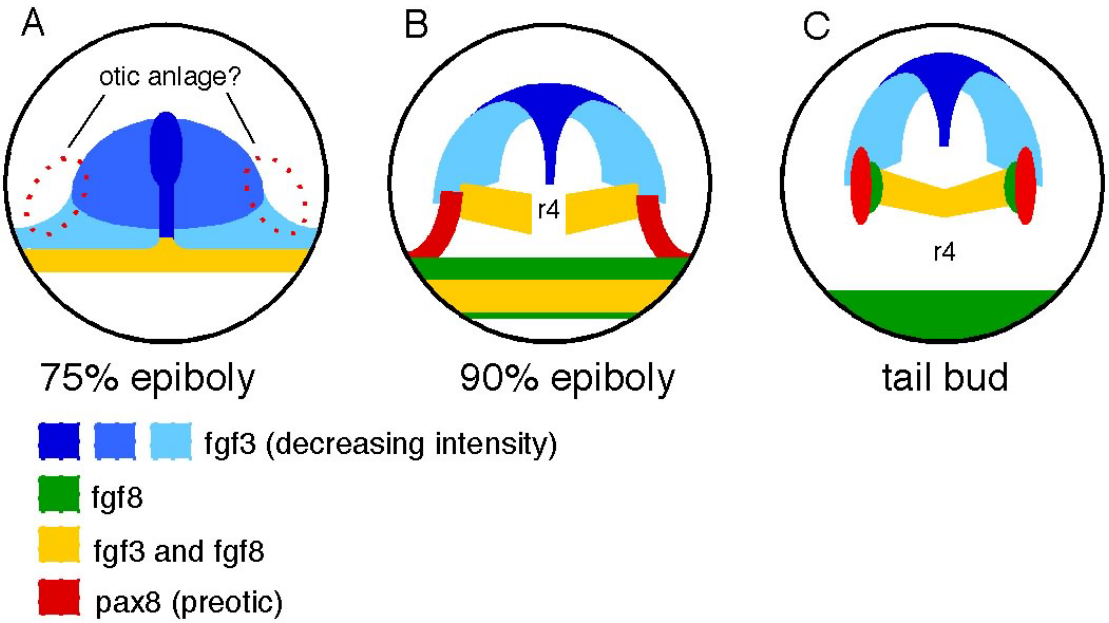

Figure 12. Summary and model of otic placode induction. (A-C) Schematic representations of gastrula stage embryos showing expression patterns of *fgf3*, *fgf8* and *pax8* as viewed from the dorsal surface. For simplicity, *pax8* expression in the pronephros is excluded. (A) At 75% epiboly, the precise location of preotic tissue is unknown, as *pax8* is not yet expressed. The dashed circles show a likely region, which was inferred by proximity to the *fgf3* expression domain and the known location of *pax8* expression one hour later. *fgf3* is heavily expressed in axial mesoderm and the germring, and at lower levels throughout the head region. *fgf8* expression is limited to the germring at this time. (B) At 90% epiboly, *pax8* expression is first detected in the preotic domain, which is in intimate contact with several regions of *fgf3* expression (paraxial cephalic mesoderm – in light blue, r4, and germring) and *fgf8* expression (r4 and germ ring). (C) At the tailbud stage, fgf8 expression in r4 directly apposes the otic domain of *pax8* expression. Nearby regions of *fgf3* expression include paraxial cephalic mesoderm (light blue) and r4.

difference is that, while the ace mutation is a null allele (Reifers et al., 1998), residual fgf3 function persists in embryos injected with fgf3-MO (Nasevicius and Ekker, 2000). It is also possible that the greater severity of the *ace* phenotype reflects the more intimate contact between the lateral hindbrain domain of *fgf8* expression and the otic anlagen (Figs. 7 and 12). Such proximity suggests that the periotic concentration of fgf8 could be greater than that of fgf3. Thus, loss of fgf8 could cause a greater deficit in signal transduction.

Although the functions of fgf3 and fgf8 are at least partially redundant (i.e. affect a common developmental pathway), it is likely that they also have distinct effects on signal transduction in responding cells. For example, fgf3 and fgf8 vary in their affinities for different receptors (Ornitz et al., 1996), and activation of different receptor isoforms can modify the nature of the signaling response (Prudovsky et al., 1996). Specifically, various receptor-ligand interactions can differentially affect cell division vs. cytodifferentiation. In addition, interactions with heparan sulfate proteoglycans with different glycosylation patterns can strongly modulate the specificity of ligand-receptor binding (Mathieu et al., 1995; Kan et al., 1999), as well as the level of signaling and the nature of the response (Amalric et al., 1994; Guimond and Turnbull, 1999; Chang et al., 2000). Currently, little is known about which receptors mediate otic induction, or how distinct FGF signaling events are integrated. However, otic induction does appear to show some ligand specificity. In contrast to the otic inducing activity of FGF3, FGF2 alone is not sufficient to induce ectopic otic placodes in chick or zebrafish (Woo and Fraser, 1997; Vendrell et al. 2000). Exogenous FGF2 was shown in one study

(Lombardo and Slack, 1998) to induce ectopic otic vesicles in *Xenopus*, but in this case the ligand was applied using FGF2-soaked heparin beads. Because the heparin could have potentiated or modified the response to the FGF2, it is possible that this treatment mimicked the activity of FGF3.

In addition to their roles in otic induction, FGF3, FGF8, and other FGF homologs cooperate to regulate later stages of otic development. *FGF8* is expressed in a region of the otic vesicle that gives rise to the vestibulo-acoustic ganglion (Hidalgo-Sanchez et al., 2000). In zebrafish *ace* mutants, the vestibulo-acoustic ganglion fails to express a regional marker, *Nkx5-1* (Adamska et al., 2000), indicating that differentiation is aberrant. *FGF3* is expressed by hair cells and support cells within the sensory patches in the otic vesicle (Wilkinson et al., 1989). Targeted disruption of *FGF3* does not prevent formation of the sensory patches (Mansour et al, 1993), possibly because *FGF10* is co-expressed in this region and might provide a redundant function there (Pirvola et al., 2000). Alternatively, expression of *FGF3* and *FGF10* might not be required for formation of the sensory patches but might facilitate morphogenesis of adjacent non-sensory structures. Both ligands strongly activate FGFR2(IIIb), a receptor isoform that is expressed in a pattern complementary to the ligands. Disruption of either *FGF3* or *FGFR2(IIIb)* leads to malformations of the semicircular canals and endolymphatic duct.

Response to otic inducing signals

Competence to respond to otic inducing signals is initially broadly distributed throughout head ectoderm but becomes increasingly restricted to the otic region as development proceeds (Yntema, 1933, 1950; Gallagher et al., 1996; Groves and

Bronner-Fraser, 2000). Presumably, reduction of the domain of otic competence involves differentiation of non-otic cells to form other cell types refractory to otic inducing signals. At the same time, prospective otic ectoderm is increasingly biased towards otic fate due to prolonged exposure to otic inducing signals. At 50% epiboly, cells fated to participate in otic development are located in the ventro-lateral blastoderm near the animal pole, far from potential sources of otic inducing signals (Kozlowski et al., 1997). Subsequent morphogenetic movements quickly bring these cells into range of marginal and axial signals. *fgf3* and *fgf8* are already expressed in the germring by the shield stage and are later induced and maintained in axial and paraxial tissues in close proximity to the prospective inner ear. FGF signaling could therefore provide continuous reinforcement of otic specification and differentiation from the shield stage to well after the close of gastrulation.

Induction of *pax8* is the earliest known manifestation of otic differentiation and is soon followed by expression of *dlx3* and *pax2.1* during early somitogenesis (Krauss et al., 1991; Ekker et al., 1992; Pfeffer et al., 1998; Heller and Brandli, 1999). It is unlikely that expression of any single early marker is sufficient to determine otic cell fate. Chick embryos also begin to express *Pax2* in pre-placode cells during early somitogenesis, yet these cells are often unable to form otic vesicles when transplanted to an ectopic location, even though they are able to maintain *Pax2* expression (Groves et al., 2000). Whether any of these early marker genes are required for placode formation remains an open question. Disruption of *Pax2* in mouse or *pax2.1* in zebrafish does not prevent placode formation, but does perturb subsequent development of the otic vesicle (Torres

et al., 1996; Riley et al., 1999). It is possible that subtle changes in early development of the placode contribute to later defects in the otic vesicle. In addition, multiple *pax* genes are coexpressed in the otic placode (Pfeffer et al., 1998; Heller and Brandli, 1999), raising the possibility that these genes provide multiple levels of redundancy.

Integration of multiple signaling events

Our loss of function data complement the gain of function data recently reported for FGF19 and Wnt-8c in the chick (Ladher et al. 2000a). It is likely that all of these factors interact in a complex network that serves to induce, maintain, and properly pattern otic tissue. In zebrafish, chick, and mouse, these factors are initially expressed in the primitive streak/germring of the gastrula and are subsequently found in head mesenchyme and/or hindbrain adjacent to the future otic tissue (Wilkinson et al., 1988; Hume and Dodd, 1993; Kelly et al., 1995; Bouillet et al., 1996; Mahmood, 1996; Fürthauer et al., 1997). Thus, this complex signaling milieu is maintained in periotic tissues for a protracted period despite the dramatic cell rearrangements that typify gastrulation. Assessing the interactions between, and relative roles of, each of these otic inducing factors remains an important task.

Several studies in zebrafish suggest that additional factors that influence otic development are expressed by the germring but not the hindbrain. For example, grafts of hindbrain can induce ventral epiblast near the germring to form ectopic otic vesicles, but hindbrain tissue is not sufficient to respecify prospective forebrain tissue to an otic fate. This does not reflect a lack of competence in the forebrain region since grafts of germring can induce cells in the prospective forebrain to form an ectopic hindbrain plus

associated otic vesicles. These data suggest that the germring modifies or potentiates otic inducing signals from the hindbrain.

A candidate for a relevant germring-derived factor is RA. Exogenous RA causes anteriorward expansion of posterior fates, including the domains of *fgf3*, *fgf8*, and*wnt8*, and also leads to formation of excess otic tissue (Papalopulu et al., 1991; Marshall et al., 1993; Simeone et al., 1995; Alexandre et al., 1996; Bouillet et al., 1996; Fig. 11). The observed expansion of otic tissue is mediated, in part, by FGF signaling since disruption of fgf3 and/or fgf8 blocks the stimulatory effects of RA (Fig. 11). In contrast to the effects of exogenous RA, absolute deficiency of RA reduces or eliminates posterior fates and causes corresponding deficiencies of otic tissue (Maden et al., 1996; Niederreither et al., 2000; White et al., 2000). Interestingly, moderate RA deficiency can lead to formation of small ectopic otic vesicles in more posterior positions, which may reflect expansion of r4-specific gene expression into the caudal hindbrain (White et al., 2000). These results could be interpreted to mean that RA acts indirectly on otic development by inducing or reinforcing FGF and Wnt signaling centers in the mesoderm and hindbrain. However, it is also possible that RA acts directly on differentiation of prospective otic tissue, perhaps by increasing the competence to respond to otic inducing signals. Further investigation of the roles of specific tissues in mediating otic induction, as well as better characterization of responses to FGF, Wnt, and RA, will help to resolve these issues.

CHAPTER III

A DIRECT ROLE FOR FGF BUT NOT WNT IN OTIC PLACODE INDUCTION*

OVERVIEW

This chapter is a published account of the epistatic relationship between Fgf and Wnt signaling (Phillips et al., 2004). The relative roles of these two signaling pathways are assessed by gain- and loss-of-function experiments. E.M. Storch is a colleague who aided in the misexpression experiments shown in Figure 15, while A.C. Lekven contributed helpful discussions, reagents and laboratory space.

SUMMARY

Induction of the otic placode, which gives rise to all tissues comprising the inner ear, is a fundamental aspect of vertebrate development. A number of studies suggest that Fgf, especially Fgf3, is necessary and sufficient for otic induction. However, an alternative model proposes that Fgf must cooperate with Wnt8 to induce otic differentiation (Ladher et al., 2000a). Using a genetic approach in zebrafish, we have tested the relative roles of Fgf3, Fgf8 and Wnt8. We demonstrate that localized misexpression of Fgf3 or Fgf8 is sufficient to induce ectopic otic placodes and vesicles even in embryos lacking Wnt8. Wnt8 is expressed in the hindbrain around the time of otic induction, but loss of Wnt8 merely delays expression of preotic markers and otic

---

*Reprinted from *Development*, Vol. 131, Phillips et al., A direct role for Fgf but not Wnt in otic placode induction, pp 923-931, Copyright (2004), with permission from the Company of Biologists Ltd.

vesicles eventually form. The delay in otic induction correlates closely with delayed expression of *fgf3* and *fgf8* in the hindbrain. Localized misexpression of Wnt8 is not sufficient to induce ectopic otic tissue. In contrast, global misexpression of Wnt8 causes development of supernumerary placodes/vesicles, but this reflects posteriorization of the neural plate and consequent expansion of the hindbrain expression domains of Fgf3 and Fgf8. Embryos that globally misexpress Wnt8 but are depleted for Fgf3 and Fgf8 produce no otic tissue. Finally, cells in the preotic ectoderm express Fgf (but not Wnt) reporter genes. Thus, preotic cells respond directly to Fgf but not Wnt8. We propose that Wnt8 serves to regulate timely expression of Fgf3 and Fgf8 in the hindbrain, and Fgf from the hindbrain then acts directly on preplacodal cells to induce otic differentiation.

INTRODUCTION

General mechanisms of neural development are broadly conserved amongst metazoans, yet components of a number of sensory organs in vertebrates are derived from evolutionarily unique structures known as cranial placodes. The inner ear in particular is remarkable in that virtually the entire organ system and the neurons that innervate it are derived from a single rudiment, the otic placode (reviewed in Baker and Bronner-Fraser, 2001; Whitfield et al, 2002; Riley and Phillips, 2003). Because the otic placode is readily accessible and undergoes such a complex morphogenesis, induction and development of the otic placode has long been a popular subject of experimental embryology studies. Considerable study has shown that even the initial steps in otic induction are highly complex. Naive ectoderm is induced to form the otic placodes

through a series of interactions with surrounding tissues during the latter half of gastrulation. The molecular players involved in otic induction have only recently begun to come to light.

A number of studies now point to members of the fibroblast growth factor (Fgf) family of peptide ligands as the best candidates for otic-inducing factors produced by periotic tissues. Fgf3 in particular appears to play a highly conserved role in otic induction. In all vertebrates examined to date, Fgf3 is expressed in the hindbrain directly between the developing otic anlage during mid-late gastrulation (Wilkinson et al., 1989; Mahmood et al., 1995, 1996; McKay et al. 1996; Lombardo et al., 1998; Philips et al., 2001), and misexpression studies in chick and *Xenopus* show that Fgf3 can induce formation of otic placodes in ectopic locations (Vendrell et al. 2000, Lombardo et al., 1998). Loss of Fgf3 function does not prevent otic induction in mouse or zebrafish, although later otic development is clearly impaired (Mansour et al., 1993; Phillips et al., 2001; Maroon et al., 2002; Leger and Brand, 2002; Kwak et al., 2003). The reason for continued otic induction is that other Fgf homologs provide redundancy in the inductive pathway. In zebrafish, *fgf8* is coexpressed with *fgf3* in the hindbrain, and loss of both functions leads to complete failure of otic induction (Phillips et al., 2001; Maroon et al., 2002; Leger and Brand, 2002; Liu et al., 2003). Fgf8 does not play a comparable role in tetrapods, although it is likely to regulate later stages of otic development (Reviewed by Riley and Phillips, 2003). Instead, other Fgfs provide redundancy. In the mouse, *Fgf10* is expressed in mesoderm just beneath the preplacode, and loss of both Fgf3 and Fgf10 totally ablates otic development (Wright and Mansour, 2003). The above studies do not

exclude a role for other inductive signals, but taken together they suggest that Fgf signaling is both necessary and sufficient for otic induction.

In contrast, an alternative model was recently proposed in which Fgf must cooperate with another factor, Wnt8, to induce the otic placode (Ladher et al., 2000a). In chick, *Fgf19* is initially expressed in subjacent mesoderm and is later found in hindbrain between prospective otic placodes. By itself, Fgf19 does not induce expression of any otic markers in explants of uncommitted ectoderm, but it does induce expression of the hindbrain factor Wnt8c, the chick ortholog of Wnt8 (Schubert et al, 2000). Exogenous Wnt8c weakly induces a subset of otic markers in explant cultures, whereas Fgf19 plus Wnt8 strongly induce a full range of otic markers. Thus, it was proposed that Fgf19 in the mesoderm induces expression of Wnt8c in the hindbrain, and then the two factors synergyze to induce the otic placodes. This model has not been previously tested in vivo. In addition, a complication of the model is that Wnt8c and Fgf19 also strongly induce expression of Fgf3, which may have played a direct role in inducing the full range of otic markers. Since FGF19 has no known ortholog in zebrafish, we addressed the question of whether known zebrafish otic inducers, Fgf3 and Fgf8, are sufficient to induce otic tissue or must cooperate with Wnt8. Our data demonstrate that Fgf signaling is both necessary and sufficient for otic induction while Wnt8 is neither necessary nor sufficient. Expression of Fgf and Wnt reporter genes suggest that Fgf, but not Wnt, signals directly to the otic anlage. Instead, Wnt8 appears to be indirectly involved in otic induction by virtue of its requirement for timely hindbrain expression of Fgf genes.

MATERIALS AND METHODS

Strains and developmental conditions

The wild-type strain was derived from the AB line (Eugene, OR). The *Dfw8* mutation was induced by γ irradiation (Lekven et al., 2000; Lekven *et al.*, 2001). Embryos were developed in an incubator at 28.5°C in water containing 0.008% Instant Ocean salts.

In situ hybridization

Embryos were fixed in MEMFA (0.1 M MOPS at pH 7.4, 2 mM EGTA, 1 mM $MgSO_4$, 3.7% formaldehyde). In situ hybridizations (Stachel et al., 1993) were performed at 67°C using probes for *pax2.1* (Krauss *et al*., 1991), *fgf8* (Reifers *et a*l., 1998), *pax8* (Pfeffer *et al*., 1998), *TOPdGFP* (Dorsky *et al.,* 2002), *erm* (Roehl and Nusslein-Volhard, 2001; Raible and Brand, 2001), *wnt8* ORF2 (Lekven *et al.*, 2001), *foxi1*(Solomon *et al.,* 2003), and *krox-20* (Oxtoby and Jowett, 1993) transcripts. The *fgf3* construct was generated by amplifying the coding sequence of *fgf3* (accession number NM 131291) and ligating it into the ClaI and EcoRI sites of pCS2+. Two-color in situ hybridization was performed essentially as described by Jowett (1996), with several modifications. RNase inhibitor (Promega 100 units/ml) was added during antibody incubation steps to help stabilize mRNA. Fast Red (Roche) was used in the first alkaline phosphatase reaction to give red color and fluorescence. Afterward, alkaline phosphatase from the first color reaction was inactivated by incubating embryos in a 4% formaldehyde solution for 2h at room temperature and then heating for 10 minutes at 37°C. NBT-BCIP (Roche) was used for the second alkaline phosphatase reaction to give

blue color. For sectioning, embryos were embedded in Immunobed resin (Polysciences No. 17324) and cut into 4 μm sections.

Morpholino oligomer injections

Morpholino oligomers obtained from Gene Tools Inc. were diluted in Danieaux solution (58 mM NaCl, 0.7 mM KCl, 0.4 mM $MgSO_4$, 0.6 mM $Ca(NO_3)_2$, 5.0 mM N-[2-Hydroxyethyl] piperazine-N'-[2-ethanesulfonic acid] (HEPES) pH 7.6) to concentrations of 2.5 μg/μl *fgf3*-MO, 2.5 μg/μl *fgf8*-MO, 1.25 μg/μl *wnt8* ORF1-MO, 1.25 μg/μl *wnt8* ORF2-MO. Filtered green food coloring was added to a concentration of 3% to visualize fluid during injections. Approximately 1-5 nl was injected into the yolk of 1- to 2-cell stage embryos. Embryos were injected and maintained in Holtfreter's solution (60 mM NaCl, 0.6 mM KCl, 0.9 mM $CaCl_2$, 5 mM HEPES pH 7.4) with 50 units/ml penicillin and 50 ug/ml streptomycin. Morpholino used were: *fgf3*-MO (Phillips et al., 2001); *fgf8*-MO (Furthauer et al., 2001); *wnt8* ORF1-MO and *wnt8* ORF*2*-MO (Lekven et al, 2001).

Misexpression

To misexpress Fgfs, we tried several approaches in which mRNA and DNA at concentrations ranging from 10-100 ng/μl were injected into embryos between 1- and 16-cell stages. Two methods were used to achieve mosaic misexpression of Fgf mRNA: injection at 1-cell stage followed by blastomere transplantation into uninjected hosts, or injection between 4- and 16-cell stages. Both methods resulted in embryos that were too severely dorsalized to study otic development. As an alternative, pCS2+ plasmid DNA containing a constitutive cytomegalovirus promoter upstream of the coding sequence of

interest was injected between 1- and 16-cell stages. The method that resulted in the greatest frequency of ectopic otic tissue was 8-cell injection of *fgf* plasmid at a concentration of 30 ng/µl. Mosaic misexpression of Wnt8 was achieved by 8-cell injection of 30-40 ng/µl of ORF1 or ORF2 plasmid. Global misexpression of Wnt8 was achieved by 1-cell injection of 80 ng/µl ORF1 or ORF2 plasmid. Global misexpression of Dkk1 was accomplished by 1-cell injection of 40 or 80 ng/µl plasmid. In all cases, injection volume was 1-5 nl. Filtered green food coloring was added to a concentration of 3% to visualize fluid during injections.

RESULTS

Wnt8 is not required for otic induction

In zebrafish, Wnt8 is the closest ortholog of chick Wnt8c (Schubert et al., 2000). The zebrafish *wnt8* locus encodes a bicistronic message consisting of two complete open reading frames, ORF1 and ORF2, which encode distinct, but highly homologous ligands. Both open reading frames are expressed at 50% epiboly in the ventral and lateral marginal zone (Kelly et al., 1995; Lekven et al., 2001). At 75% epiboly (8 hours post fertilization, hpf) ORF2 transcripts can be detected in rhombomeres 5 and 6 (r5/6), immediately adjacent to the otic placode anlagen, and persist until at least the 6 somite stage. To test the possibility that preotic cells require Wnt8, we examined otic development in embryos injected with morpholinos directed against ORF1 and/or ORF2. Knockdown of ORF1 alone causes mild dorsalization but results in no apparent otic defects (not shown). In contrast, the ORF2-MO injected embryos consistently produce small otic vesicles shortened by roughly 50% (not shown). To ensure more complete

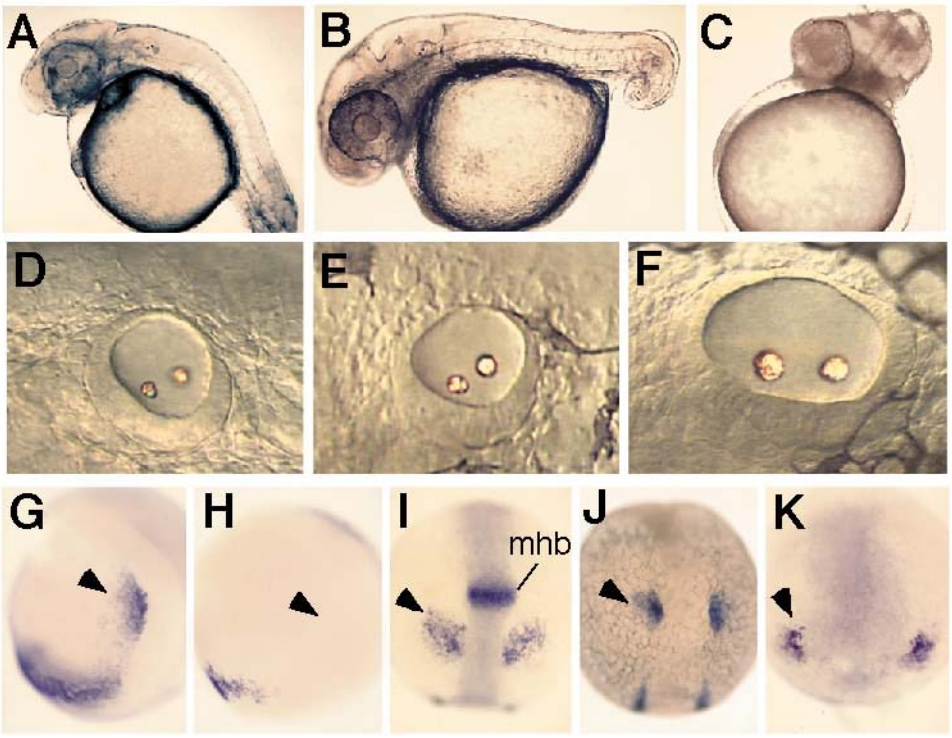

Figure 13. Effects of disrupting Wnt8 function. (A-F) Lateral views of live embryos at 30 hpf. (A) *wnt8* morphant, (B) moderately affected *dkk1*-injected wild-type embryo and, (C) severely affected *dkk1*-injected wild-type embryo lacking hindbrain and otic tissue. Enlarged view otic vesicles of (D) *wnt8* morphant, (E) moderately affected *dkk1*-injected wild-type embryo and (F) wild-type embryo. (G and H) lateral views of *pax8* expression at tailbud stage in a (G) wild-type embryo and (H) *wnt8* morphant lacking the otic domain. (I-K) dorsal views of *pax8* expression at 6-somite stage in a (I) wild-type embryo, (J) severely affected *dkk1*-injected embryo and (K) *Dfw8* homozygote. Arrowhead indicates preotic region. Abbreviation: mhb, midbrain-hindbrain border. (A-F) Anterior is to the left and dorsal upward. (G and H) Lateral views with anterior upward. (I-K) Dorsal views with anterior upward. Scale bar, 150 µm (A-C), 30 µm (D-F), 200 µm (G-K).

loss of Wnt8 function, embryos were coinjected with ORF1-MO and ORF2-MO (hereafter termed *wnt8* morphants). Ear development was impaired to roughly the same degree as in embryos injected with ORF2-MO alone (Fig. 13A, D). Despite the small size of these otic vesicles, they always contained anterior and posterior sensory maculae and associated otoliths, suggesting that key aspects of morphogenesis and differentiation occur normally. To ascertain whether the observed ear defects were caused by faulty otic induction, we examined the expression of the preotic marker, *pax8*. Preotic expression of *pax8* begins by 90% epiboly (9 hpf) in wild-type embryos (Pfeffer et al., 1998, Phillips et al., 2001), but is still not evident at tailbud stage (10 hpf) in *wnt8* morphants (Fig 13 G,H). Similarly, preotic *pax8* is also not observed at tailbud stage in embryos homozygous for a chromosomal deficiency, *Df(LG14)wnt8*^{w8} (hereafter termed *Dfw8*), which deletes both *wnt8* open reading frames (Lekven et al., 2001 and data not shown). However, *pax8* is eventually expressed in the preotic domain in both *Dfw8* mutants and *wnt8* morphants by the 6 somite stage (12 hpf), 2 hours later than normal (Fig. 13K and not shown). This demonstrates that Wnt8 is not necessary for otic induction per se, but is required for timely initiation of the otic field.

To address the possibility that another, as yet unknown, Wnt protein partially compensates for the loss of Wnt8, we misexpressed the Wnt antagonist Dickkopf-1 (Dkk-1). Zebrafish Dkk-1 is a homologue of *Xenopus* Dkk-1, which has been shown to be a potent extracellular antagonist of Wnt activity in vivo (Glinka, et al., 1998; Hashimoto, et al. 2000). 165/239 (69%) of *dkk1* plasmid injected embryos displayed a dorsalized and anteriorized phenotype characterized by severe truncation of posterior

tissues similar to *wnt8* morphants (Fig 13A,B). These *dkk1*-injected embryos possessed otic vesicles. The remainder (74/239, 31%) exhibited a more severe loss of posterior structures, including hindbrain, than was observed for *wnt8* morphants (Fig 13C). These severe embryos did not appear to possess otic vesicles. However, analysis of *pax8* expression at 6-somite stage (12 hpf) showed that otic induction had occurred in all (21/21) *dkk-1* injected embryos (Fig 13J). These data demonstrate that placode induction can occur despite globally compromised Wnt function.

Wnt8 regulates timely expression of *fgf3* and *fgf8* in the hindbrain

To clarify whether the delay in otic induction observed in Wnt8 loss of function embryos was due to indirect effects, we examined expression of previously identified otic inducers, Fgf3 and Fgf8, in embryos lacking Wnt8 function. *fgf3* is normally expressed in r4 by 90% epiboly (9 hpf). However, the hindbrain domain of *fgf3* was barely visible at tailbud stage (10 hfp) in over half (71/128) of *wnt8* morphants and is undetectable at this stage in *Dfw8* mutants (Fig 14B,C). Strong r4 expression of *fgf3* becomes evident by the 6 somite stage (12 hpf) in *Dfw8* homozygotes (Fig. 14D). The hindbrain domain of *fgf8* becomes evident by 75% epiboly (8 hpf) in wild-type embryos but was only weakly expressed in most (61/81) *wnt8* morphants even as late as 90% epiboly (9 hpf). Furthermore, 10% of *wnt8* morphants still had reduced expression at tailbud stage (10 hpf, Fig. 14F). Expression of *fgf8* is also delayed in *Dfw8* homozygotes, in which expression cannot be detected in the hindbrain until tailbud stage (10 hpf, Fig. 14G). *Dfw8* mutants and *wnt8* morphants show strong *fgf8* expression by the 6 somite stage (12 hpf, Fig. 14H and data not shown). This indicates that Wnt8 is

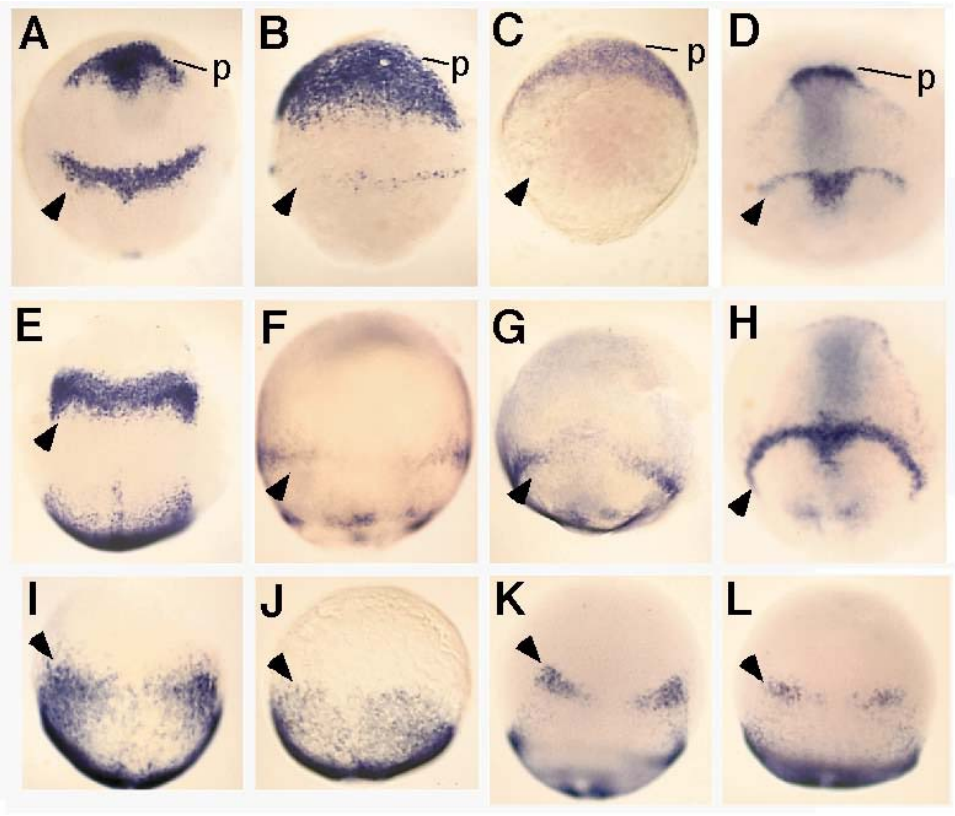

Figure 14. Cross regulation of Wnt8 and Fgf. (A-D) *fgf3* expression in the hindbrains of (A) tailbud stage wild-type embryo, (B) tailbud stage *wnt8* morphant, (C) tailbud stage *Dfw8* homozygote, and (D) 6-somite stage *Dfw8* homozygote. (E-H) *fgf8* expression in the hindbrains of (E) tailbud stage wild-type embryo, (F) tailbud stage *wnt8* morphant, (G) tailbud stage *Dfw8* homozygote, and (H) 6-somite stage *Dfw8* homozygote. (I-K) *wnt8* ORF2 expression in the hindbrains of a (I) wild-type embryo at 90% epiboly, (J) wild-type embryo injected with *fgf3*- and *fgf8*-MOs at 90% epiboly, (K) wild-type embryo at tailbud stage and, (L) tailbud stage wild-type embryo injected with *fgf3*- and *fgf8*-MOs. Arrowheads indicate hindbrain domain. p, prechordal plate. Dorsal views with anterior upward. Scale bar = 200 µm.

necessary for timely expression of both *fgf3* and *fgf8* in the hindbrain. The delay in Fgf expression correlates well with the delay in otic induction and suggests that the otic defects observed in these embryos may be an indirect effect resulting from a deficiency in Fgf signaling. The possibility remains, however, that Wnt signaling regulates later aspects of otic development (see Discussion).

Fgf signaling regulates *wnt8* in the hindbrain

To more fully understand the epistatic relationship between Wnt and Fgf signaling, we examined *wnt8* expression in embryos knocked down for Fgf3 and Fgf8. Expression of ORF2 in the r5/6 domain normally begins by 75% epiboly (8 hpf) but did not begin until 90% epiboly (9 hpf) in embryos depleted for Fgf3 and Fgf8 (Fig. 14J). ORF2 continued to be expressed at lower than normal levels in the r5/6 domain through tailbud stage (10 hpf, Fig 14L). The *wnt8* germring domain appeared unaffected, however. The finding that Fgf and Wnt positively regulate each other is reminiscent to the model proposed by Ladher et al. (2000a), in which chick Fgf19 is proposed to induce expression of *Wnt8c* and Wnt8c induces expression of *Fgf3* (see Discussion).

Misexpression of Fgf3 or Fgf8 induces ectopic otic tissue

Although loss-of-function studies indicate that Fgf3 and Fgf8 but not Wnt8 are necessary for otic induction, we sought to test whether any of these factors are sufficient for otic induction. To misexpress Fgf3 or Fgf8, we injected at various stages either synthetic RNA or plasmid DNA containing Fgf cDNA under the control of a constitutive promoter. We find that embryos are extremely sensitive to Fgf misexpression since both

Figure 15. Effects of Fgf misexpression. (A and B) Two-color in situ hybridization of 3-somite stage. (A) wild-type and (B) *fgf3* plasmid-injected embryos showing *pax8* expression (blue) and *krox-20* expression (red). The left preotic domain is significantly enlarged and a region with ectopic upregulation of *pax8* (arrowhead) is evident. (C and D) Two color *in situ* hybridization of 3-somite stage embryo injected with *fgf3* plasmid showing *fgf3* expression (blue) and *pax8* expression (red). (C) Brightfield and (D) fluorescent images showing relationship between ectopic *fgf3*-expressing cells (arrow) and ectopic *pax8*-expressing cells (arrowhead). The area boxed in C is enlarged in D. The endogenous preotic domain on the left is enlarged in the vicinity of misexpressed *fgf3*. The r4 domain of *fgf3* is faintly visible in C. (E and F) *foxi1* expression at 3-somite stage in (E) wild-type and (F) *fgf8* plasmid-injected embryo. Ectopic expression in anterior region of the injected embryo is indicated (arrowhead). (G) Ectopic *pax2.1* expression (arrowhead) adjacent to the midbrain of a 4-somite stage embryo injected with *fgf3*-plasmid. (H) Low magnication view of a 30 hpf wild-type embryo injected with *fgf8*-plasmid showing that overall axial development is essentially normal, although development of anterior sensory structures is perturbed. (I) Higher magnification of the same embryo shown in H. Ectopic otic vesicles are indicated (arrowheads). Development of adjacent eye tissue is perturbed, but general features of brain development, such as the epiphysis (e) and midbrain-hindbrain boundary (mhb) are produced. (J) Frontal/lateral view of an embryo injected with *fgf3*-plasmid. An ectopic otic vesicle is indicated (arrowhead). Development of adjacent nasal and eye tissue is severely perturbed. (K) Lateral view of a *wnt8* morphant injected with *fgf8*-plasmid. Ectopic otic vesicles (arrowheads) are seen next to the midbrain-hindbrain boundary (mhb). Abbreviations: mhb, midbrain-hindbrain border; r3, rhombomere 3; r4, rhombomere 4; r5, rhombomere 5; op, endogenous otic placode; e, epiphysis. (A-E,G) Dorsal view with anterior upward. (F) Dorsal-anterior view. (H,I and K) Lateral views with anterior to the left. (J) Frontal-lateral view with anterior to the left. Scale bar, 150 μm (A-C, E-G), 175 μm (H), 75 μm (I-K).

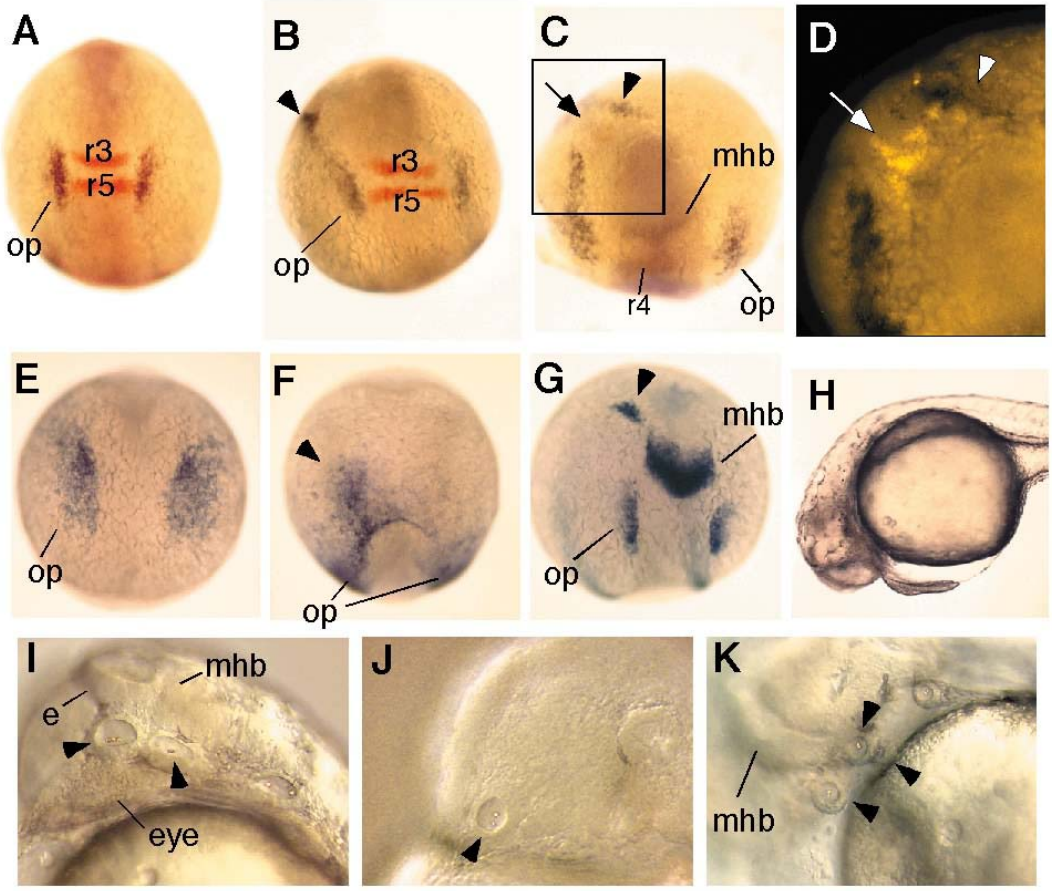

mRNA and early stage plasmid injection lead to severe dorsalization and expansion of the neural plate at the expense of epidermal and preplacodal ectoderm (data not shown). This most likely reflects an early function of Fgf signaling in dorsal/ventral patterning (Fürthauer et al., 1997; Koshida et al., 2002). However, injection of plasmid into wild-type embryos at the 8-cell stage results in belated, mosaic Fgf expression. With this technique, some embryos still exhibit moderate dorsalization, but by co-staining injected embryos for neural marker and Fgf expression, we determined that the majority had only

small, scattered patches of expressing cells and did not show overt signs of dorsalization. Of the non-dorsalized class, 26% (30/118) of Fgf3 misexpressing embryos and 15% (14/94) of Fgf8 misexpressing embryos showed ectopic patches of *pax8* expression and/or significant expansion of the endogenous preotic domain. Such expression did not result from expansion of the otic-inducing portion of the hindbrain since *krox-20* expression was normal (Fig. 15B). Instead, sites of ectopic *pax8* correlated with sites of Fgf3 or Fgf8 misexpression (Fig. 15C,D; and data not shown). Furthermore, Fgf misexpression was able to induce ectopic domains of expression of *foxi1*, which encodes an upstream regulator of *pax8* (Solomon et al., 2003; Fig. 15F). Fgf misexpression also led to ectopic or expanded expression of later preotic markers *pax2a* and *dlx3b* (Fig. 15G and data not shown). When allowed to develop further, 9% (17/196 non-dorsalized) of embryos injected with *fgf3* plasmid and 8% (37/464 non-dorsalized) of embryos injected with *fgf8* plasmid displayed ectopic vesicles containing differentiated sensory patches and associated otoliths (Fig. 15H-J, Table 1). Formation of ectopic vesicles was limited to the periphery of the anterior neural plate, although during earlier developmental stages isolated *pax8* expressing cells were occasionally observed elsewhere, including the neural plate (not shown). Importantly, coinjection of *fgf8* and *wnt8* plasmids did not significantly increase the number of embryos displaying ectopic vesicles, indicating that Wnt8 does not augment Fgf's ability to induce otic tissue.

To address the possibility that Fgf acts by inducing ectopic Wnt8, we injected Fgf plasmid into *wnt8* morphants. 8% (5/64) of Fgf3 misexpressing and 9% (5/58) of Fgf8 misexpressing *wnt8* morphants showed ectopic patches of *pax8* expression in the

head (not shown). In another experiment, 12% (2/17) of *wnt8* morphants injected with *fgf8* plasmid produced ectopic otic vesicles (Fig. 15K). As an additional test, embryos were injected with *dkk1*-plasmid at the one-cell stage, followed by *fgf8*-plasmid at the 8-cell stage. The dorsalizing effects of *dkk1* and *fgf8* strongly potentiate each other such that severely affected embryos were more numerous when compared to *fgf8* injection alone. Hence, embryonic patterning cannot be easily interpreted in most (176/196) embryos. However, of more moderately affected embryos, 15% (3/20) formed ectopic otic vesicles (not shown). Thus, Fgf misexpression can still induce ectopic otic tissue in embryos depleted for Wnt8 or otherwise blocked in Wnt signaling activity.

Table 1. Effects of Fgf misexpression

	Morphology at 30 hpf		Expression of preotic markers	
Phenotype	*fgf3* injected	*fgf8* injected	*fgf3* injected	*fgf8* injected
Normal	75	270	132	99
Ectopic otic tissue	17 (8.7%)*	37 (8.0%)*	29 (16%)*	16 (12.8%)*
Enlarged otic tissue	n.d.	n.d.	20 (11%)*	10 (8%)*
Other head defects	104	157	N/A	N/A
Dorsalized	190	48	151	15
Total	386	512	332	140
Non-dorsalized	196	464	181	125

*percentages reflect ratio of indicated class to non-dorsalized embryos

Wnt8 cannot induce ectopic otic tissue without Fgf

To test whether mosaic misexpression of Wnt8 is sufficient to induce ectopic otic tissue, we injected *wnt8* ORF1 or ORF2 plasmid into wild-type embryos at the 8-cell stage. None of the embryos injected with ORF2-plasmid showed ectopic otic vesicles (n=50). A small fraction (5/249) of embryos injected with ORF1-plasmid produced supernumerary otic vesicles. In these few cases, embryos appeared to be severely posteriorized: They showed bilateral loss of nasal pits and eyes, and they showed no morphological development of the epiphysis or midbrain-hindbrain boundary (not shown). We infer that these are phenotypes resulting from more widespread expression of Orf1. To test the effects of increasing Wnt8 signaling, we doubled the concentration of *wnt8* plasmid and injected embryos at the 1-cell stage. Injection of ORF2-plasmid caused mild posteriorization in some embryos but had no visible effect on otic development (n=118, data not shown). In contrast, 73% (129/177) of embryos injected with ORF1-plasmid were strongly posteriorized, and these included the 5-6% (10/177) of embryos that produced supernumerary otic vesicles (Fig. 16E). Analysis at earlier stages showed that 22% (10/45) of ORF1-misexpressing embryos produced enlarged domains of *pax8* wrapping around the anterior neural plate (Fig. 16C). This correlates with expanded hindbrain domains of *fgf3, fgf8* and *erm,* a reporter of Fgf activity (Fig. 16 A,B and data not shown) reminiscent of the patterns seen in embryos posteriorized with retinoic acid (Phillips et al., 2001). When *fgf3*-MO and *fgf8*-MO were coinjected with ORF1-plasmid at the 1-cell stage, preotic expression of *pax8* was severely reduced or ablated (n=150; Fig. 16D,F). At later stages, most embryos appeared posteriorized

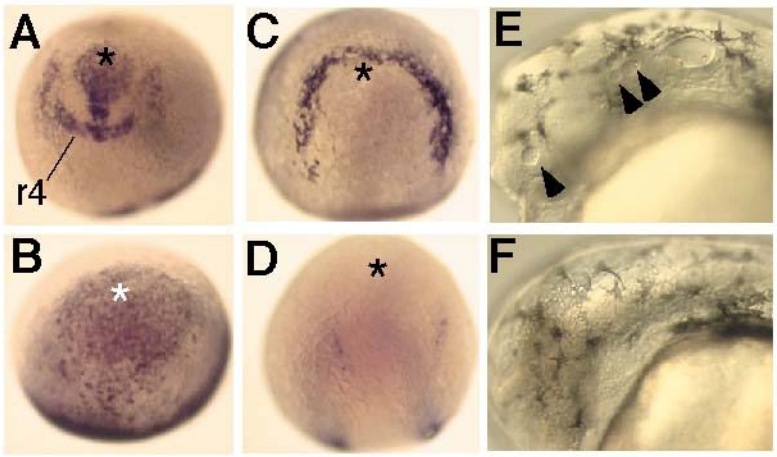

Figure 16. Effects of Wnt8 misexpression. (A-C) 3 somite stage embryos globally expressing *wnt8* ORF1 showing expression of (A) *fgf8,* (B) *erm,* and (C) *pax8*. The r4 domain of *fgf8* is indicated. The weaker anterior *fgf8* expression corresponds to midbrain-hindbrain boundary. Asterisks mark the anterior limit of the neural plate. (D) *pax8* expression in an embryo globally expressing ORF1 and coinjected with *fgf3*- and *fgf8*-MOs. Preotic expression is nearly ablated. (E) Ectopic otic vesicles (arrowheads) in a live 30 hpf embryo globally expressing ORF1. Note that anterior sensory structures and morphological landmarks in the brain such as the midbrain-hindbrain boundary and epiphysis are not produced. (F) Loss of otic tissue in a 30 hpf embryo globally expressing ORF1 and coinjected with *fgf3*- and *fgf8*-MOs. (A-D) Dorsal views with anterior upward. (E and F) Lateral views with anterior to the left. Scale bar, 200 μm (A-D), 75 μm (E-F).injected with ORF1-plasmid alone. These data indicate that Wnt8 cannot directly induce otic tissue in the absence of Fgf.

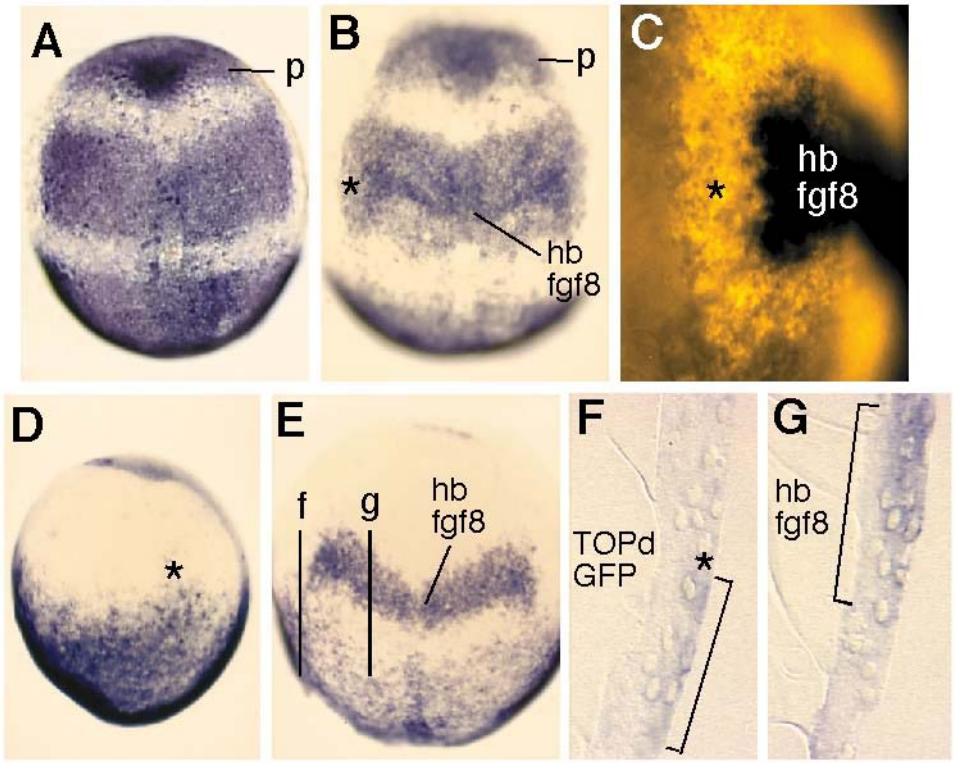

Figure 17. Expression of Fgf- and Wnt-inducible reporter genes.

All images show gene expression patterns in wild-type embryos at tailbud stage. (A) expression of *erm*. (B) costaining of *erm* and *fgf8* (darker staining). (C) two-color staining showing expression of *erm* (red) and *fgf8* (blue). (D) *TOPdGFP* expression. (E) costaining of *TOPdGFP* and *fgf8*. (F and G) parasagittal sections at the locations indicated in (E) showing. (F) *TOPdGFP* expression in a domain lateral and posterior to the hindbrain. (G) *fgf8* expression in the hindbrain. Preotic domains are indicated by asterisks. Abbreviations: p, prechordal plate; hb, hindbrain. (A,B and E) Dorsal views with anterior upward. (C) Dorsolateral view with anterior upward. (D) Lateral view with anterior upward and dorsal to the right. (F and G) Dorsal is to the right and anterior is upward. Scale bar, 150 μm (A, B, E), 40 μm (C), 175 μm (D), 25 μm (F, G).

but none produced any ectopic otic tissue (n=240). This finding was highly significant ($p < 0.0005$) when compared to the moderate level of ectopic ear formation in embryos

Fgf, but not Wnt, reporter genes are expressed in preotic cells

To determine whether Fgf signaling acts directly upon preotic cells, we examined expression of the Fgf reporter gene *erm*. Erm is a member of the ETS family of transcription factors that is expressed in response to Fgf signaling and its expression is ablated by disrupting Fgf signaling (Roehl and Nusslein-Volhard, 2001; Raible and Brand, 2001). Accordingly, *erm* is expressed in a pattern corresponding to known Fgf expression domains, including tissues surrounding the prechordal plate, the hindbrain, and the germring (Fig 17A). When visualized along with *fgf8*, which serves to mark the lateral edge of hindbrain abutting the otic anlage (Phillips et al., 2001), *erm* expression appears to encompass all or most of the preotic field (Fig. 17B,C). Thus, preotic cells respond directly to Fgf signaling.

To ascertain whether the otic anlage actively responds to Wnt signaling, we examined the expression of the Wnt reporter gene, *TOPdGFP* (Dorsky et al., 2002). This is a transgene consisting of a GFP coding sequence downstream of a minimal promoter and four Lef binding sites. Although the transgene does eventually lead to detectable levels of GFP fluorescence, wholemount in situ hybridization is a more sensitive means of detecting transgene expression during early stages of development (Dorsky et al, 2002). *TOPdGFP* is expressed in a pattern similar to that of *wnt8* (Fig 17D). Moreover, *TOPdGFP* expression is dependent upon Wnt8 function since both *wnt8* morphants and *Dfw8* homozygotes lack expression (not shown). Thus, *TOPdGFP*

expression faithfully reports Wnt8 activity during late gastrula stages. Although previously reported to be expressed only in mesendoderm during gastrulation (Dorsky et al., 2002), we find upon sectioning that *TOPdGFP* is also expressed in dorsal ectoderm (Fig. 17F). Co-staining of *TOPdGFP* with *fgf8* reveals a small group of *TOPdGFP* expressing cells lying posterior and lateral to the hindbrain domain of *fgf8* (Fig 17E-G). These cells could mark the posterior edge of the preotic domain. However, the majority of preotic cells do not express *TOPdGFP*. Thus, preotic cells may not respond directly to Wnt signaling, or if they do the level is too low to activate expression of the transgene.

DISCUSSION

We have assessed two competing models for otic induction: In one model, Fgfs expressed in the hindbrain and subjacent mesendoderm are necessary and sufficient for otic induction. In the other model, Fgf must cooperate with Wnt8 to fully induce otic development. Our data suggest that, in zebrafish, Fgf signaling is directly responsible for otic induction whereas Wnt8 acts indirectly by promoting timely expression of Fgf3 and Fgf8 in the hindbrain. As discussed below, the role of Fgf and Wnt signaling are likely to be conserved from teleosts through tetrapods.

A direct role for Fgf signaling in otic induction

Comparative studies in zebrafish, *Xenopus*, chick, and mouse suggest that Fgf, especially Fgf3, plays a broadly conserved role in otic induction. However, these model systems have historically used different experimental approaches, each of which only partially addresses the nature of Fgf function. Misexpression studies in chick and frog

show that Fgf signaling is able to induce ectopic otic tissue (Vendrell et al., 2000; Lombardo et al., 1998), but this need not reflect the normal function of the specific ligands under study. Loss-of-function studies in zebrafish and mouse confirm an essential role for Fgf3 and, in addition, show that either Fgf8 or Fgf10, respectively, play partially redundant roles in otic induction (Phillips et al., 2001; Maroon et al., 2002; Leger and Brand, 2002; Liu et al., 2003; Wright and Mansour, 2003). However, these studies did not address whether any of these ligands are sufficient for otic induction. We show here that misexpression of either Fgf3 or Fgf8 is able to induce ectopic otic tissue in zebrafish (Fig. 15), demonstrating for the first time in a single species that Fgf is both necessary and sufficient for otic induction.

While we cannot exclude the possibility that Fgf3 and Fgf8 induce expression of another hindbrain signal that is directly responsible for otic induction, this seems unlikely for several reasons. First, the Fgf reporter gene *erm* is expressed in ectoderm adjacent to the hindbrain during late gastrulation, indicating that preotic cells receive and respond to Fgf signals (Fig. 17). Furthermore, preplacodal *erm* expression is ablated in embryos depleted for Fgf3 and Fgf8 (our unpublished observations). Finally, mosaic misexpression of Fgf can induce ectopic otic development without inducing hindbrain markers such as *krox20* and *wnt8* (Fig. 15B and data not shown). The simplest interpretation for these data is that Fgf3 and Fgf8 act directly on preplacodal ectoderm to induce the otic placode.

The function of Fgf signaling is clearly context-dependent. Fgf misexpression induced ectopic otic tissue only in ectoderm immediately surrounding the anterior neural

plate. This probably corresponds to the preplacodal domain, a distinct domain of the ectoderm lying between neural and epidermal ectoderm. The preplacodal domain is marked by expression of a number of transcription factors genes, including *Six*, *Msx*, *Dlx*, and *Eya*-related homologs (Reviewed by Baker and Bonner-Fraser, 2001; Whitfield et al., 2002; Riley and Phillips, 2003). The signaling interactions that regulate these genes are not well understood, but BMP signaling from ventral tissue is required for *Msx* and *Dlx* gene expression, and signals from the organizer and/or neural plate are also required (Feledy et al., 1999; Pera et al., 1999; Beanan et al., 2000; McClarren et al., 2003). A balance of these competing axial signals may be crucial for establishing an uncommitted preplacodal region along the neural non-neural interface, which is then subdivided into different kinds of placodes by specific local cues. The hindbrain domain of Fgf3 and Fgf8 appears to constitute an essential part of the local trigger for otic development. It is interesting to note that Fgf3 and Fgf8 are also expressed in more anterior tissues, including the prechordal plate and midbrain-hindbrain boundary, yet these alternate sources do not normally trigger otic development in more anterior locations. This might reflect insufficiency in the level, timing, or duration of Fgf signaling, and the presence of other factors could modify the response to Fgf. In any case, locally augmenting Fgf signaling can overcome the restrictions on otic development in more anterior regions. It is also noteworthy that Fgf misexpression did not induce formation of ectopic otic tissue in regions posterior to the endogenous otic placodes. This might be because retinoic acid (RA), a posteriorizing agent synthesized

by posterior mesoderm, strongly modifies the response to Fgf signaling (Kudoh et al., 2002).

An indirect role for Wnt8 in otic induction

Although *wnt8* is expressed in the hindbrain by 75% epiboly – at the right time and place to influence otic induction – it is neither necessary nor sufficient for this process. Loss of all *wnt8* activity delays but does not block expression of the preotic marker *pax8* (Fig. 14). The initial delay in otic induction is likely due to a similar delay observed for expression of *fgf3* and *fgf8* in the hindbrain. Most embryos knocked down for *wnt8* ORF1 and ORF2, as well as embryos that misexpress the Wnt antagonist Dkk1, go on to produce small but well differentiated otic vesicles containing sensory maculae and associated otoliths (Fig. 13). Misexpression of *wnt8* did occasionally lead to production of supernumerary otic vesicles. However, all such embryos appeared severely posteriorized, failing to develop any anterior sensory structures, midbrain-hindbrain border or epiphysis. Analysis at earlier stages confirmed that misexpression of *wnt8* caused the hindbrain domains of *fgf3* and *fgf8* to shift almost to the anterior limit of the embryo (Fig. 17). Moreover, the lateral edges of the hindbrain domain extend forward to form a U-shaped arc of staining that is complementary to an inverse arc of preotic *pax8* that wraps around the anterior limit of the neural plate. Knockdown of *fgf3* and *fgf8* blocked preotic *pax8* expression and totally ablated formation of otic vesicles in all embryos injected with *wnt8*-plasmid. These data support the conclusion that Wnt8 acts indirectly in otic induction by influencing expression of *fgf3* and *fgf8* in the hindbrain.

Additional evidence for an indirect role for Wnt8 is that expression of *TOPdGFP*, a Wnt-inducible transgene, is not detected in preotic cells during gastrulation (Fig. 17). It should be pointed out that one limitation of this transgene is that it reports only transcriptional activation by Lef1, a mediator of the canonical Wnt pathway, but it does not reflect signaling via alternate Wnt mediators, Tcf3 and Tcf3b (Dorsky et al., 2002). Analysis of Tcf3 and Tcf3b in zebrafish suggests that these proteins normally act as transcriptional repressors that are inactivated upon Wnt signaling (Kim, 2000; Dorsky, 2003). There are as yet no genes identified that specifically report Wnt-mediated derepression of Tcf3 activity. Despite this caveat, the failure to detect *TOPdGFP* expression shows that Wnt8 signaling is not sufficient to strongly activate the Lef1-dependent pathway in preotic cells. It is also worth noting that, of the known Frizzled receptors examined in various vertebrate species, none is expressed at appreciable levels in prospective otic ectoderm during late gastrulation when otic development is initiated (Deardorf and Klein, 1999; Stark et al., 2000; Momoi et al., 2003). Expression of multiple *Frizzled* genes can be detected later within the nascent otic placode, suggesting that Wnt signaling could play a role in later stages of otic development. Indeed, *TOPdGFP* expression is first detected in prospective otic ectoderm between 12 and 13 hpf (6-8 somites), just prior to morphological formation of the otic placode (not shown). This is also consistent with the observation that, in rat, periotic accumulation of nuclear β-catenin is first detected just after formation of the otic placode (Matsuda and Keino, 2000). In addition, secreted Frizzled proteins, which are induced by Wnt signaling, are expressed in chick otic tissue only after formation of the

otic placode (Baranski et al., 2000; Ladher et al., 2000b; Esteve et al., 2000; Terry et al., 2000). While we find no evidence to support a direct role for Wnt8 in otic induction, zebrafish embryos lacking Wnt8 function produce smaller vesicles suggesting that Wnt8 signaling might stimulate proliferation in the developing otic placode. Thus, later Wnt signaling could also regulate morphogenesis or differentiation of ear tissue during post-placodal stages.

Although ORF1 and ORF2 show very close sequence homology, their functions are not identical. Knockdown of ORF1 alone has negligible effects on inner ear development whereas knockdown of ORF2 alone significantly delays otic induction and leads to production of small otic vesicles. These effects are not significantly worsened by knockdown of both ORF1 and ORF2, suggesting a more critical role for ORF2. It is possible that this reflects the proximity of the hindbrain domain of ORF2 to r4, the site of expression of both *fgf3* and *fgf8*. In contrast, misexpression of ORF2 had only mild effects and did not induce excess or ectopic otic tissue, whereas misexpression of ORF1 posteriorized the neural plate and led to production of supernumerary otic vesicles in 2-5% of embryos. This could reflect enhancement of an early posteriorizing function normally associated with the germring domain of Wnt8. It is not clear why global misexpression of ORF2 does not have similar effects, but sequence differences between the ligands could be critical for differential receptor binding.

Feedback between the Fgf and Wnt pathways

While Wnt8 is required for normal expression of *fgf3* and *fgf8* in the hindbrain, Fgf signaling is also required for proper expression of *wnt8*-ORF2 in the r5/6 domain. It

is not known whether this mutual regulation is direct or indirect, but it could reflect the activity of a positive feedback loop operating within the hindbrain. The purpose of such a feedback loop could be analogous to that of the midbrain-hindbrain boundary (MHB), wherein an anterior domain of *Wnt1* abuts a posterior domain of *Fgf8*, and the two factors cooperate to organize surrounding brain tissue (reviewed by Wurst and Bally-Cuif, 2001). Induction of both genes is under the control of a variety of upstream regulators. Both factors are required to maintain the MHB and they therefore indirectly require each other. The r4 region of the hindbrain appears to be a second signaling center that helps pattern the hindbrain. Expression of *fgf3* and *fgf8* in the r4 domain is necessary to establish the identities of rhombomeres 5 and 6 (Walshe et al., 2002; Maves et al., 2002; Wiellette and Sive, 2003). This could partly explain why Fgf signaling is required for proper expression of *wnt8* in the r5/6 region. The requirement for Wnt8 ORF2 on hindbrain patterning has not been examined, but this domain may help to establish and stabilize the r4 signaling center and thereby provide a sustained source of Fgf3 and Fgf8 required for otic induction.

Whether a similar mechanism operates in other vertebrates remains to be fully tested. In chick and mouse, *Wnt8* is expressed in a domain in the hindbrain consistent with the role proposed in our study (Hume and Dodd, 1993; Bouillet et al., 1996). The only functional analysis of this domain in amniotes is a study by Ladher and colleagues (2000a) examining the effects of Fgf19 and Wnt8c on gene expression in chick explant cultures. From that study it was proposed that Fgf19 from periotic mesendoderm induces expression of *Wnt8c* in the hindbrain, and the two factors then induce otic

development in adjacent ectoderm. However, a key observation in the study was that exogenous Wnt8c induced prospective otic ectoderm to express *Fgf3*, which was interpreted as a marker of early otic differentiation. This presents a conundrum because *Fgf3* is not expressed in the chick ear until well after formation of the otic vesicle, yet Wnt8c did not induce expression of any earlier markers of otic development. On the other hand, *Fgf3* is expressed in the chick hindbrain by the 1-somite stage (Mahmood et al. 1995), raising the possibility that induction of *Fgf3* by Wnt8c mimics an early aspect of hindbrain development. In this scenario, Wnt8c could facilitate a feedback loop that augments and maintains Fgf signaling long enough to induce otic development. Thus, the ability to induce a full range of early otic markers in cultures exposed to Fgf19 and Wnt8c might actually reflect the additive effects of exogenous Fgf19 plus newly synthesized Fgf3. More complete analysis of the relative roles of Fgf and Wnt signaling will require Wnt8 misexpression in vivo and loss-of-function studies using morpholinos in chick (Kos et al., 2003) and gene knockouts in mouse.

CHAPTER IV

FUNCTIONAL ANALYSIS OF THE ZEBRAFISH MSX FAMILY OF TRANSCRIPTION FACTORS

OVERVIEW

This chapter analyses the function of a family of transcription factors expressed in the preplacodal domain and neural tube. It represents a collaboration with Dr. A. Fritz, who mapped the *Df(LG1)msxB*^{x8} mutation, Dr. H.-J. Kwon, who performed the RT-PCR analysis in Figure 19, C. Melton, an undergraduate researcher working under my direction, and Dr. B. Riley in whose laboratory this work was completed.

SUMMARY

Metazoan development requires a proper balance of transcriptional activation and repression. The muscle segment homeobox (Msx) family represents a group of homeodomain containing proteins with repressive functions at both the transcriptional level and during protein-protein interactions. Though much is known about the function of *msx* genes later in development, potential roles for Msx function in early embryonic patterning remain unknown. Here I analyze the function of three Msx family members in zebrafish: *msxB, msxC* and *msxE.* These genes are expressed early in development in the ventral ectoderm. By the end of gastrulation they are expressed in and around the preplacodal domain and come to be maintained in the dorsal neural tube, the site of neural crest induction. Loss-of-function studies demonstrate that Msx regulates signaling interactions which refine the neural-nonneural border through inhibitory

interactions with Dlx proteins. Embryos depleted for Msx display severe developmental defects, including cell death, within the placodal, neural crest and dorsal CNS tissues.

INTRODUCTION

Cell-cell communication in metazoans elicits tissue-specific expression of transcriptional mediators. A balance of both transcriptional activators and repressors are necessary to achieve a proper target gene activity. One family of repressive transcription factors is the muscle segment homeobox (Msx) family of homeodomain containing proteins. The Msx family has been proposed to have general roles in nearly every aspect of cellular development including proliferation, specification, differentiation, and cell death (reviewed by Bendall and Abate-Shen, 2000).

All studies to date suggest a transcriptional repressing activity for Msx when binding DNA (Catron et al., 1995; Zhang et al., 1997). Studies using reporter plasmids show that the homeodomain binds DNA, while residues located near the N terminus confer the repressive abilities (Catron et al., 1993, 1995). It is also the N terminus which interacts with and represses TATA binding protein (Zhang et al., 1996). An additional conserved 12 residue motif similar to the Engrailed repressor domain is also located near the N-terminus, although the function of this domain is unclear since deletion studies demonstrate that this motif does significantly contribute to repression of target genes. Additional repressive functions can also take place through protein-protein interactions (Zhang et al., 1997). Msx functionally antagonizes Dlx proteins through interactions in the homeodomain. This interaction appears independent of DNA-binding and the Msx-Dlx complex is transcriptionally inactive (Zhang et al., 1997). Further studies using

chimeric Msx proteins also support a repressive role for Msx. Expressing a form of Msx1 where the N terminus has been replaced with an Even-skipped repressor domain gives similar phenotypes as overexpression of wild-type Msx1 in *Xenopus* (Yamamoto et al., 2000). The Msx1 overexpression phenotype can be reversed by injection of a VP-16 activator domain fused to the Msx1 homeodomain (Yamamoto et al., 2000; Ishimura et al., 2000). This again indicates that the normal function of Msx is repressive in nature and that the VP-16 fusion may serve as a dominant negative protein.

Studies of Msx function in various systems have shown that Msx expression may be under the control of early axial signaling pathways, namely BMP and Wnt. Recent data indicate that the Wnt pathway effector β-catenin can activate murine *msx2* expression via two Lef/TCF binding sites, while two binding sites for the BMP mediator Smad4 can also activate *msx2* expression (Hussein et al., 2003). Loss of function studies in zebrafish and *Xenopus* indicate that Msx genes respond to intermediate levels of BMP (Tribulo et al., 2003). Consistent with this, Msx genes are expressed ventrally during gastrulation. Msx appears able to mediate the ventralizing activity of BMP, in both in mesoderm and ectoderm. Overexpression of *Xenopus* Msx1 in mesodermal tissues expands somitic mesoderm at the expense notochord (Maeda et al., 1997), while in the ectoderm Msx1 overexpression expands epidermal fates at the expense of neural tissue (Suzuki et al., 1997). Msx has also been shown to mediate the effects of BMP-induced neural crest specification and can induce the expression of neural crest makers such as *snail* and *foxD3* (Tribulo et al., 2003). Finally, Msx1 overexpression can rescue dominant-negative BMP dorsalized embryos (Suzuki et al., 1997). However,

interpretation of these overexpression experiments is somewhat complicated since these are multifunctional proteins which may have context-dependent functions. The dominant-negative studies are likewise complicated by the fact that replacement of a functional Msx domain with a VP-16 activator domain may endow these proteins with non-native activities. Hence, it is a formal possibility that the functions proposed by these overexpression studies do not reflect the endogenous biological activity of Msx.

The loss of function experiments in mouse may provide the data with fewest caveats. Mouse Msx1 and Msx2 have been shown to be redundantly required in tooth organogenesis downstream of BMP signaling (Jernvall and Theslaff, 2000). Msx1 and Msx3 are also required for BMP-mediated specification of the roofplate of the neural tube (Bach et al., 2003). As yet, no role for Msx function in axial specification has been shown by these mutant analyses. One reason for this may be that redundancy within the Msx family is masking the role of Msx in early BMP-mediated dorsal-ventral patterning. Compound mutant analysis would address this issue but removal of all three mouse *msx* genes may be required. Hence, this remains an open question because of the difficulty of generating mouse triple mutants. Complete analysis of Msx function may require the loss of several family members to eliminate redundant functions as well as removal of interacting partners. The large brood size and loss of function techniques available in zebrafish makes this model system an excellent one for determining the role of Msx in vertebrate development. Here, we analyze the function of the three zebrafish Msx family members expressed during gastrulation, *msxB*, *msxC* and *msxE*. In addition to their early expression domains in ventral tissues, each of these genes is also expressed in

or around the preplacodal domain, a crescent-shaped field lateral to the neural plate which gives rise to all placodal fates. These three *msx* genes are later expressed in the neural plate proper. Interestingly, we find no evidence for an early role in ventral fate specification. Instead, we propose a role for Msx genes in neural-nonneural boundary positioning and maintenance of cell fate within the neural tube and placodal derivatives.

MATERIALS AND METHODS

Strains and developmental conditions

The wild-type strain was derived from the AB line (Eugene, OR). The *b380* mutation was induced by γ irradiation (Solomon and Fritz, 2002). The *Df(LG1)msxB*^{x8} mutation was induced by ENU. Embryos were developed in an incubator at 28.5°C in water containing 0.008% Instant Ocean salts.

In situ hybridization

Embryos were fixed in MEMFA (0.1 M MOPS at pH 7.4, 2 mM EGTA, 1 mM $MgSO_4$, 3.7% formaldehyde). In situ hybridizations (Stachel et al., 1993) were performed at 67°C using probes against *msxB, msxC, msxE* (Ekker et al, 1997), *dlx3* (Ekker et al, 1992), *eya1* (Sahly et al., 1999), *krox-20* (Oxtoby and Jowett, 1993), *myoD* (Weinberg et al., 1996), *six4.1* (Seo et al., 1998), *zlens1, pax8* (Pfeffer et al., 1998), *foxD3* (Odenthal and Nusslein-Volhard, 1998), *sna2* (Thisse et al., 1995), and *wnt1* (Kelly and Moon, 1995). Two-color in situ hybridization was performed essentially as described by Jowett (1996), with several modifications. RNase inhibitor (Promega 100 units/ml) was added during antibody incubation steps to help stabilize mRNA. Fast Red (Roche) was used in the first alkaline phosphatase reaction to give red color and

fluorescence. Afterward, alkaline phosphatase from the first color reaction was inactivated by incubating embryos in a 4% formaldehyde solution for 2h at room temperature and then heating for 10 minutes at 37°C. NBT-BCIP (Roche) was used for the second alkaline phosphatase reaction to give blue color. For sectioning, embryos were embedded in Immunobed resin (Polysciences No. 17324) and cut into 4 μm sections.

Immunolocalization

Antibody staining was performed essentially as described by Riley et al., (1999). Embryos were incubated with the polyclonal primary antibody pax2 (Berkeley Antibody Company, diluted 1:100), zn-8, zn-12, phosphorylated histone H3, BrdU, or Islet. Embryos were then washed and incubated with one of the following secondary antibodies: Alexa 546 goat anti-rabbit IgG (Molecular Probes A-11010, diluted 1:50), Alexa 488 goat anti-mouse IgG (molecular Probes A-11001, diluted 1:50) or horseradish peroxidase secondary antibody (Sigma A-0545, diluted 1:200).

Morpholino oligomer injections

Morpholino oligomers obtained from Gene Tools Inc. were diluted in Danieaux solution (58mM NaCl, 0.7mM KCl, 0.4mM $MgSO_4$, 0.6mM $Ca(NO_3)_2$, 5.0mM N-[2-Hydroxyethyl] piperazine-N'-[2-ethanesulfonic acid] (HEPES) pH 7.6) to a concentration of 4-5μg/μl. Filtered green food coloring was added to a concentration of 3% to visualize fluid during injections. Approximately 1 nl (5ng MO) was injected into the yolk of one- to two-cell stage embryos. Embryos were injected and allowed to briefly recover in fish water. Morpholino sequences were as follows. *msxB* 5`TATACT

TACGAGGAGGAGATGTGAA3`;*msxC* 5`ATTATTGCTGAGGTGCTTACTTGGC3`; *msxE* 5`CCGAGCATCACTGTTACCACTGGG 3`

Alcian blue staining

See Solomon et al., (2003) for protocol.

RESULTS

***msxB*, *msxC* and *msxE* are dynamically expressed early in zebrafish development**

msxB expression is first observed just before gastrulation begins. It is weakly expressed in the ventral and lateral epiblast at 5 hpf and is strongly expressed in the ventrolateral domain at 8 hpf (Fig 18A). Near the end of gastrulation, the dorsal and lateral *msxB* domain expands into the underlying hypoblast (Fig 18G, arrow). By tailbud stage this dorsal domain also begins to extend in the ectoderm along the edge of the neural plate (and underlying mesoderm, Fig. 18B,C,G). At this time *msxB* is expressed in overlapping domains with preplacodal marker *dlx3b,* although *msxB* also is expressed in the lateral neural plate as well (Fig 18I). Expression of *msxB* is then lost from the preplacodal domain but is maintained in the lateral neural plate, the site of neural crest induction. Dorsal convergence later joins the two lateral domains in the dorsal neural tube by 12 hpf (Fig 18D, H).

msxC is largely coexpressed with *msxB*. Like *msxB*, *msxC* is initially expressed in ventrolateral ectoderm (Fig 18J and data not shown) and during the latter half of gastrulation, *msxC* expression is upregulated in a dorsoanterior location (Fig 18K, L). However, unlike *msxB, msxC* forms two pairs of bilateral stripes. The more medial stripe appears limited to the lateral neural plate just medial to the *dlx3b* domain while the

Figure 18. Expression of *msxB, msxC,* and *msxE.* Wild type embryos at 8 hpf (A,J and R), 10 hpf (B,C,E-G,K,L,N-O,S and T), 11 hpf (I and Q), and 12 hpf (D,M, and U) showing *msxB* expression (A-I), *msxC* expression (J-Q), and *msxE* expression (R-U). (E) *msxB* cross-section at the level indicated in (B), high magnification views in (F and G) are indicated. Note the expression of *msxB* in both tissue layers (arrow in G). (H) High magnification view of a cross-sectioned embryo similar to (D). (N) *msxC* cross-section at the level indicated in (K). High magnification views in (O and P) are indicated. Note that the lateral *msxC* domain appears limited to the mesendoderm in (P). *msxE* is expressed in a unique periotic domain (arrow in S). (I and Q) 10 hpf double stained embryos showing *dlx3b* expression (red) and *msxB* expression (black in I) or *msxC* expression (black in Q). (A,B,J,K,R and S) lateral views with dorsal to the right and anterior up. (C,D,I,L,M,Q,T, and U) Dorsal views with anterior to the top. (E-G) Cross-sections with dorsal to the right. (N-P) Cross-sections with dorsal to the top.

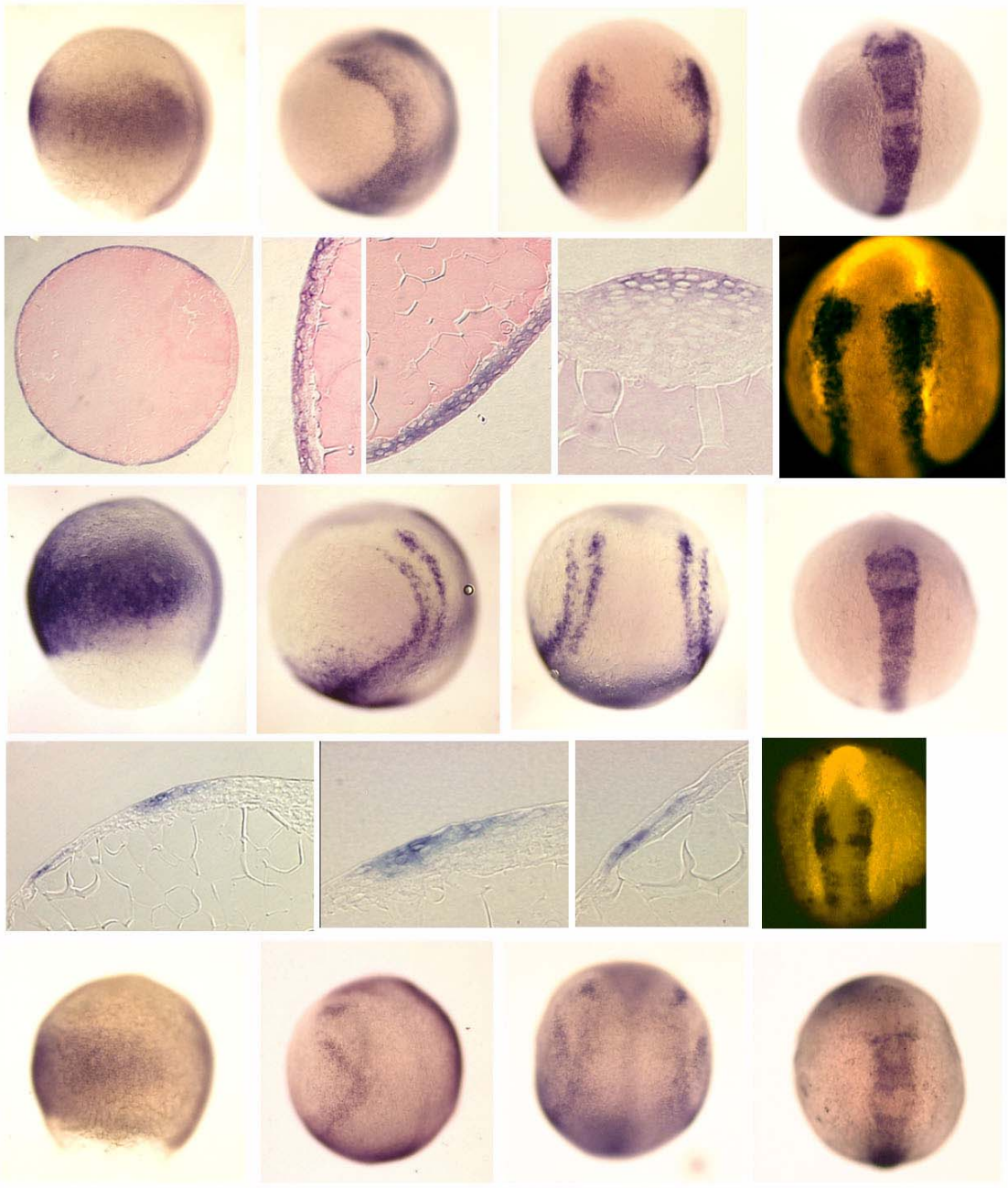

more lateral stripe marks expression in cephalic mesoderm (Fig. 18N-P). During somitogenesis, *msxC* expression is maintained in the dorsal neural tube throughout the first three days of development whereas the mesoderm expression can no longer be detected after 14 hpf (Fig. 18M). *msxE* is expressed in overlapping domains with *msxB*and *msxC*. It is also first observed in the ventrolateral domain adjacent to the germring (Fig. 18R) and later is expressed in the dorsal CNS (Fig. 18U). However, a unique domain is also observed near the preotic ectoderm (arrow in Fig 18S), though sectional analysis is required to verify whether this domain is in otic ectoderm or underlying mesoderm. As these three family members are similarly expressed and may share common roles in development, we sought to further investigate the function of MsxB, MsxC, and MsxE in embryonic development.

Morphology of Msx loss of function embryos

To analyze the function of these *msx* family members, we undertook a loss of function approach using both splice-blocking morpholino oligos (MOs) and a deficiency of *msxB*, termed *Df(LG1)msxB*^{x8}, hereafter termed *x8*. We generated splice-blocking MOs that are both potent and specific as shown by RT-PCR analysis on *msx* morphants (Fig 19A). Each morpholino injection results in complete or nearly complete knockdown of the targeted transcript without affecting other, closely related gene products.

Embryos with perturbed MsxB function, either mutant or *msxB*-MO injected, have head defects at 24 hpf characterized by necrosis and small head size (Fig 19C,D). They also display mild axial defects such as an undulating notochord and a short tail

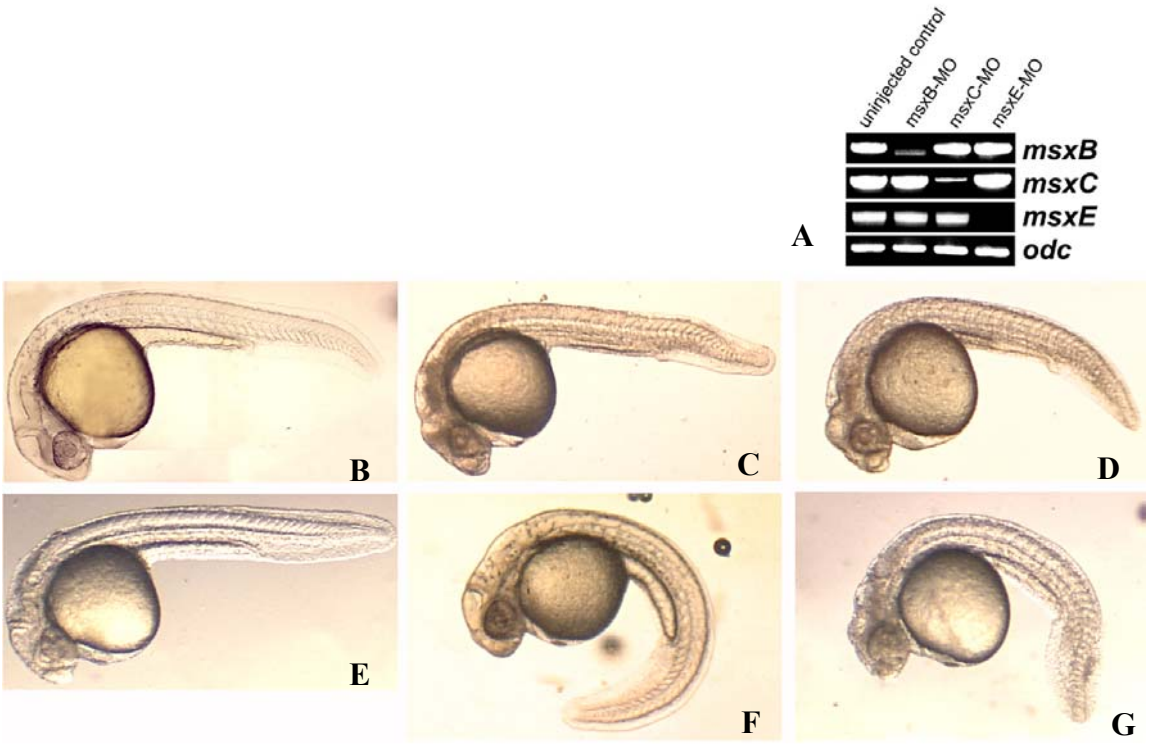

Figure 19. Morphology of *msx* loss of function embryos. (A) RT-PCR analysis of morpholino knockdown. Primers for the indicated genes (right) were applied to the morpholino-injected embryos indicated (top). *odc* expression was used as a procedural control. (B-G) 28 hpf embryos (B) wild-type, (C) *x8/x8,* (D) *msxB* morphant, (E) *msxE* morphant, (F) *msxC* morphant, (G) *msxBCE* morphant. Lateral views with dorsal to the top and anterior to the left.

consistent with deficiencies in mesodermal tissues. Axial defects are more pronounced in *msxC* morphants which show a severe ventral tail curvature while having no noticeable head defects (Fig 19F). *msxE* morphants are most similar to *msxB* mutants in that they also show necrosis in the head, though much less severe (Fig. 19E). To morecompletely analyze the function of these Msx family members and to rule out the possibility of redundancy, we examined the phenotype of embryos injected with *msxB*, *msxC* and *msxE* MOs (*msxBCE*-MO). These triple morphants have more severe necrosis and axial defects than loss of any one *msx* gene function (Fig. 19G). The head phenotypes together with the expression pattern suggested role(s) for Msx in development of placodal or dorsal CNS fates as well as possible interactions along the neural plate boundary. Hence, we proceeded with our analyses utilizing these triple morphants to uncover any redundant functions as well as single MO injections to identify gene specific functions (Table 2).

Msx and Dlx have opposing roles in BMP regulation at the neural plate boundary

In examining expression of various markers of the preplacodal domain we noticed that the bilateral stripes were reproducibly too close together, indicating a narrow neural plate. This was confirmed by examination of several preplacodal markers including *dlx3b* (Fig. 20 B,F), *eya1* (Fig. 20D) and *six4.1* (Fig. 21E) as well as the neural marker *krox-20* (Fig. 20F). On average the Msx morphants displayed a 21% reduction in neural plate width (wild-type: 105 +/- 11.7 μm; *msxBCE*-MO: 82.5 +/- 3.3 μm). This change suggested that *msxBCE* morphants are mildly ventralized, which is not consistent

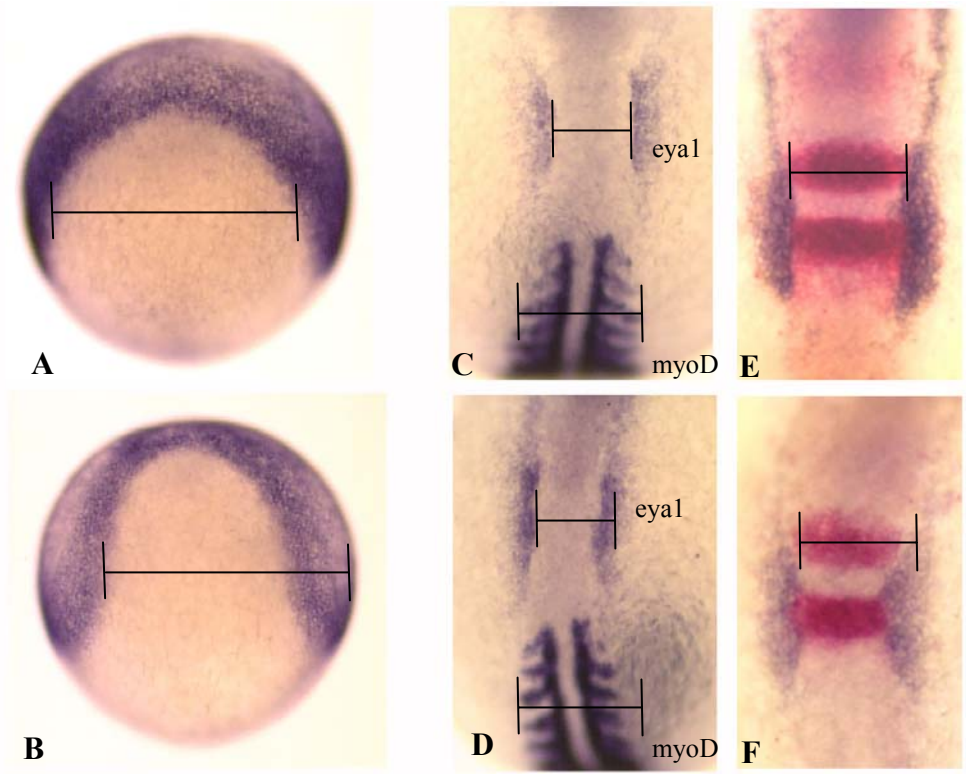

Figure 20. *msxBCE* morphants are ventralized. Wild-type (A,C and E) or *msxBCE* morphant showing 9.5 hpf *dlx3b* (A and B), 12 hpf *eya1* and *myoD* (C and D) and 12 hpf *dlx3b* in blue and *krox-20* in red (E and F). Dorsal views with anterior to the top. For comparison, measurement bars are used corresponding to the width of the wild-type expression domiains. The width of A is also indicated in B, the width of C is also indicated in D and the width of E is also indicated in F.

with the hypothesis that Msx proteins help mediate BMP ventralization. Instead the *msxBCE*-MO phenotype is consistent with increased BMP activity indicating that Msx normally represses BMP activity. However, we observe no observable change in BMP expression in *msxBCE* morphants (not shown). To explain this phenotype, we considered another proposed function of Msx, functional antagonism of Dlx proteins (Zhang et al., 1997). *dlx3b* and *dlx4b* are both expressed in the preplacodal domain with *msx* genes (Solomon and Fritz, 2002, Fig. 20A). Furthermore, Dlx misexpression narrows the neural plate, suggesting that Dlx may have a moderate ventralizing function to (McLarren et al., 2003), while our data indicates that Msx functions to dorsalize the embryo. To determine if an inhibitory Msx-Dlx mechanism operates within the preplacodal domain we injected *msxBCE*-MO into a *dlx* deficiency mutant, *b380,* which removes *dlx3b* and *dlx4b*. We reasoned that loss of Msx function may lead to narrowing of the neural plate because Dlx proteins are too overly active. In support of this, *b380* suppresses the ventralizing effects of *msxBCE*-MO (Fig. 21D; neural plate widths: *msxBCE*-MO into wild-type 95.2 +/- 9.5 μm and *msxBCE*-MO into *b380 -/-* 128.4 +/- 15.9 μm). This is consistent with a model where protein-protein interactions between Dlx and Msx restrain the ability of Dlx to activate the transcription of target genes. Interestingly, in *msxBCE* morphants we also observe a ventralization of somitic mesoderm markers such as *myoD* (Fig. 20D; width of *myoD* domain in wild-type: 161.1 +/- 0.2 μm and *msxBCE* morphants: 135.7 +/- 9.5μm) indicating that Msx may also have roles in repressing transcriptional activators in the mesoderm as well as ectoderm. Dlx3b and Dlx4b promote general preplacodal identity (Solomon and Fritz, 2002) and,

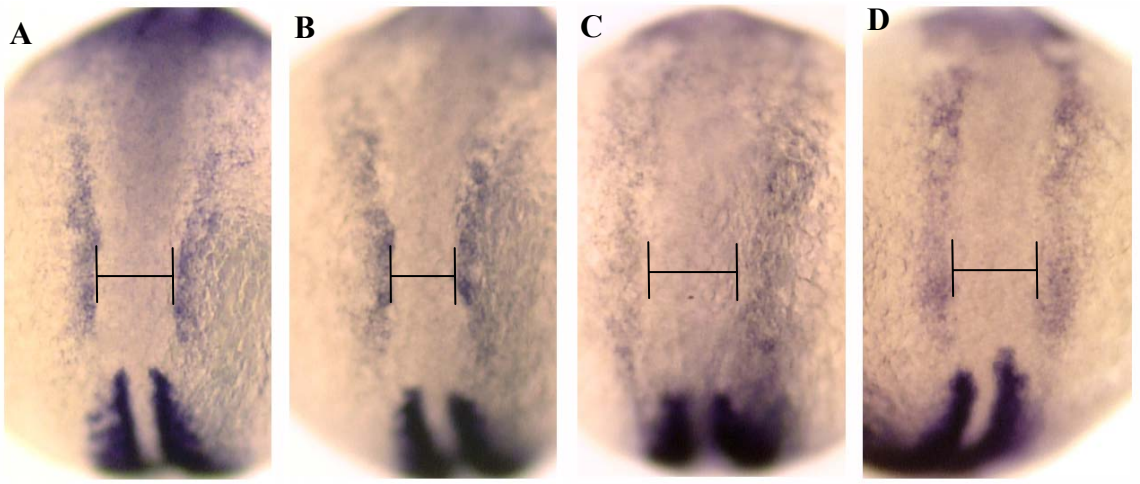

Figure 21. ***b380* can rescue the constricted neural plate phenotype of *msxBCE* morphants.** (A-D) 12 hpf *six4.1* and *myoD* expression in wild-type (A), *msxBCE* morphant (B), *b380* (C), and *b380* injected with *msxBCE*-MO (D). Dorsal views with anterior upward. For comparison, measurement bars corresponding to wild-type (A) neural plate width are used in each panel.

when deleted in *b380*, the expression of *six4.1* is considerably reduced (Fig. 21C). However, the expression level of *six4.1* is nearer wild-type levels in *b380* mutants injected with *msxBCE*-MO (Fig. 21D). This suggests that *msx* gene products have additional preplacodal-repressing functions in addition to being antagonists of Dlx proteins. The effects of relieving this repression is not seen in wild type embryos depleted for Msx function, but are only uncovered in a genetic background with weakened preplacodal character. Taken together, these data indicate that Msx acts through repressive interactions with Dlx proteins to refine the border between the preplacodal ectoderm and the neural ectoderm and that Msx generally represses preplacodal development.

Posterior placodal tissues are perturbed in embryos depleted for Msx

We next sought to determine the specific function of *msx* genes on preplacodal development. The anterior placodal tissues, lens and olfactory epithelium do not express *msx* genes and hence appear to develop normally in *msxBCE* morphants as assessed by the anterior preplacodal marker *zlens1* and morphant morphology (Fig. 22 A-D). Posterior placodal fates which develop in or near the *msx* domain are induced normally (Fig. 23) but are not maintained properly. The monoclonal antibody zn12 marks several neuronal cell types including those of the trigeminal ganglion. *msxBCE* morphants have smaller trigeminal ganglia which display reduced arborization patterns compared to uninjected controls (Fig 23A). The otic placode is another placodal tissue within the *msx* expression domain. Otic induction appears normal as assessed by expression of *pax8* and *pax2a* otic markers (Fig 23 and data not shown). However, growth of the otic

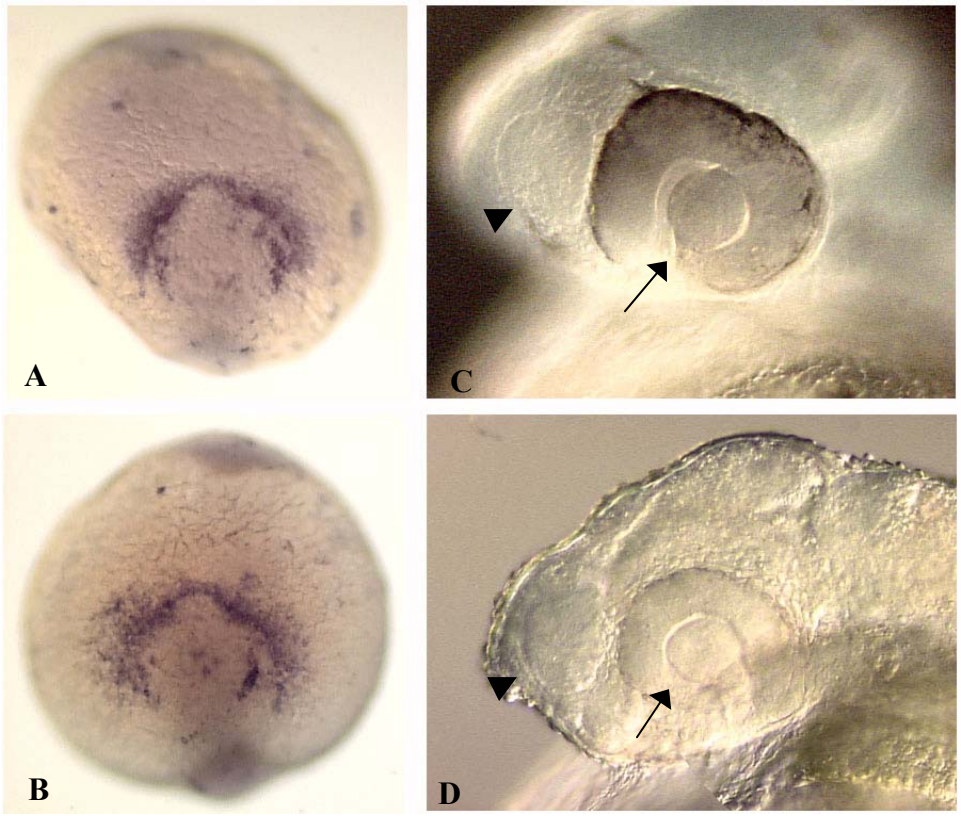

Figure 22. Normal nasal and lens placode development in *msxBCE* morphants. *zlens1* expression in wild-type **(**A) and *mscBCE* morphant (B). 28 hpf wild-type (C) and *msxBCE* morphant (D). The nasal epithelium (arrowhead) and lens (arrow) are visible. (A and B) Anterior views with dorsal down. (C and D) Lateral views with anterior to the left and dorsal up.

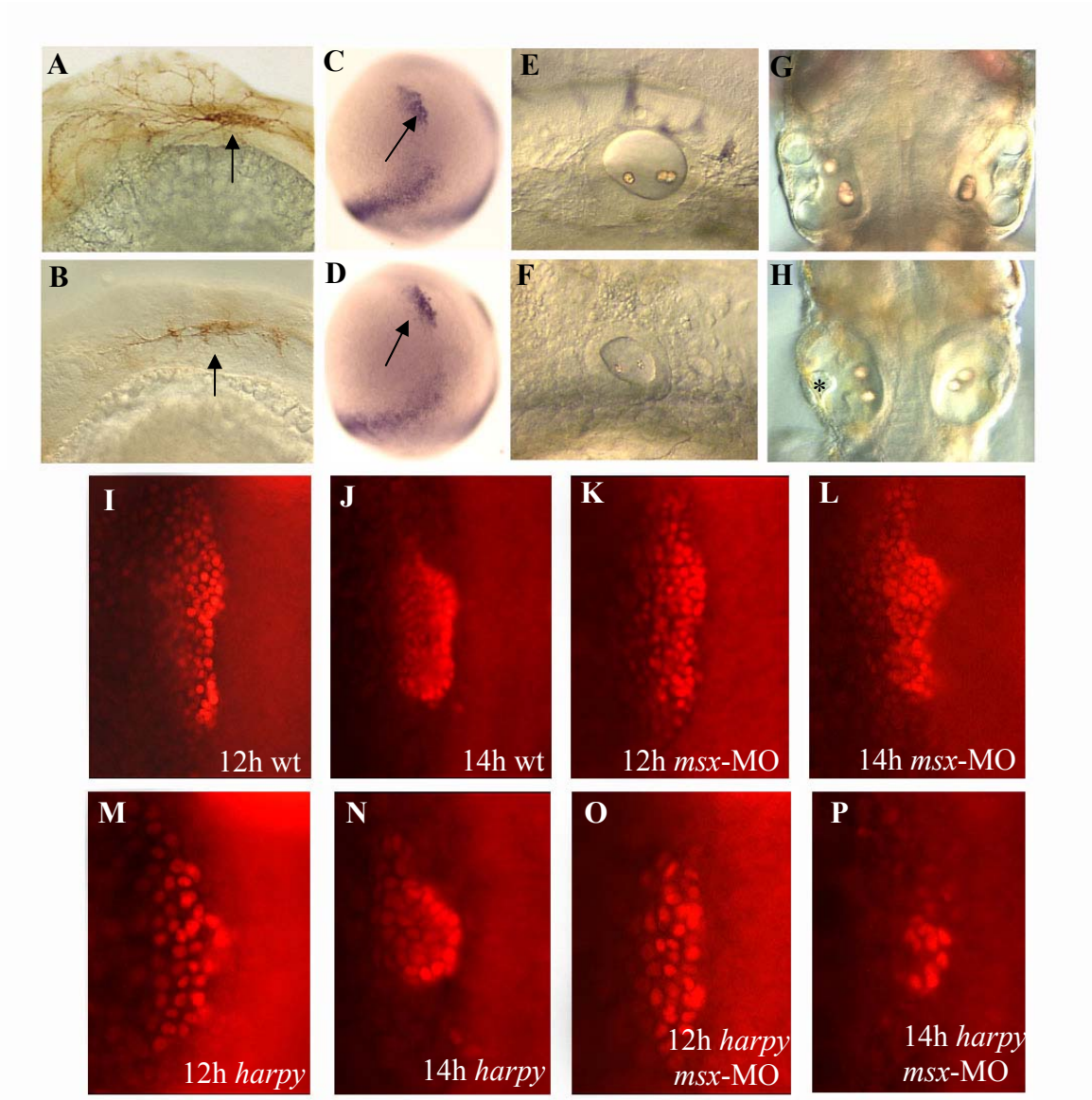

Figure 23. Trigeminal and otic placodal derivatives are abnormal in *msxBCE* morphants. zn12 staining show trigeminal ganglia (arrows) in wild-type (A) and *msxBCE* morphant (B). 10 hpf *pax8* expression in wild-type (C) and *msxBCE* morphant (D). 28 (E and F) and 75 (G and H) hpf ear morphology of wild-type (E and G) and *msxBCE* morphant (F and H). Note the semicircular canal projection defect (*). (I-P) Pax2 staining on stages, morphants and mutants as indicated. (A,B,E and F) Later views with dorsal up and anterior to the left. (C and D) Lateral views with dosal to the right and anterior up. (G-P) Dorsal views with anterior up.

field typically seen in wild type embryos does not occur in *msxBCE* morphants. Therefore, the otic vesicle is small and malformed and later defects in semicircular canal formation are also evident (Fig 23F,H and L), though the sensory epithelia are present and the axial markers reveal the inner ear is relatively well patterned (data not shown). To more thoroughly investigate these otic defects, we quantitated the number of otic cells at various times of development using an antibody which recognizes Pax2a. The number of otic cells is initially normal (wt: 94.7+/-3.9 cells; *msxBCE*-MO: 87.2+/-7.2 cells at 12 hpf, Fig. 23I,K), but the otic field fails to expand and there are approximately 40% fewer otic cells compared to wild-type at 14 hpf (wt: 135.3+/-0.1 cells; *msxBCE*-MO: 83.5+/-8.1 cells; Fig. 23J,L). *x8* mutants injected with *msxCE* morpholinos show a similar phenotype (not shown). This suggests that in the absence of Msx function, the otic primordium prematurely stops expanding at about 12 hpf.

In addition to the reduced number of otic cells, *msxBCE* morphants show a morphogenetic defect characterized by delayed consolidation of the otic field. At 12 hpf wild-type otic tissue is diffuse and spread out over a large area (Fig. 23I). By 14 hpf, however, the otic field has converged into a smaller grouping of tightly packed cells (Fig. 23J). This convergence is delayed in embryos depleted for Msx and therefore at 14 hpf the otic field more closely resembles a 12 hpf wild-type embryo (Fig. 23L). Consolidation of otic tissue eventually occurs, however, and at 24 hpf *msxBCE* morphants do form a small, though correctly patterned, otic vesicle (Fig. 23F).

Increased cell death in Msx loss of function embryos

One hypothesis which would explain the small size of otic tissue in Msx loss of function embryos is that Msx proteins act to stimulate otic cell proliferation. To test this hypothesis, we utilized the zebrafish mutant *harpy,* which lacks all cell division after gastrulation begins (6 hpf; our unpublished observations). Otic induction in *harpy* mutants occurs normally with the exception that the otic anlage contains too few cells (31.8+/-3.2 cells at 12 hpf; Fig. 23M). Despite the absence of any cell division, *harpy* mutant ears still grow at approximately the same rate as wild type embryos (40.7+/-0.1 cells at 14 hpf; Fig. 23N). This indicates that cell division is not essential for otic expansion in normal zebrafish embryos and that loss of Msx function may affect another process. If this is the case, we predicted that *msxBCE*-MO injection into *harpy* would cause a similar phenotype as injection into wild type embryos. Indeed, *harpy* embryos depleted for Msx initially have a similar number of otic cells as uninjected *harpy* (29.9+/-0.1 cells at 12 hpf; Fig. 23) but by 14 hpf display a significantly reduced ear size (24.6+/-0.1 cells Fig. 23P). Furthermore, Msx depletion produces no noticeable defects in cell cycle progression as assayed by the mitosis marker phosphorylated histone H3 (wt: 15+/- 2.4 cells; *msxBCE*-MO: 13.9+/-3 cells; Fig 24B) or by BrdU incorporation during S phase (wt: 39.6+/-0.3 cells; *mscBCE*-MO: 37.7+/-6.7 cells; Fig. 24D). These data indicate that loss of Msx function does not perturb cell division and hence is unlikely to be the root cause of the small ear phenotype.

We next assayed whether the otic phenotype was due to increased levels of cell death. Acridine orange is a hydrophilic DNA intercalating agent which only gains

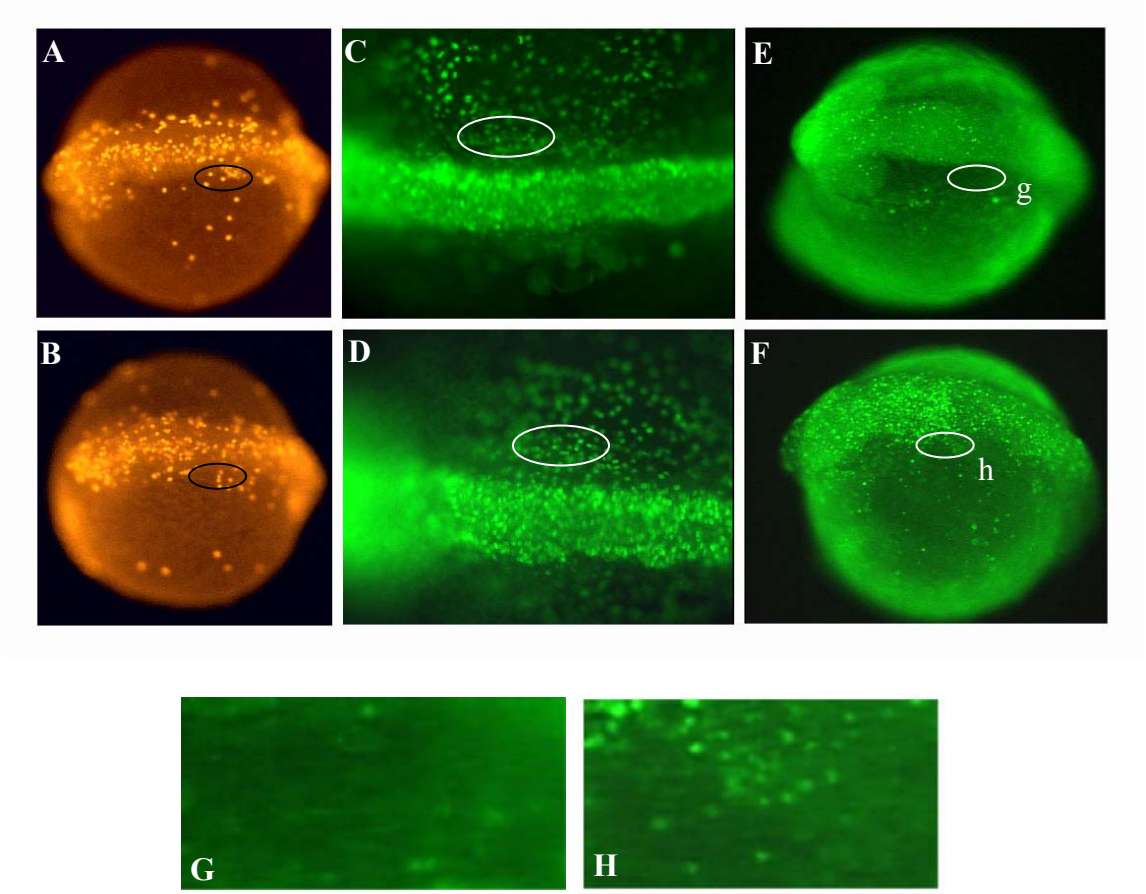

Figure 24. Cell division and cell death in *msxBCE* morphants. Phosphorylated histone H3 expression in wild-type (A) and *msxBCE* morphants (B). BrdU incorporation in wild-type (C) and *msxBCE* morphants (D). Acridine orange staining in wild-type (E) and *msxBCE* morphants (F) (G and H) High magnification view of otic regions indicated in (E and F). Otic regions are indicated by the ovals. Dorsal views with anterior to the left.

access to the nucleus if the cell membrane is compromised, as in cells undergoing apoptosis. Healthy cells remain unstained by this dye. We incubated wild-type and *msxBCE* morphants in an acridine orange solution to identify dying cells. Control embryos show few dying cells at 14 hpf (Fig. 24E). Conversely, in *msxBCE*-MO injected embryos, tissues which normally express *msx* undergo extensive cell death, including the hindbrain and the otic region (Fig. 24F). These data indicate that increased cell death is likely one of the factors responsible for the small ear phenotype observed in embryos depleted for Msx. However, increasing cell number in *harpy* mutant ears suggests that the mechanism of growth in normal embryos is more complex than simple proliferation. Other mechanisms of otic tissue expansion and possible roles for Msx proteins in this process are discussed below (see Discussion).

Dorsal CNS tissues are reduced in embryos lacking Msx function

Since *msxB*, *msxC* and *msxE* all are expressed in the dorsal neural tube, we examined development of different tissues located within this domain. Neural crest is induced at the lateral edges of the neural plate during early stages of segmentation (10-11 hpf) by an intermediate dose of BMP (Nguyen et al., 1998). FoxD3 is a forkhead class transcription factor which has been proposed to act early during neural crest specification and can induce the expression of other neural crest-specific transcription factors (Sasai et al., 2001). At 11 hpf, *foxD3* expression is expressed at high levels in newly specified neural crest precursors in wild type embryos. *msxBCE* morphants express normal levels of *foxD3* (Fig. 25B), though in a narrower domain consistent with the constricted neural plate phenotype discussed above. Snail2 is downstream of FoxD3

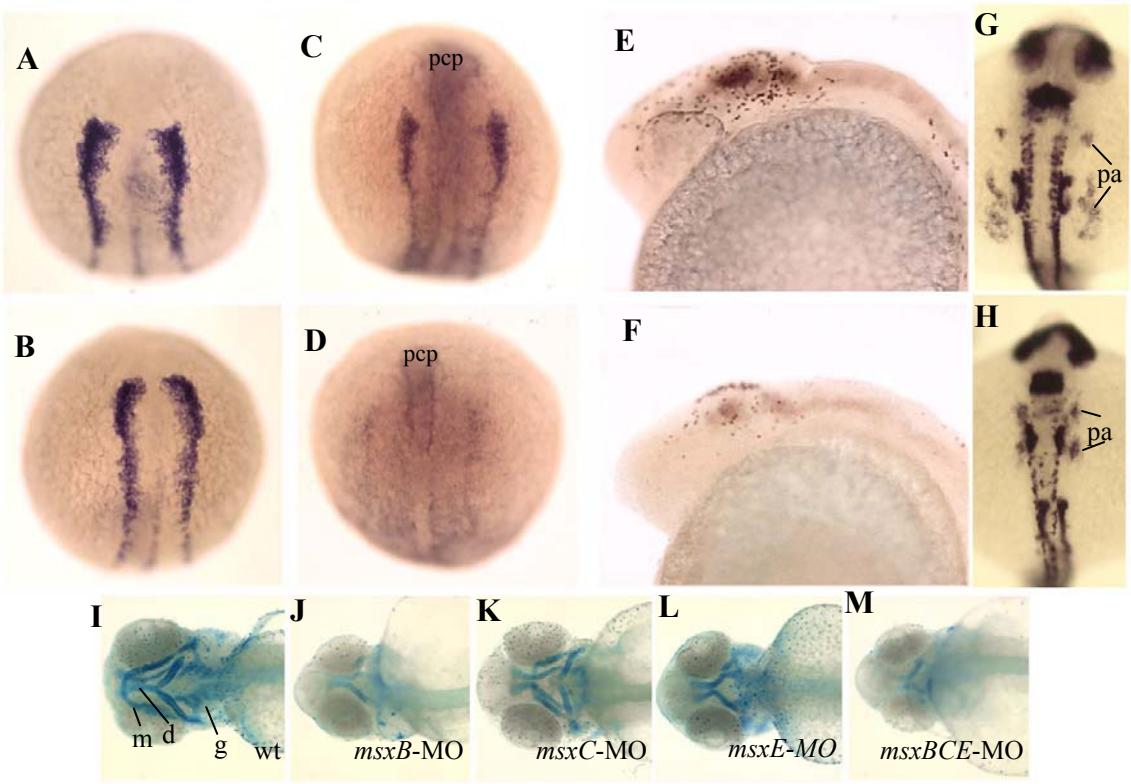

Figure 25. Impaired neural crest development in *msxBCE* morphants. *foxd3* expression at 11 hpf in wild-type (A) and *msxBCE* morphants (B). *snail2* expression at 11 hpf in wild-type (C) and *msxBCE* morphants (D). Pax7 at 24 hpf expression in wild-type (E) and *msxBCE* morphants (F). *pax2a* expression at 24 hpf in wild-type (G) and *msxBCE* morphants (H). Pharyngeal arches (pa) are indicated. (I-M) Alcian blue cartilage staining on 75 hpf embryos injected with the indicated morpholinos. pcp, prechordal plate; m, mandibular jaw; g, gill arches; d, dorsal palate. (A-D,G,H) Dorsal views with anterior up. (E and F) Lateral views with dorsal up and anterior to the left. (I-M) Ventral views with anterior to the left.

in the genetic cascade of neural crest specification and is expressed in a similar domain in neural crest progenitors. In *msxBCE* morphants, however, this marker is expressed at very low levels in future neural crest tissue, though expression is retained in other expressing tissues (i.e. prechordal plate, Fig. 25D). This indicates that neural crest specification occurs normally, but that later stages of neural crest development are perturbed. Consistent with this, migrating neural crest cells are markedly decreased in number at 24 hpf as viewed by Pax7 expression (wt: 66+/-7.4; *msxBCE*-MO: 37.7+/-15.1, Fig. 25F). In addition to defects in neural crest differentiation, cell death in the dorsal neural tube probably contributes to the deficiency in migrating neural crest.

Migrating neural crest go to on adopt many different cell fates, including elements of the jaw. Alcian blue staining of jaw cartilage in 3d *msx* morphants indicates that loss of any one *msx* function results in jaw defects (Fig. 25I-M), consistent with the reduction in migrating neural crest seen at 24 hpf. The ventral elements, including the gill cartilages and the mandibular cartilages, are most severely affected. Each element is either reduced in size or absent in these single MO injected embryos. Jaw defects are most severe in triple morphants which have defects in the dorsal palate in addition to complete loss of ventral elements (Fig. 25M). Pigment cells are another derivative of neural crest tissue and are severely reduced in number at two days of development in *msxBCE* morphants (not shown). Finally, neural crest contributes to pharyngeal arch tissue. The pharyngeal arches are present in *msxBCE* morphants, but are reduced in size and do not extend properly as shown by expression of *pax2a* (Fig. 25H). These data indicate that neural crest specification occurs in the absence of Msx function, but that

differentiation and survival are impaired and too few migrating neural crest cells are produced.

Rohon-Beard sensory neurons are another cell type present in the dorsal CNS and located within the Msx expression domain. An antibody directed against Islet marks the Rohon-Beards and allows quantitation of these sensory neurons. At 19 hpf *msxBCE* morphants have approximately 30% fewer Rohon-Beard neurons than uninjected controls (wt: 16.5+/-2.4; *msxBCE*-MO: 11.4+/-1.9, Fig. 26A,B). This is most likely due to cell death as morphants have similar numbers of Rohon-Beard neurons at 12hpf (not shown). The lateral edges of the neural plate form the roofplate of the neural tube, an important signaling center within the CNS. The roofplate expresses secreted molecules such as *wnt1*. Furthermore, roofplate defects are observed in knockout mice lacking Msx1 and Msx2 function (Bach et al., 2003). The roofplate forms in *msxBCE* morphants and expresses *wnt1,* but fails to resolve itself into the stereotyped striped expression pattern (Fig. 26D). Hence, other dorsal cell types such as commissural neurons are not present in 71% *msx* morphants as viewed by zn8 antibody staining (n=21; Fig. 26F). These data indicate that, like neural crest, msx is not required for specification of dorsal CNS tissues, but for cell survival and refinement of neural patterning.

Embryos lacking Msx have defects in fin growth and heart looping

Msx expression has been shown to be activated by Fgf signaling in the developing fin/limb bud mesenchyme. In this context, Msx proteins may be necessary for continued proliferation and growth of the extending limb bud. Consistent with this hypothesis, embryos lacking MsxB function have a mild reduction in pectoral fin tissue

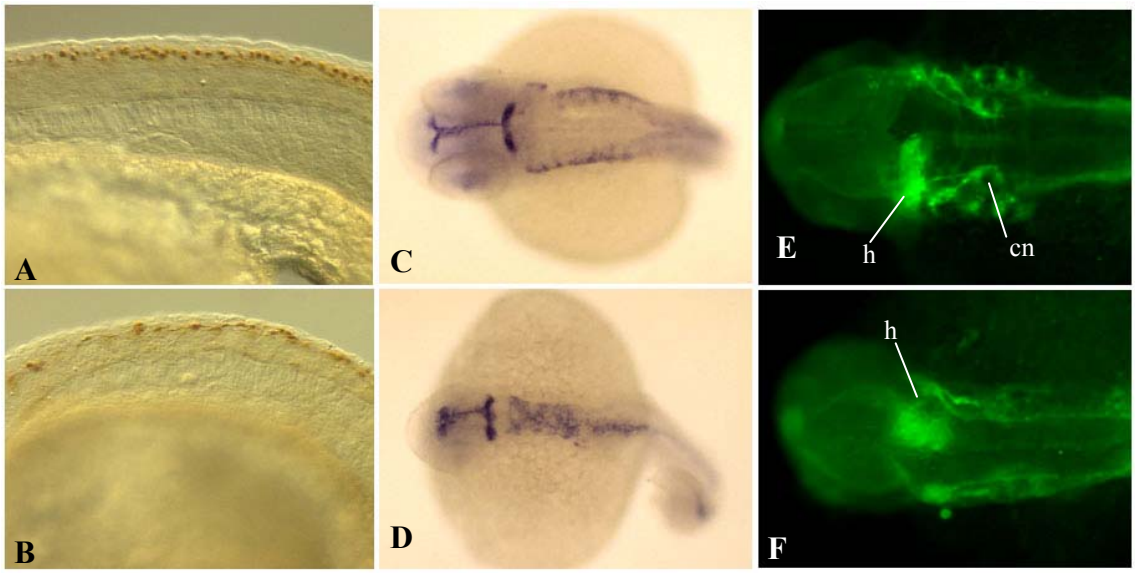

Figure 26. Disrupted dorsal CNS development in *msxBCE* morphants. Islet expressing Rohon-Beard sensory neurons in 19 hpf wild-type (A) and *msxBCE* morphants (B). *wnt1* expression in the roofplate of 30 hpf wild-type (C) and *msxBCE* morphants (D). zn8 expression in 30 hpf wild-type (E) and *msxBCE* morphants (F). Note heart (h) expression of zn8 is located on the right side while the commissural neurons (cn) are missing in the morphant.

Table 2. Summary of *msx* phenotypes

Tissue examined	BCE-MO	x8	B-MO	C-MO	E-MO
Neural Crest					
FoxD3	WT	ND	WT	WT	WT
Sna2	***	WT	ND	WT	WT
Pax7	***	**	ND	ND	ND
Pigment	***	*	*	WT	WT
Placodes					
Nasal	WT	WT	WT	WT	WT
Lens	WT	WT	WT	WT	WT
Trigeminal	***	ND	ND	ND	ND
Otic					
# pax2 cells	***	*	ND	WT	WT
small vesicle	***	**	**	WT	WT
delayed HC dev	ND	**	ND	ND	ND
SSC dev	***	***	***	ND	*
cristae	***	WT	WT	ND	ND
Pharyngeal arches	***	ND	*	WT	WT
Jaw defects	***	ND	***	*	*
Pectoral fin	**	**	*	WT	WT
Median fin fold	*	WT	WT	WT	WT
Ventral tail curvature	***	*	WT	***	WT
Heart laterality	Random	Random	Random	Random	WT
Dorsal CNS					
Rohon Beard neurons	**	*	ND	ND	ND
Commissural neurons	***	***	***	WT	WT
Brain necrosis	***	**	**	WT	*

(*) indicates degree of severity. ND, not determined

while *msxBCE* morphants show a more severe loss of fin tissue (Table 2). During examination of the zn8 staining pattern in commissural neurons, we noted defects in heart tissue which is also marked by zn8. Asymmetrical heart looping appears to be randomized in *msxBCE* morphants with 48% of embryos displaying a right-sided heart, 29% with a left-sided heart and 23% of embryos with a heart that did not appear to loop

away from the midline (n=21; Fig. 26F). Further analysis with single mutants and morphants shows that MsxB and MsxC are each required for proper asymmetric heart looping, while embryos depleted for MsxE display normal heart looping. Further analysis of this phenotype will be required to put forward a specific model for Msx function in left-right asymmetry, but this process has been proposed to involve BMP and Nodal signaling, both potential regulators of *msx* expression.

DISCUSSION

We have undertaken functional analyses of members of the Msx family expressed early in zebrafish development. *msxB, msxC* and *msxE* are all expressed in ventral tissues during gastrulation and later are expressed in the preplacodal domain and dorsal neural tube. We utilize a loss of function approach to remove or knockdown multiple Msx proteins to eliminate the possibility of redundant functions. Contrary to predictions in most current models, our findings indicate that Msx genes do not act as simple mediators of BMP signaling. Instead, *msx* morphants are partially ventralized suggesting over-activity of BMP. As we observe no difference in BMP expression levels in *msx* morphants, regulation of BMP is most likely an indirect effect of repressive protein-protein interactions with Dlx transcriptional activators. Posterior placodal and dorsal neural cell types, including neural crest, within the Msx domain are specified but later many of these cells die in Msx loss of function embryos. The increased cell death results in malformed patterning of *msx* expressing tissues.

Msx genes act to refine the neural plate border

Overexpression of wild-type and dominant negative forms of Msx suggest that a primary role of Msx proteins is to mediate early ventralization by BMP signaling. This predicts that Msx loss of function embryos should be dorsalized. To the contrary, we show that embryos depleted for Msx show mild ventralizaion. Ventral tissues such as the median fin fold are specified normally. Instead, *msxBCE* morphants display a moderate ventralization phenotype, contrary to expectations if Msx mediates ventral signals. A deletion which removes two *dlx* genes expressed in the neural-nonneural border rescues the Msx ventralization phenotype consistent with the inhibitory interaction of Dlx and Msx proteins. The action of Msx proteins results in the proper balance of Dlx activity. Although, the function of Dlx remains unknown, Msx-Dlx interactions allow for refinement of the boundary between the preplacodal domain and neural ectoderm. Support for this model is seen in recent studies in chick examining the effects of Dlx5 misexpression indicate that Dlx result in narrowing of the neural plate (McLarren et al., 2003).

Why do studies in *Xenopus* studies suggest an early role for Msx genes in axial specification (Maeda, et al. 1997; Suzuki et al., 1997; Ishimura et al., 2000; Yamamoto et al., 2000)? One possibility is that the phenotypes observed following the overexpression and dominant negative techniques employed for these experiments may not reflect normal Msx function. Msx repression is likely to be context dependent; i.e. Msx function changes depending upon the molecular identity of the cell in which it is expressed because of the presence of different interacting partners. *msx* expression is

not normally present in neural tissue until after gastrulation, while misexpression studies force global expression of *msx*. Hence, the antineural properties which Msx proteins appear to possess in misexpression assays may not reflect normally occurring protein interactions and makes interpretation of these experiments difficult. Further, major axial defects in *msx1;msx2* or *msx1;msx3* compound mutant mice have not been reported. This supports the notion that Msx does not function in early axial specification, although triple mutant analysis may uncover a role for Msx in dorsal-ventral patterning.

Msx genes are required for normal development of placodal fates

Msx is only transiently expressed in preplacodal tissue. However, loss of Msx function results in otic defects 3-4 hours after *msx* expression shifts out of the preplacodal domain. Embryos depleted for Msx initiate placodal development normally. Early preplacodal markers are expressed at the proper time although in a more medial position. Likewise, early markers of otic tissue are also expressed in an appropriate manner, indicating that otic induction has taken place. However, the otic vesicle is small and malformed and later otic tissues such as the semicircular canals fail to form. Conversely, *msx* morphants undergo a slight decrease in otic cell number during this period indicating that some property required for expansion of the otic tissue is perturbed by loss of Msx function. Since cell division defects are not apparent, the one possible explanation for this small ear phenotype is that Msx regulates a subtle aspect of early differentiation without which a subset of otic cells die. Alternatively, ongoing cell death in the dorsal CNS could disrupt signals required for continued development of otic tissue. Though the hindbrain factors Fgf3 and Wnt8b are expressed normally in *msx*

morphants (our unpublished ovservations), other factors might be deficient. Protein and transcriptional targets of Msx repression are unrestrained, causing an imbalance of transcriptional activity. The result of this imbalance presumably causes defects in cellular identity and cell death is the ultimate effect.

Our observations of the lack of otic tissue expansion in *msxBCE* morphants led us ask whether cell division was perturbed in the otic region of the embryos. Progression through the cell cycle appeared normal. Furthermore, injection of *msxBCE*-MO into a mutant background (*harpy)* lacking cell division produced a similar lack of otic expansion as Msx knockdown in wild-type. The most likely mode of Msx action, therefore, is probably in preventing cell death as we see an increase in dying cells in these Msx depleted embryos. However, the observation that *harpy* embryos undergo otic tissue expansion in the absence of cell division prompts the question: what mechanism causes growth of the otic primordium? One intriguing possibility is the recruitment of neighboring, non-otic cells into the otic field by the preotic cells themselves. This suggests a diffusible factor emitted by newly specified otic tissue instructing neighboring cells to enlist in the otic formation process. Until this hypothesis is tested we cannot rule out the possibility that *msx* genes play a role in this process.

Another observation that suggests a role for Msx in signaling within the otic field is that, in addition to increased cell death and inhibited otic expansion, *msx* morphants are defective in the morphogenetic process which consolidates the otic field. Importantly, this defect seems specific to otic tissue since other cell movements, such as convergence of the neural plate, appear normal. The morphogenetic defects in *msxBCE*

morphants suggest that a signaling pathway within the otic field has been perturbed. This may be the same signaling pathway which is acting during otic recruitment. Hence, Msx may be participating in a pathway which directs both recruitment and morphogenesis as well as preventing cell death. Impairing this pathway would then produce a phenotype similar to the one seen in Msx morphants. Further analysis of signaling pathways within the otic field will be needed to rigorously test this model. It should be noted that members of both the Wnt and Fgf families of secreted ligands are active in preotic tissue at approximately 12 hpf based on expression of the Wnt reporter *TOPdGFP* and the *fgf24* expression pattern (Draper et al., 2003; our unpublished observations) and that binding sites for the Wnt mediators TCF/Lef are present in the mouse *msx1* promoter. Identification of new Msx targets of will also help facilitate many aspects of this work.

A role for Msx in the neural plate

foxD3 is an early marker in neural crest development and is expressed normally in embryos lacking Msx (Fig. 25B). However this tissue does not express proper levels of a downstream neural crest marker, *snail2,* indicating that neural crest is specified but that differentiation is perturbed. *msx* morphants are deficient in migrating neural crest at 24 hpf and defects are observed in all neural crest derivatives examined, including melanocytes, pharyngeal arch and jaw elements. Cell death may contribute to this later phenotype, as we note increased cell death relative to wild-type after 14 hpf. However, cell death is unlikely to explain the lack of *snail2* expression at 11 hpf as we see no evidence of increased cell death at this time. Therefore, we conclude that Msx is

necessary for early stages of neural crest differentiation and that it is perturbed early neural crest development which results in later cell death.

Msx functions in dorsal CNS tissue differentiation as well. Rohon-Beard sensory neurons are evident in the correct position and number at 12 hpf but are underproduced by 19 hpf in *msx* morphants. Commissural neurons, whose soma are located dorsolaterally, are also absent. These phenotypes may reflect the increased cell death observed in the dorsal CNS. Alternatively, loss of Msx may result in disrupted patterning events this tissue. Perturbed *wnt1* expression in the roofplate supports this notion of dysfunctional signaling events. It should be noted that these hypotheses need not be mutually exclusive. Increased cell death in the dorsal neural tube could cause general CNS disorganization resulting in alterations in the expression of signaling factors such as *wnt1*. Likewise, lack of *wnt1* expression at rhombomere boundaries (the normal site of *wnt1* upregulation) could cause patterning defects and cell death throughout the neural tube.

CHAPTER V

SUMMARY AND CONCLUSIONS

This dissertation largely focuses on development of vertebrate placodal tissues. Placodes are derivatives of a common domain originating adjacent to the anterior neural plate and give rise to the sense organs associated with the head. After specification of a general preplacodal domain, these cells are primed to differentiate and await local inducers of each specific placodal fate. In chapter II, I showed that Fgf3 and Fgf8 are redundantly required for otic placode induction. While my analyses indicate that Fgf3 and Fgf8 are necessary for otic induction but whether Fgf activity directly induced the otic placode and whether Fgf cooperates with other signaling pathways remain open questions. These questions are addressed in Chapter III, where we determine the relative roles of the Fgf and Wnt pathways in otic induction as well as provide evidence of the direct action of Fgf3 and Fgf8. The gain-of function experiments used in this study demonstrate that Fgf signaling was able to induce ectopic otic tissue but only within the preplacodal domain. This prompted us to begin a study of a family of transcription factors expressed in and around the preplacodal domain, the muscle segment homeobox (Msx) family of transcriptional repressors. In chapter IV, I address the function of this family and demonstrate that Msx proteins function in refining the boundary between the preplacodal domain and the neural plate. While *msx* genes are unnecessary for specification of placodal fates, they do play a role in differentiation, morphogenesis and survival in placodal tissues as well as neural crest and dorsal CNS most likely by restraining the function of tissue-specific transcription factors. This dissertation as a

whole provides important insights which will hopefully serve as a framework for future discoveries in placodal development.

FGF3 AND FGF8 ARE REDUNDANTLY REQUIRED FOR OTIC INDUCTION

The loss of function studies described in Chapter II demonstrate that Fgf3 and Fgf8, emanating from several periotic tissues, are necessary for otic placode induction. Identifying the molecular nature of the otic-inducing signals had been a long-standing goal in vertebrate embryology. The Fgf3 and Fgf8 loss of function data builds on and reconciles much of the data gathered on otic induction. For example, the hindbrain has been proposed to be a source of otic-inducing signals because of its ability to induce ectopic otic tissue when grafted (Woo and Fraser, 1998). The finding that both Fgf3 and Fgf8 are expressed in the zebrafish hindbrain and are required for otic induction provides a mechanism for the hindbrain's otic-inducing properties. In addition, Fgf3 had been proposed to play a role in otic induction based on its expression pattern, misexpression studies and knockdown experiments (Wilkinson et al., 1989; Represa et al., 1991; Lombardo and Slack, 1998; Vendrell et al., 2000). However, the finding that Fgf3 knockout mice still form otic tissue suggests that Fgf3 may be unnecessary for otic induction (Mansour et al., 1993). Our finding that Fgf3 acts redundantly during otic induction sheds light on the mouse Fgf3 mutant phenotype and suggests that mouse Fgf3 may also be acting in a redundant fashion with another Fgf ligand. Mouse Fgf8 is an unlikely candidate in this process since, unlike in zebrafish, is not expressed in a pattern consistent with a role in otic induction (Crossley and Martin, 1995). Instead, mouse Fgf10 emanating from subjacent mesoderm acts redundantly with Fgf3 from the

hindbrain and loss of both Fgf3 and Fgf10 totally ablates otic development (Wright and Mansour, 2003). This discovery suggests that the mechanism of multiple, redundant Fgf ligands signaling to induce the otic placode may be well conserved among vertebrates.

A DIRECT ROLE FOR FGF BUT NOT WNT DURING OTIC INDUCTION

The finding that Fgf3 and Fgf8 are necessary for otic induction in zebrafish does not preclude the possibility that the Fgf pathway may act in concert with other otic-inducing signals. It remains possible that loss of Fgf3 and Fgf8 function lowers the sum total of otic-inducing signals below a critical threshold, enabling visualization of a molecular and morphological phenotype. In support of additional otic-inducing signals, Ladher and colleagues (2000a) proposed a model where Fgf19 signals in parallel with a Wnt ligand, Wnt8c. This conclusion was based on the ability of these factors to induce otic markers in chick tissue explants. To test the relative roles of Fgf and Wnt signaling, we used both loss of function and misexpression techniques available in zebrafish. Our findings indicate that Wnt8 serves to regulate the expression of Fgf3 and Fgf8 and that it is these Fgf ligands which directly signal to preotic tissue to induce the otic placode. We therefore propose a linear pathway where Fgf signaling is a necessary intermediate between the Wnt pathway and otic induction. Figure 27 depicts a model for otic placode induction in zebrafish. Wnt8 is required to induce timely *fgf3* and *fgf8* expression in rhombomere 4 of the hindbrain. Fgf3 and Fgf8 are in turn required for high levels of *wnt8* expression in rhombomeres 5 and 6. Analysis of the expression pattern of the Fgf reporter gene *erm* indicates that Fgf3 and Fgf8 are then directly received by preotic cells. Reception of Fgf ligands by the preplacodal domain triggers

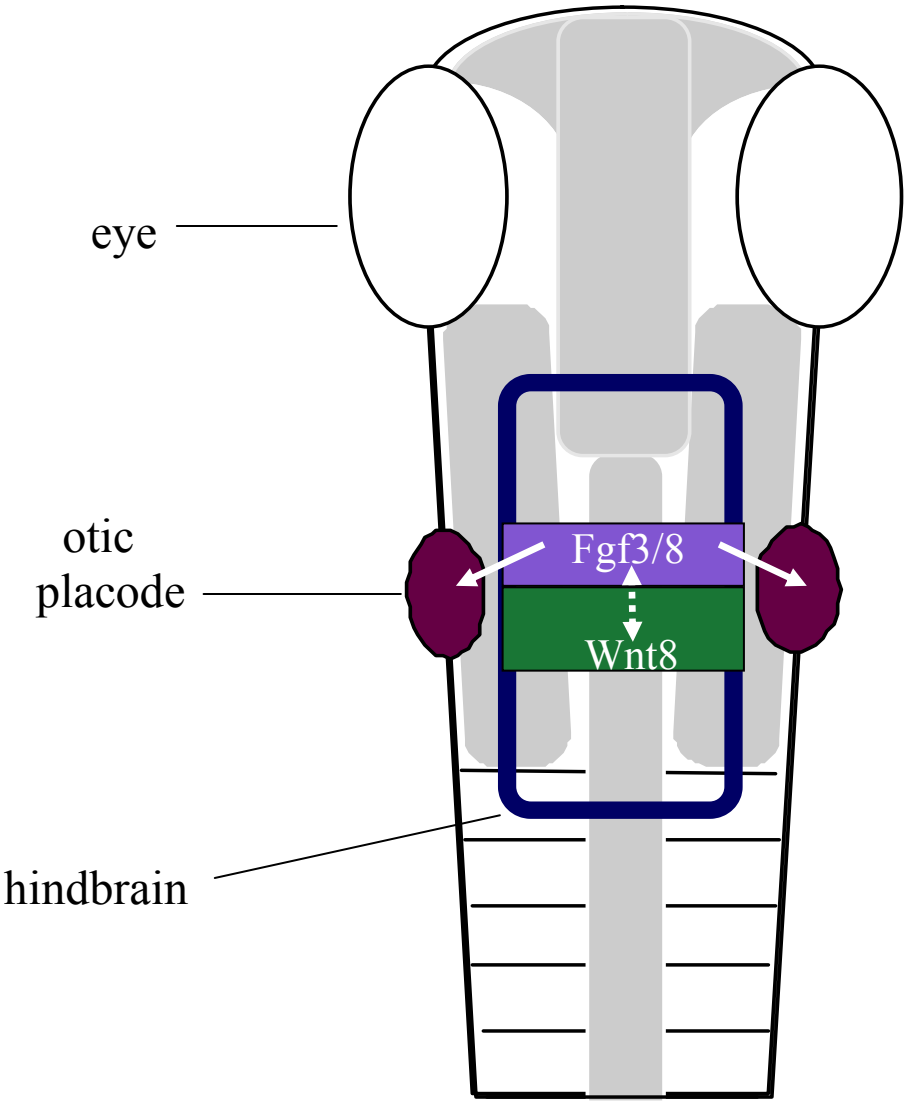

Figure 27. A model for otic induction. Positive interactions between the Fgf and Wnt signaling pathways are required to establish *fgf3* and *fgf8* expression domains in r4 (blue) as well as *wnt8* expression in r5 and 6 (green). Fgf3 and Fgf8, but Wnt8, then signal directly to the preotic cells to induce the otic placode (red).

the expression of otic genes such as *pax8* and the newly induced otic cells go on to form the otic placode.

These results may also shed light on results observed by Ladher and colleagues who report activation of *Fgf3* expression in explant cultures exposed to Wnt8c. This *Fgf3* expression was interpreted as an indicator of otic placode induction even though *Fgf3* expression is not observed in the chick otic region until after the formation of the otic vesicle. *Fgf3* is expressed in the early chick hindbrain (Mahmood et al. 1995), however, suggesting that Wnt8c induction of *Fgf3* may reflect an early aspect of hindbrain development. Therefore, exogenous Wnt8c could initiate a feedback loop similar to the one seen in zebrafish. The endogenous Fgf3 may then cooperate with exogenous Fgf19 to induce a full range of otic markers, producing the results observed by Ladher and colleagues.

Surprisingly, our Fgf misexpression experiments only produced ectopic otic tissue when the misexpressing cells resided near the endogenous preplacodal domain. We occasionally observed scattered cells expressing otic markers in other locations, such as the neural plate, but these cells did not display the characteristic cohesive grouping we usually observe along the preplacodal domain. Furthermore, these cells never differentiate into a vesicle-like structure. Therefore, we conclude that cells in the preplacodal domain are the most competent to respond to Fgf inducers. This suggests that the preplacodal cells are partially specified toward placodal fate and is evidence for the existence of a general state which all placodal tissues must pass through. This notion supports the preplacodal field hypothesis discussed in the Introduction which states that

all placodes emerge from a common ectodermal region with unique developmental history and molecular character. Our current model of placode induction details that the preplacodal domain is specified by an intermediate level of axial signals. In response to these signals, the preplacodal domain upregulates tissue-specific transcription factors such as Dlx. The preplacodal domain is therefore a tissue set apart from the neural and epidermal ectodermal tissues to await local inducers which provide specific placodal fate. The otic and the lens placodes, for instance, both derive from cells with similar molecular history but it is the different local inducers which direct ultimate cell fate. Fgf signaling is normally the trigger for otic induction. However, when misexpressed in more anterior regions of the preplacodal domain, Fgf signals can override lens induction, for example, and result in the formation of ectopic otic tissue.

FEEDBACK BETWEEN THE WNT AND FGF PATHWAYS

While Wnt8 is required for normal expression of *fgf3* and *fgf8* in the hindbrain, Fgf signaling is also required for proper expression of *wnt8*-ORF2 in the r5/6 domain. It is not known whether this mutual regulation is direct or indirect, but it could reflect the activity of a positive feedback loop operating within the hindbrain. A similar Fgf-Wnt feedback loop acts in other tissues in developing vertebrate embryos. Midbrain-hindbrain boundary (MHB) tissue expresses an anterior domain of Wnt1 immediately anterior to an Fgf8 expression domain. These two factors are required to maintain MHB tissue and they therefore are each necessary for the other's expression. Wnt1 and Fgf8 then cooperate to organize surrounding neural tissue (reviewed by Wurst and Bally-Cuif, 2001). Induction of both genes is under the control of a variety of upstream regulators.

The r4 region of the hindbrain appears to be a second signaling center that helps pattern the hindbrain. Expression of *fgf3* and *fgf8* in the r4 domain is necessary to pattern more posterior hindbrain segments, including r5 (Walshe et al., 2002; Maves et al., 2002; Wiellette and Sive, 2003). A role for Fgf3 and Fgf8 in hindbrain patterning may explain our observation that Fgf knockdown embryos fail to express normal levels of *wnt8* in r5 and 6. The posteriorizing function of Wnt8 may likewise be required for proper hindbrain pattering, including *fgf3* and *fgf8* expression in r4.

Fgf signaling has long been known to operate in limb formation (reviewed by Tickle and Munsterberg, 2001). Fgf10 in the limb mesenchyme induces expression of *fgf8* in the apical ectodermal ridge (AER). Fgf8 signaling to the underlying mesenchyme is then required for proper limb outgrowth. More recently, Wnt signaling has been shown to act in a positive feedback loop with Fgf in chick limb tissue. Wnt2b (in the forelimb) and Wnt8c (in the hindlimb) appear to be necessary for *fgf10* expression in the limb mesenchyme. In the ectoderm Fgf10 induces *fgf8* expression via activation of Wnt3a signaling. The loop is completed by Fgf8 maintenance of *fgf10* expression. Hence, a signaling network involving the positive action of both Wnt and Fgf family members may be acting via tissue-tissue organogenesis signaling to pattern the MHB, hindbrain and the limb bud.

FUTURE DIRECTIONS IN FGF FUNCTION DURING OTIC INDUCTION

There remain several unresolved issues relating to Fgf-induced otic placode development. One area which remains unexplored is determining the relative roles of Fgf3 and Fgf8 in otic induction. These Fgf ligands appear to share some functions and

therefore may be signaling through the same molecular pathway. In fact, any Fgf ligand binding to its tyrosine kinase receptor would be predicted to have the same effect: activation of the Ras pathway culminating in nuclear localization of MAP kinase and activation of target genes. In this context, it is feasible that Fgf3 and Fgf8 are activating identical downstream mediators even though they have differential receptor affinities. Their redundant functions, therefore, would refer to the sum total of activated receptor complexes. Loss of one ligand would decrease the effective range of Fgf signaling and could result in the small ear phenotype we observe. However, ligand-specific functions are also a possibility. It has been shown that different ligand-receptor interactions result in differential cellular responses (Prudovsky et al., 1996). Fgf3 and Fgf8 activate different receptor isoforms (Ornitz et al., 1996) which may modulate the effect on downstream transcriptional effectors. This hypothesis suggests that Fgf3 and Fgf8 have distinct functions and may function in parallel pathways.

The molecular effects of Fgf signaling to otic tissue also remain largely unknown. Expression of otic markers such as *pax8* and *pax2a* are dependent upon Fgf signaling but it is not known whether they are direct targets of FGF/MAPK activity. In addition, the targets of these transcription factors and their ultimate role in otic development are unknown. The complete picture of the role of Fgf signaling in otic induction will remain unclear until the identity and functions of all the downstream effectors are uncovered.

Our data indicate that Wnt signaling is not operating in parallel with Fgf3 and Fgf8. However, this does not rule out the possibility that there are still other otic-

inducing factors in addition to these Fgf ligands. One observation which supports this idea is the recent finding that at least one early otic marker is retained in embryos lacking Fgf3 and Fgf8 function (our unpublished observations). This marker is the forkhead class transcription factor, *foxi1*. Functional analyses of Foxi1 have demonstrated a role in otic development (Solomon et al., 2003). Severe *foxi1* mutants lack otic tissue as viewed by both morphology and otic marker expression suggesting otic induction is impaired. Importantly, the early otic marker *pax8* is ablated in *foxi1* mutants and Foxi1 misexpression can cell-autonomously induce expression of *pax8*. *foxi1* is initially expressed throughout the ventral and lateral ectoderm and is then later retained in preotic tissue. This expression domain is reminiscent of the expression pattern of BMP ligands. Hence, it remains a possibility that BMP is also playing a role in otic placode induction by inducing *foxi1* expression. Alternatively, Foxi1 and BMP may be providing competence to respond to otic-inducing signals. Indeed, loss of otic competence would be predicted to cause a similar phenotype as failure of otic induction. Whether BMP signaling is providing competence to respond to otic inducers or acting as an otic inducer itself remains to be seen. An early BMP function in axial patterning complicates analysis of this pathway, since complete loss of BMP results in expansion of the neural plate at the expense of preplacodal and ventral ectoderm (Nguyen et al., 1998). Conditional mutant alleles of BMP pathway components would help determine the role of this pathway in otic induction.

MSX REPRESSION IS REQUIRED FOR PLACODAL DEVELOPMENT

Our current model of placodal development involves the setting aside of a general preplacodal domain which can later be specified by local inducers. Msx repressors have been shown to inhibit differentiation by preventing withdrawal from the cell cycle (Hu et al., 2001). Several Msx family members are expressed in and around the preplacodal domain (this work). To further our understanding of placodal development, we sought to analyze the function of these Msx transcription factors via loss-of-function studies. We find that embryos depleted for Msx undergo normal placode induction, but that later differentiation is perturbed and placodal tissues undergo increased levels of cell death. How Msx functions within the context of placode induction is unclear, since premature differentiation of the preplacodal domain in *msx* morphants would be expected to impair competence to local placode inducing signals. Impaired competence would be expected to lead to perturbed placodal specification, a phenotype we do not observe. Instead, *msx* may function by restricting the activity of transcriptional activators such as Dlx. This suggests that, in *msx* morphants, Dlx activity is heightened. Moderate overexpression of Dlx proteins causes widespread necrosis (our unpublished observations); indicating Dlx function must be attenuated for proper development. Hence, an increased level of active Dlx proteins is a potential explanation for the cell death we observe in placodal tissues. A similar mechanism may be in place in neural crest progenitors and the dorsal CNS. Since Dlx is not expressed in the neural plate Msx would have other as yet unidentified targets. Indeed, molecular identification

of additional Msx target genes or proteins would allow for future studies on Msx function in different contexts, such as roles in mesoderm and neural patterning.

Although the molecular function of Msx proteins remains unclear, we present two general models of possible Msx roles in placodal development. The first is the more direct. Msx may be required cell-autonomously in placodal tissues to inhibit the function of transcriptional activators such as Dlx as discussed above. Alternatively, Msx function may be more indirect. Msx repression may be required within the neural plate, a tissue which expresses *msxB, msxC* and *msxE* at the time we note defects in placodal development. This model suggests a non-autonomous function for Msx, where Msx might be required for the production or repression of an unknown signal emanating from the neural plate. Little evidence exists which demonstrates the presence of such a signal however, studies of Fgf3 function show that this hindbrain factor is responsible for both inducing and pattering the otic placode. Fgf3 expression is retained in r4 of the hindbrain well after otic induction has occurred and has the ability to induce anterior character to rostral regions of the otic placode (Kwak et al., 2002). A role for Msx in regulating the expression of another hindbrain-derived factor required for normal placodal development has yet to be demonstrated. Identifying new Msx target genes or proteins would prove invaluable in demonstrating a function for Msx in neural signaling.

MSX-DLX INTERACTIONS

We provide evidence that *msx* genes play a role in the refinement of the boundary between the preplacodal domain and the neural plate by inhibitory interactions with Dlx family members. This is consistent with proposed roles for Msx and Dlx in

tissue-tissue interactions (reviewed by Bendall and Abate-Shen, 2000). In mammals, Msx1 and Msx2 are expressed in tooth mesenchyme and the overlying dental epithelium. In this context, Msx mediates signaling interactions, including BMP and Fgf signaling, between these two tissue layers (Jernvall and Theslaff, 2000). Msx1 and Msx2 are redundantly required for early tooth development as shown by the *Msx1 -/-; Msx2 -/-* mutant phenotype (Bei and Maas, 1998). These double mutants fail to undergo early tooth differentiation, a phenotype similar to the *Dlx1; Dlx2* mutant phenotype (Thomas et al., 1997). These *dlx* genes are expressed in an overlapping domain with *msx1* and *msx2*. This observation suggests that Msx and Dlx may not always act in opposition and suggests context-dependent inhibitory interactions between these two families. Alternatively, the level of Dlx function may be critical during tooth development and therefore increasing or decreasing Dlx activity by modulating Msx function could result in the same developmental defects.

msx and *dlx* genes are also expressed in the limb bud, another system that involves extensive tissue-tissue interactions (Bendall and Abate-Shen, 2000). In the mouse, *Msx1* and *Msx2* are both expressed in the AER and underlying mesenchyme along with several *Dlx* genes. While a role for Msx or Dlx in these tissues has not yet been reported, the expression domains are consistent with a function in maintenance of an undifferentiated population of cells which is actively dividing. Downregulation of *msx* expression correlates with decreased cell proliferation and discontinuation of limb outgrowth. Hence, one model for Msx function in the limb is inhibitory interactions with Dlx proteins resulting in delayed differentiation. Relieving the Msx repression

would enable Dlx to activate differentiation. Further analysis of Msx and Dlx mutants will be required to test this hypothesis.

CONCLUSION

This dissertation focuses on the molecular mechanisms of inner ear development as well as preplacodal development as a whole. General mechanisms of pattern formation are presented which will hopefully bring to light new paradigms of cell-cell communication, tissue interactions and the cellular response resulting in these events. Future goals of this research will be to elucidate the ultimate molecular players regulating cell rearrangements which result in the intricate three-dimensional pattern within developing placodal derivatives as well as identifying new genes linked to human deafness and vestibular defects.

REFERENCES

Adamska, M., Leger, S., Brand, M., Hadrys, T., Braun, T., and Bober, E. (2000). Inner ear and lateral line expression of a zebrafish *Nkx5-1* gene and its downregulation in the ears of *FGF8* mutant, *ace*. *Mechanisms of Development* **97**, 161-165.

Alexandre, D., Clarke, J. D., Oxtoby, E., Yan, Y. L., Jowett, T., and Holder, N. (1996). Ectopic expression of Hoxa-1 in the zebrafish alters the fate of the mandibular arch neural crest and phenocopies a retinoic acid-induced phenotype. *Development* **122**, 735-746.

Amalric, F., Bouche, G., Bonnet, H., Brethenou, P., Roman, A. M., Truchet, I., and Quarto, N. (1994). Fibroblast growth factor-2 (FGF-2) in the nucleus: translocation process and targets. *Biochem. Pharmacol*. **47**, 111-115.

Appel, B. and Eisen, J. S. (1998). Regulation of neuronal specification in the zebrafish spinal cord by *Delta* function. *Development* **125**, 371-380.

Bach, A. Lallemand, Y., Nicola, M. A., Ramos, C., Mathis, L. Maufras, M., and Robert, B. (2003). Msx1 is required for dorsal diencephalon patterning. *Development* **130,** 4025-4036.

Baker, C. V. and Bronner-Fraser, M. (2001) Vertebrate cranial placodes I. Embryonic induction. *Dev. Biol.* **232**, 1-61.

Baranski, M., Berdougo, E., Sandler, J.S., Darnell, D.K., and Burrus, L.W. (2000). The dynamic expression pattern of frzb-1 suggests multiple roles in chick development. *Dev. Biol.* **217**, 25-41.

Beanan, M. J., Feledy, J. A. and Sargent, T. D. (2000). Regulation of early expression of *Dlx3*, a *Xenopus* anti-neural factor, by β-catenin signaling. *Mech. Dev*. **91**, 227-235.

Begbie, J. and Graham, A. (2001). The ectodermal placodes: a dysfunctional family. *Phil. Trans. R. Soc. Lond.* **356**, 1655-1660.

Bei, M. and Maas, R. (1998). FGFs and BMP4 induce both *Msx1*-independent and *Msx1*-dependent signaling pathways in early tooth development. *Development* **125,** 4325-4333.

Bendall, A. J. and Abate-Shen, C. (2000). Roles for Msx and Dlx homeoproteins in vertebrate development. *Gene* **247**, 17-31.

Bever, M. M. and Fekete, D. M. (2002). Atlas of the developing inner ear in zebrafish. *Dev. Dyn*. **223**, 536-543.

Bouillet, P., Oulad-Abdelghani, M., Ward, S. J., Bronner, S., Chambon, P. and Dolle, P. (1996). A new mouse member of the *Wnt* gene family, *mWnt-8,* is expressed during early embryogenesis and is ectopically induced by retinoic acid. *Mech. Dev*. **58**, 141-152.

Brand, M. Heisenberg, C.-P., Jiang, Y.-L., Beuchle, D., Lun, K., Furutani-Seiki, M., Granato, M., Hafter, P., Hammerschmidt, M., Kane, D., Kelsh, R., Mullins, M., Odenthal, J., van Eeden, F. J. M., and Nüsslein-Valhard, C. (1996). Mutations in zebrafish genes affecting the formation of the boundary between the midbrain and hindbrain. *Development* **123**, 179-190.

Brigande, J. V., Keirnan, A. E. Gao, X., Iten, L. E. and Fekete, D. M. (2000). Molecular genetics of pattern formation in the inner ear: do compartment boundaries play a role? *Proc. Natl. Acad. Sci. USA* **97**, 11700-11706.

Catron, K. M., Iler, N., and Abate, C. (1993). Nucleotides flanking a conserved TAAT core dictate the DNA binding specificity of three murine homoedomain proteins. *Mol. Cell Biol.* **13**, 2354-2365.

Catron, K. M., Zhang, H., Marshall, S. C., Inostroza, J. A., Wilson, J. M., and Abate, C. (1995). Transcriptional repression by Msx-1does not require homeodomain DNA binding sites. *Mol. Cell Biol.* **15,** 861-871.

Chang, Z., Meyer, K., Rapraeger, A. C., and Friedl, A. (2000). Differential ability of heparan sulfate proteoglycans to assemble the fibroblast growth factor receptor complex in situ. *FASEB J.* **14**, 137-144.

Chisaka, O., Musci, T. S., and Capecchi, M. R. (1992). Development defects of the ear, cranial nerves and hindbrain resulting from targeted disruption of the mouse homeobox gene *Hox-1.6*. *Nature* **355**, 516-520.

Cordes, S. P., and Barsh, G. S. (1994). The mouse segmentation gene *kr* encodes a novel basic domain-leucine zipper transcription factor. *Cell* **79**, 1025-1034.

Crossley, P. H. and Martin, G. R. (1995). The mouse *Fgf8* gene encodes a family of polypeptides and is expressed in regions that direct outgrowth and patterning in the developing embryo. *Development* **121,** 439-451.

Deardorf, M. A. and Klein, P. S. (1999). *Xenopus frizzled-2* is expressed highly in the developing, otic vesicle and somites. *Mech. Dev.* **87**, 229-233.

Deol, M. S. (1964). The abnormalities of the inner ear in *kreisler* mice. *J. Embryol. Exp. Morph.* **12**, 475-490.

Deol, M. S. (1966). Influence of the neural tube on differentiation of the inner ear in the mammalian embryo. *Nature* **209,** 219-220.

Depew, M. J., Liu, J. K., Long, J. E., Presley, R., Meneses, J. J., Pedersen, R. A. and Rubenstein, J. L. R. (1999). *Dlx5* regulates regional development of the branchial arches and sensory capsules. *Development* **126**, 3831-3846.

Dorsky, R. I., Sheldahl, L. C. and Moon, R. T. (2002). A transgenic Lef1/ß-catenin-dependent reporter is expressed in spatially restricted domains throughout zebrafish development. *Dev. Biol.* **241**, 229-237.

Dorsky, R. I., Itoh, M., Moon, R. T. and Chitnis, A. (2003) Two tcf3 genes cooperate to pattern the zebrafish brain. *Development* **130**, 1937-1947.

Draper, B. W., Stock, D. W., and Kimmel, C., B. (2003). Zebrafish *fgf24* functions with *fgf8* to promote posterior mesodermal development. *Development* **130,** 4639-4654.

Ekker, M., Akimenko, M. A., Bremiller, R., and Westerfield, M. (1992). Regional expression of three homeobox genes in the inner ear of zebrafish embryos. *Neuron* **9**, 27-35.

Ekker, M., Akimenko, M. A., Allende, M. L., Smith, R., Drouin, G., Langille, R. M., Weinberg, E. S., and Westerfield, M. (1997). Relationships among *msx* gene structure and function in zebrafish and other vertebrates. *Mol. Biol. Evol.* **14,** 1008-1022.

Epstein, D. J., Vekemans, M., and Gros, P. (1991). *splotch* (*sp2H*), a mutation affecting development of the mouse neural tube, shows a deletion within the paired homeodomain of *Pax-3*. *Cell* **67**, 767-774.

Esteve, P., Morcillo, J. and Bovolenta, P. (2000). Early and dynamic expression of cSfrp1 during chick embryo development. *Mech. Dev.* **97**, 217-221.

Feledy, J. A., Beanan, M. J., Sandoval, J. J., Goodrich, J. S., Lim, J. H., Matsuo-Takasaki, M., Sato, S. M. and Sargent, T. D. (1999). Inhibitory patterning of the anterior neural plate in *Xenopus* by homeodomain factors *Dlx3* and *Msx1*. *Dev. Biol*. **212**, 455-464.

Fürthauer, M., Thisse, C. and Thisse, B. (1997). A role for FGF-8 in the dorsoventral patterning of the zebrafish gastrula. *Development* **124**, 4253-4264.

Fürthauer, M., Reifers, F., Brand, M., Thisse, B. and Thisse, C. (2001). *sprouty4* acts in vivo as a feedback-induced antagonist of FGF signaling in zebrafish. *Development.* **128**, 2175-2186.

Gallagher, B. C., Henry, J. J., and Grainger, R. M. (1996). Inductive processes leading to inner ear formation during *Xenopus* development. *Dev. Biol.* **175**, 95-107.

Glinka, A., Wu, W., Delius, H., Monaghan, A. P., Blumenstock, C. and Niehrs, C. (1998). Dickkopf-1 is a member of a new family of secreted proteins and functions in head induction. *Nature* **391**, 357-362.

Goulding, M. D., Chalepakis, G., Deutsch, U., Erselius, J. R., and Gruss, P. (1991). Pax-3, a novel murine DNA binding protein expressed during early neurogenesis. *EMBO J.* **5,** 1135-1147.

Graham, A. and Begbie, J. Neurogenic placodes: a common front. *Trends Neurosci.* (2000) **23,** 313-316.

Gritsman, K. Zhang, J., Cheng, S., Heckscher, E., Talbot, W. A., and Schier, A. F. (1999). The EGF-CFC protein one-eyed pinhead is essential for nodal signaling. *Cell* **97**, 121-132.

Groves, A. K., and Bronner-Fraser, M. (2000). Competence, specification and commitment in otic placode induction. *Development* **127,** 3489-3499**.**

Guimond, S. E., and Turnbull, J. E. (1999). Fibroblast growth factor receptor signalling is dictated by specific heparan sulphate saccharides. *Current Biology* **9**, 1343-1346.

Haddon, C. and Lewis, J. (1996). Early ear development in the embryo of the zebrafish, *Danio rerio*. *J. Comp. Neurol*. **365**, 113-128.

Haddon, C., Jiang, Y.-L., Smithers, L. and Lewis, J. (1998a). *Delta-Notch* signalling and the patterning of sensory cell differentiation in the zebrafish ear: evidence from the *mind bomb* mutant. *Development* **125**, 4637-4644.

Haddon, C., Smithers, L., Schneider-Maunoury, S., Coche, T., Henrique, D. and Lewis, J. (1998b). Multiple *delta* genes and lateral inhibition in zebrafish primary neurogenesis. *Development* **125**, 359-370.

Harrison, R. G. (1935). Factors concerned in the development of the ear in *Ablystoma punctatum*. *Anat. Rec.* **64** (suppl. 1) 38-39.

Hashimoto, H., Itoh, M., Yamanaka, Y., Yamashita, S., Shimizu, T., Solnica-Krezel, L., Hibi, M. and Hirano, T. (2000). Zebrafish Dkk1 functions in forebrain specification and axial mesendoderm formation. *Dev. Biol.* **217**, 138-152.

Hauptmann, G. and Gerster, T. (2000). Combined expression of zebrafish *Brn-1*- and *Brn-2*-related POU genes in the embryonic brain, pronephric primordium, and pharyngeal arches. *Dev. Dyn*. **218**, 345-358.

Heller, N., and Brandli, A. W. (1999). *Xenopus Pax-2/5/8* orthologues: novel insights into *Pax* gene evoulution and identification of *Pax8* as the earliest marker for otic and pronephric cell lineages. *Dev. Genet.* **24**, 208-219.

Hidalgo-Sanchez, M., Alvarado-Mallart, R. M., and Alvarez I. S. (2000). *Pax2*, *Otx2*, *Gbx2* and *FGF8* expression in early otic vesicle development. *Mechanisms of Development* **95**, 225-229.

Hu, G., Lee, H., Price, S. M., Shen, M. M., and Abate-Shen, C. (2001). Msx homeobox genes inhibit differentiation through upregulation of *cyclin D1*. *Development* **128,** 2373-2384.

Hume, C. R. and Dodd, J. (1993). *Cwnt-8c:* a novel Wnt gene with a potential role in primitive streak formation and hindbrain organization. *Development* **119**, 1147-1160.

Hussein, S. M., Duff, E. K., and Sirard, C. (2003). Smad4 and beta-catenin co-activators functionally interact with lymphoid-enhancing factor to regulate graded expression of Msx2 *J. Biol. Chem.* **278,** 48805-48814.

Hutson, M. R., Lewis, J. E., Nguyen-Luu, D., Lindberg, K. H. and Barald, K. F. (1999). Expression of Pax2 and patterning of the chick inner ear. *J. Neurocytol.* **28**, 795-807.

Ishimura, A., Maeda, R., Takeda, M., Kikkawa, M., Daar, I. O., and Maeno, M. (2000). Involvement of BMP-4/msx1 and FGF pathways in neural induction in the *Xenopus* embryo. *Develop. Growth. Differ.* **42,** 307-316.

Jacobson, A. G. (1963). The determination and positioning of the nose, lens, and ear. I. Interactions within the ectoderm, and between the ectoderm and underlying tissue. *J. Exp. Zool.* **154**, 273-283.

Jernvall, J. and Thesleff, I. (2000). Reiterative signaling and patterning during mammalian tooth morphogenesis. *Mech Dev.* **92,** 19-29.

Jowett, T. (1996). Double fluorescent in situ hybridization to zebrafish embryos. *Trends Genet.* **12**, 387-389.

Kan, M., Wu, X., Wang, F., and McKeehan, W. L. (1999). Specificity for fibroblast growth factors determined by heparan sulfate in a binary complex with the receptor kinase. *J. Biol. Chem.* **274**, 15947-15952.

Kelly, G. M. and Moon, R. T. (1995). Involvement of *wnt1* and *pax2* in the formation of the midbrain-hindbrain boundary in the zebrafish gastrula. *Dev. Genet.* **17,** 129-140.

Kelly, G. M., Greenstein, P., Erezyilmaz, D. F. and Moon, R. T. (1995). Zebrafish *wnt8* and *wnt8b* share a common activity but are involved in distinct developmental pathways. *Development* **121**, 1787-1799.

Kiefer, P. Strahle, U., and Dickson, C. (1996a). The zebrafish *Fgf-3* gene: cDNA sequence, transcript structure and genomic organization. *Gene* **168**, 211-215.

Kiefer, P., Mathieu, M., Mason, I., and Dickson, C. (1996b). Secretion and mitogenic activity of zebrafish FGF3 reveal intermediate properties relative to mouse and *Xenopus* homologs. *Oncogene* **12**, 1503-1511.

Kim, C. H., Oda, T., Itoh, M., Jiang, D., Artinger, K. B. Chandrasekharappa, S. C., Driever, W. and Chitnis, A. B. (2000). Repressor activity of Headless/Tcf3 is essential for vertebrate head formation. *Nature* **407**, 913-916.

Knouff R. A. (1935). The developmental pattern of ectodermal placodes in *Rana pipiens*. *J. Comp. Neurol.* **62,** 17-71.

Kohan, R. (1944). The chordomesoderm as an inducer of the ear vesicle. *C. R. (Dokl.) Acad. Sci. URSS* **45,** 39-41.

Kos, R., Tuker, R. P., Hall, R., Duong, T. D. and Erickson, C. A. (2003). Methods for introducing morpholinos into the chick embryo. *Dev. Dyn.* **226**, 470-477.

Koshida, S., Shinya, M., Nikaido, M., Uneo, N., Schulte-Merker, S., Kuroiwa, A. and Takeda, H. (2002). Inhibition of BMP activity by the FGF signal promotes posterior neural development in zebrafish. *Dev. Biol.* **244**, 9-20.

Kozlowski, D. J., Murakami, T., Ho, R. K., and Weinberg, E. S. (1997). Regional cell movement and tissue patterning in the zebrafish embryo revealed by fate mapping with caged fluorescein. Biochem. *Cell Biol.* **75**, 551-562.

Krauss, S., Johansen, T., Korzh, V. and Fjose, A. (1991). Expression of the zebrafish paired box gene *pax[zf-b]* during early neurogenesis. *Development* **113**, 1193-1206.

Krauss, P. and Lufkin, T. (1999). Mammalian *Dlx* homeobox gene control of craniofacial and inner ear morphogenesis. *J. Cell. Biochem*. **Suppl. 32/33**, 133-140.

Kudoh, T., Wilson, S. W. and Dawid, I. B. (2002). Distinct roles for Fgf, Wnt and retinoic acid in posteriorizing the neural ectoderm. *Development* **129**, 4335-4346.

Kwak, S.-J., Phillips, B. T., Heck, R. and Riley, B. B. (2002). An expanded domain of *fgf3* expression in the hindbrain of zebrafish *valentino* mutants results in mis-patterning of the otic vesicle. *Development* **129**, 5279-5287.

Ladher, R. K., Anakwe, K. U., Gurney, A. L., Schoenwolf, G. C. and Francis-West, P. H. (2000a). Identification of synergistic signals initiating inner ear development. *Science* **290**, 1965-1968.

Ladher, R.K., Church, V.L., Allen, S., Robson, L., Abdelfattah, A., Brown, N.A., Hattersley, G., Rosen, V., Luyten, F.P., Dale, L., and Francis-West, P.H. (2000b). Cloning and expression of the Wnt antagonist Sfrp-2 and Frzb during chick development. *Dev. Biol.* **218**, 183-198.

Leger, S. and Brand, M. (2002). Fgf8 and Fgf3 are required for zebrafish ear placode induction, maintenance, and inner ear patterning. *Mech. Dev.* **119**, 91-108.

Lekven, A. C., Helde, K. A., Thorpe, C. J., Rooke, R. R. and Moon, R. T. (2000). Reverse genetics and zebrafish. *Physiol. Genomics* **2**, 37-48.

Lekven, A. C., Thorpe, C. J., Waxman, J. S. and Moon, R. T. (2001). Zebrafish *wnt8* encodes two Wnt8 proteins on a bicistronic transcript and is required for mesoderm and neurectoderm patterning. *Dev. Cell* **1**, 103-114.

Lewis, E. R., Leverenz, E. L. and Bialek, W. S. (1985). *The vertebrate inner ear.* CRC Press, Boca Raton, FL.

Li, Y., Allende, M. L., Finkelstein, R. and Weinberg, E. S. (1994). Expression of two zebrafish *orthodenticle*-related genes in the embryonic brain. *Mech. Dev*. **48**, 229-244.

Li, X., Oghi, K. A., Zhang, J., Krones, A., Bush, K. T., Glass, C. K., Nigam, S. K., Aggarwal, A. K., Maas, R., Rose, D. W., and Rosenfeld, M. G. (2003). Eya protein phosphatase activity regulates Six-Dach-Eya transcriptional effects in mammalian organogenesis. *Nature* **426**, 247-254.

Liu, D., Chu, H., Maves, L., Yan, Y-L., Morcos, P.A., Postlewait, J. H.,and Westerfield, M. (2003). Fgf3 and Fgf8 dependent and independent transcription factors are required for otic placode induction. *Development* **130**, 2213-2224.

Lombardo, A., Isaacs, H. V. and Slack, J. M. W. (1998). Expression and functions of *FGF-3* in *Xenopus* development. *Int. J. Dev. Biol*. **42**, 1101-1107.

Lombardo, A., and Slack, J. M. W. (1998). Postgastrulation effects of fibroblast growth factor on *Xenopus* development. *Developmental Dynamics* **212,** 75-85.

Lufkin, T., Dierich, A. LeMeur, M., Mark, M., and Cahmbon, P. (1991). Disruption of the *Hox 1.6* homeobox gene results in defects in a region corresponding to its rostral domain of expression. *Cell* **66**, 1105-1119.

Maden, M., Gale, E., Kosteeskii, and Zile, M. (1996). Vitamin A-deficient quail embryos have half a hindbrain and other neural defects. *Curr. Biol.* **6**, 417-426.

Maeda, R., Kobayashi, A., Sekine, R., Lin, J.-J., Kung, H., and Maeno, M. (1997). *Xmsx-1* modifies mesodermal tissue pattern along dorsoventral axis in *Xenopus laevis* embryo. *Development* **124**, 2553-2560.

Mahmood, R., Kiefer, P., Guthrie, S., Dickson, C. and Mason, I. (1995). Multiple roles for FGF-3 during cranial neural development in the chicken. *Development* **121**, 1399-1410.

Mahmood, R., Mason, I. J. and Morrisskay, G. M. (1996). Expression of *FGF-3* in relation to hindbrain segmentation, otic pit position and pharyngeal arch morphology in normal and retinoic acid exposed mouse embryos. *Anat. & Embryol.* **194**, 13-22

Mansour, S. L., Goddard, J. M. and Capecchi, M. R. (1993). Mice homozygous for a targeted disruption of the proto-oncogene *int-2* have developmental defects in the tail and inner ear. *Development* **117**, 13-28.

Maroon, H., Walshe, J., Mahmood, R., Keifer, P., Dickson, C. and Mason, I. (2002) Fgf3 and Fgf8 are required together for formation of the otic placode and vesicle. *Development* **129**, 2099-2108.

Marshall, H., Nonchev, S., Sham, M. H., Muchamore, I., Lumsden, A., and Krumlauf, R. (1992). Retinoic acid alters hindbrain Hox code and induces transformation of rhombomeres 2/3 into a 4/5 identity. *Nature* **360**, 737-741.

Mathieu, M., Chatelain, E., Ornitz, D., Bresnick, J., Mason, I., Kiefer, P., and Dickson, C. (1995). Receptor binding and mitogenic properties of mouse fibroblast growth factor 3 – modulation of response by heparin. *J. Biol. Chem.* **270**, 24197-24203.

Matsuda, M. and Keino, H. (2000). Roles of ß-catenin in inner ear development in rat embryos. *Anat. Embryol.* **202**, 39-48.

Maves, L., Jackman, W. and Kimmel, C.B. (2002). FGF3 and FGF8 mediate a rhombomere 4 signaling activity in the zebrafish hindbrain. *Development.* **129,** 3825-3837.

Mazan, S., Jailard, D, Baratte, B. and Janvier, P. (2001). *Otx1* gene-controlled morphogenesis of the horizontal semicircular canal and the origin of the gnathostome characteristics. *Evol & Dev*. **2**, 186-193.

McKay, I. J., Lewis, J. and Lumsden, A. (1996). The role of *FGF-3* in early inner ear development: an analysis in normal and *kreisler* mutant mice. *Dev. Biol.* **174**, 370-378.

McLarren, K. W., Litsiou, A. and Streit A. (2003). DLX5 positions the neural crest and preplacode region at the border of the neural plate. *Dev. Biol*. **259**, 34-47.

Mendonsa, E. S., and Riley, B. B. (1999). Genetic analysis of tissue interactions required for otic placode induction in the zebrafish. *Dev. Biol.* **206**, 100-112.

Meyers, E. N., Lewandoski, M., and Martin, G. R. (1998). An *FGF8* mutant alleleic series generated by Cre- and FLP-mediated recombination. *Nature Genetics* **18**, 136-141.

Moens, C. B., Yan, Y-L., Appel, B., Force, A. G. and Kimmel, C. B. (1996). *valentino*: a zebrafish gene required for normal hindbrain segmentation. *Development* **122**, 3981-3990.

Moens, C. B., Cordes, S. P., Giorgianni, M. W., Barsh, G. S., and Kimmel, C. B. (1998). Equivalence in the genetic control of hindbrain segmentation in fish and mouse. *Development* **125**, 381-391.

Momi, A., Yoda, H., Steinbessier, H., Fagotto, F., Kondoh, H., Kudo, A., Driever, W. and Furutani-Seiki, M. (2003). Analysis of Wnt8 for neural posteriorizing factor by identifying Frizzled 8c and Frizled 9 as functional receptors for Wnt8. *Mech. Dev.* **120**, 477-489.

Morsli, H., Tuorto, F., Choo, D., Postiglione, M. P., Simeone, A. and Wu, D. K. (1999). *Otx1* and *Otx2* activities are required for the normal development of the mouse inner ear. *Development* **Suppl.126**, 2333-2343.

Nguyen, V. H., Schmid, B., Trout, J., Connors, S. A., Ekker, M., Mullins, M. C. (1998) Ventral and lateral regions of the zebrafish gastrula, including the neural crest progenitors, are established by a *bmp2b/swirl* pathway of genes. *Dev. Biol.* **199,** 93-110.

Nasevicius, A., and Ekker, S. C. (2000). Effective targeted gene 'knockdown' in zebrafish. *Nature Genetics* **26**, 216-220.

Niederreither, K., Vermot, J., Schuhbaur, B., Chambon, P., and Dolle, P. (2000). Retinoic acid synthesis and hindbrain patterning in the mouse embryo. *Development* **127**, 75-85.

Odenthal, J., and Nusslein-Volhard, C. (1998). *fork head* domain genes in zebrafish. *Dev. Genes Evol.* **208,** 245-258.

Ornitz, D. M., Xu, J., Colvin, J. S., McEwen, D. G., CacArthur, C. A., Coulier, F., Gao, G., and Goldfarb, M. (1996). Receptor specificity of the fibroblast growth factor family. *J. Biol. Chem.* **271**, 15292-15297.

Oxtoby, E. and Jowett, T. (1993) Cloning of the zebrafish *krox-20* gene *(krx-20)* and its expression during hindbrain development. *Nucleic Acid Res.* **21**, 1087-1095.

Ozaki H., Nakamura K., Funahashi J., Ikeda K., Yamada G., Tokano H., Okamura H. O., Kitamura K., Muto S., Kotaki H., Sudo K., Horai R., Iwakura Y., Kawakami K. (2004) *Six1* controls patterning of the mouse otic vesicle. *Development* **131,** 551-562.

Papalopulu, N., Clarke, J. D. W., Bradley, L., Wilkinson, D., Krumlauf, R., and Holder, N. (1991). Reinoic acid causes abnormal development and segmental patterning of the anterior hindbrain in *Xenopus* embryos. *Development* **113**, 1145-1158.

Pera, E., Stein, S. and Kessel, M. (1999). Ectodermal patterning in the avian embryo: epidermis versus neural plate. *Development* **126**, 63-73.

Pfeffer, P. L., Gerster, T., Lun, K., Brand, M. and Busslinger, M. (1998). Characterization of three novel members of the zebrafish *Pax2/5/8* family: dependency of *Pax5* and *Pax8* on the *Pax2.1* (*noi*) function. *Development* **125**, 3063-3074.

Phillips, B. T., Bolding, K. and Riley, B. B. (2001). Zebrafish *fgf3* and *fgf8* encode redundant functions required for otic placode induction. *Dev. Biol.* **235**, 351-365. doi: 10.1006/dbio.2001.0297.

Phillips, B. T., Storch, E. M., Lekven, A. C., and Riley, B. B. (2004). A direct role for Fgf but not Wnt in otic placode induction. *Development* **131,** 923-931.

Pirvola, U., Spencer-Dene, B., Xing-Qun, L., Kettunen, P., Thesleff, I., Fritzsch, B., and Dickson, C. (2000). FGF/FGFR-2 (IIIb) signaling is essential for inner ear morphogenesis. *J. Neurosci.* **20**, 6125-6134.

Prince, V. E., Moens, C. B., Kimmel. C. B. and Ho, R. K. (1998). Zebrafish *hox* genes: expression in the hindbrain region of the wild-type and mutants of the segmentation gene, *valentino*. *Development* **125**, 393-406.

Prudovsky, I. A., Savion, N., LaVallee, T. M., and Maciag, T. (1996). The nuclear trafficking of extracellular fibroblast growth factor (FGF)-1 correlates with the perinuclear association of the FGF receptor-1 alpha isoforms but not the FGF receptor-1 beta isoforms. *J. Biol. Chem.* **271**, 14198-14205.

Raible, F. and Brand, M. (2001). Tight transcriptional control of the ETS domain factors Erm and Pea3 by Fgf signaling during early zebrafish development. *Mech. Dev.* **107**, 105-117.

Reifers, F., Bohli, H., Walsh, E. C., Crossley, P. H. and Stanier, D. Y. R. (1998). *Fgf8* is mutated in zebrafish *acerebellar (ace)* mutants and is required for maintenance of the midbrain-hindbrain boundary and somitogenesis. *Development* **125**, 2381-2395.

Represa, J., Leon, Y., Miner, C., and Giraldez, F. (1991). The *int-2* proto-oncogene is responsible for induction of the inner ear. *Nature* **353**, 561-563.

Riley, B. B., Zhu, C., Janetopoulos, C. and Aufderheide, K. J. (1997). A critical period of ear development controlled by distinct populations of ciliated cells in the zebrafish. *Dev. Biol*. **191**, 191-201.

Riley, B. B. Chiang, M.-Y., Farmer, L., and Heck, R. (1999). The *deltaA* gene of zebrafish mediates lateral inhibition of hair cells in the inner ear and is regulated by *pax2.1*. *Development* **126**, 5669-5678.

Riley, B. B. and Phillips, B. T. (2003) Ringing in the new ear: resolutions of cell interactions in otic development. *Dev. Biol*. 261, 289-312.

Roehl, H. and Nusslein-Volhard, C. (2001). Zebrafish *pea3* and *erm* are general targets of FGF8 signaling. *Curr. Biol.* **11**, 503-507.

Sahly, I., Andermann, P., and Petit, C. (1999). The zebrafish *eya1* gene and its expression pattern during embryogenesis. *Dev. Genes Evol.* **209,** 399-401.

Sasai, N. Mizuseki, K., and Sasai, Y. (2001). Requirement of FoxD3-class signaling for neural crest determination in *Xenopus*. *Development* **128,** 2525-2536.

Schier, A. F., Neuhauss, S. C. F., Helde, K. A., Talbot, W. S., and Driever, W. (1997). The *one-eyed pinhead* gene functions in mesoderm and endoderm formation in zebrafish and interacts with *no tail*. *Development* **124**,327-342.

Schier, A. F. (2001). Axis formation and patterning in zebrafish. *Curr. Opin. Genet. Dev.* **11,** 393-404.

Schubert, M., Holland, L. Z., Holland, N. D. and Jacobs, D. K. (2000). A phylogenetic tree of the *Wnt* genes based on all available full-length sequences, including five from the cephalochordate Amphioxus. *Mol. Biol. Evol.* **17**, 1896-1903.

Seo, H.C., Drivenes, O., and Fjose, A. (1998). A zebrafish Six4 homologue with early expression in head mesoderm. *Biochim. Biophys. Acta.* **1442,** 427-431.

Simeone, A., Avantaggiato, V., Moroni, M. C., Mavilio, F., Arra, C., Cotelli, F., Nigro, V., and Acampora, D. (1995). Retinoic acid induces stage-specific atnero-posterior transformation of rostral central nervous system. *Mech. Dev.* **51**, 83-98.

Solomon, K. S., and Fritz, A. (2002). Concerted action of two *dlx* paralogs in sensory placode formation. *Development* **129,** 3127-3136.

Solomon, K. S., Kudoh, T., Dawid, I. G. and Fritz, A., (2003). Zebrafish *foxi1* mediates otic placode formation and jaw development. *Development* **130**, 929-940.

Stachel, S. E., Grunwald, D. J. and Myers, P. Z. (1993). Lithium perturbations and *goosecoid* expression identify a dorsal specification pathway in the pregastrula zebrafish. *Development* **117**, 1261-1274.

Stark, M. R., Biggs, J. J., Schoenwolf, G. C. and Rao, M. S. (2000). Characterization of avian *frizzeld* genes in cranial placode development. *Mech. Dev.* **93**, 195-200.

Stone, L. S. (1931). Induction of the ear by the medulla and its relation to experiments on the lateralis system in amphibia. *Science* **74**, 577.

Sun, X., Meyers, E. N., Lewandoski, M., and Martin, G. R. (1999). Targeted disruption of *Fgf8* causes failure of cell migration in the gastrulating mouse embryo. *Genes & Development* **13**, 1834-1846.

Suzuki, A., Ueno, N., and Hemmati-Brivanlou, A. (1997). *Xenopus msx1* mediates epidermal induction and neural inhibition by BMP4. *Development* **124,** 3037-3044.

Terry, K., Magan, H., Baranski, M., and Burrus, L.W. (2000). Sfrp-1 and sfrp-2 are expressed in overlapping and distinct domains during chick development. *Mech. Dev.* **97**, 177-182.

Thisse, C. Thisse, B., and Postlethwait, J. H. (1995). Expression of *snail2*, a second member of the zebrafish Snail family, in cephalic mesoderm and presumptive neural crest of wild-type and *spadetail* mutant embryos. *Dev. Biol.* **172,** 86-99.

Thomas, B. L., Tucker, A. S., Qiu, M., Ferguson, C. A., Hardcastle, Z., Rubenstein, J. L. R., and Sharpe, P. T. (1997). Role of *Dlx-1* and *Dlx-2* genes in patterning of the murine dentition. *Development* **124,** 4811-4818.

Tickle, C. and Munsterberg, A. (2001). Vertebrate limb development-the early stages in chick and mouse. *Curr. Opin. Genet. Dev.* **11,** 476-481.

Torres, M., Gomez-Padro, E., and Gruss, P. (1996). *Pax2* contributes to inner ear patterning and optic nerve trajectory. *Development* **122**, 3381-3391.

Tribulo, C., Aybar, M. J., Nguyen, V. H., Mullins, M. C., and Mayor, R. (2003). Regulation of Msx genes by a Bmp gradient is essential for neural crest specification. *Development* **130,** 6441-6452.

van Oostrom, C. G., and Verwoerd, C. D. A. (1972). The origin of the olfactory placode. *Acta Morphol. Neerl. Scand.* **9**, 160.

Vendrell, V. Carnicero, E., Giraldez, F., Alonso, M. T. and Schimmang, T. (2000). Induction of inner ear fate by FGF3. *Development* **127**, 155-165.

Vendrell, V., Gimnopoulos, D., Beckler, T. and Schimmang, T. (2001). Functional analysis of FGF3 during zebrafish inner ear development. *Int. J. Dev. Biol.* **45 (S1)**, S105-S106.

Waddington, C. H. (1937). The determination of the auditory placode in the chick. *J. Exp. Bio.* **14**, 232-239.

Walsh, J., Maroon, H., McGonnell, I.M., Dickson, C. and Mason, I. (2002). Establishment of hindbrain segmental identity requires signaling by FGF3 FGF8. *Curr. Biol.* **12,** 1117-1123.

Weinberg, E. S., Allende, M. L., Kelly, C. S., Abdelhamid, A., Murakami, T., Andermann, P., Doerre, O. G., Grunwald, D. J., and Riggleman, B. (1996). Developmental regulation of zebrafish *myoD* in wild-type, *no tail* and *spadetail* embryos. *Development* **122,** 271-280.

White, J. C., Highland, M., Kaiser,M., and Clagett-Dame, M. (2000). Vitamin A deficiency results in the dose-dependent acquisition of anterior character and shortening of the caudal hindbrain of the rat. *Dev. Biol.* **220**, 263-284.

Whitfield, T. T., Granato, M., van Eeden, F. J. M., Schach, U., Brand, M., Furutani-Seiki, M., Hafter, P., Hammerschmidt, M., Heisenberg, C.-P., Jiang, Y.-J., Kane, D. A., Kelsh, R. N., Mullins, M. C., Odenthal, J., and Nüsslein-Volhard, C. (1996). Mutations affecting development of the zebrafish inner ear and lateral line. *Development* **123**, 241-254.

Whitfield, T. T., Riley, B. B., Chiang, M-Y. and Phillips, B. T. (2002) Development of the zebrafish inner ear. *Dev. Dyn.* **223**, 427-458.

Wiellette, E.L., and Sive, H. (2003) vhnf1 and Fgf signals synergize to specify rhombomere identity in the zebrafish hindbrain. *Development.* **130,** 3821-3829.

Wilkinson, D. G., Peters, B., Dickson, C. and McMahon, A. P. (1988). Expression of the FGF-related proto-oncogene *int-2* during gastrulation and neurulation in the mouse. *EMBO J.* **7**, 691-695.

Wilkinson, D. G., Bhatt, S. and McMahon, A. P. (1989). Expression pattern of the FGF-related proto-oncogene *int-2* suggests multiple roles in fetal development. *Development* **105**, 1331-1336.

Woo, K., and Fraser, S. E. (1997). Specification of the zebrafish nervous system by nonaxial signals. *Science* **277**, 254-257.

Woo, K., and Fraser, S. E. (1998). Specification of the hindbrain fate in the zebrafish. *Dev. Biol.* **197**, 283-296.

Wright, T. J. and Mansour, S. L. (2003). *Fgf3* and *Fgf10* are required for mouse otic placode induction. *Development* **130**, 3379-3390.

Wu, D. K., Nunes, F. D. and Choo, D. (1998). Axial specification for sensory organs versus non-sensory structures of the chicken inner ear. *Development* **125**, 11-20.

Wurst, W. and Bally-Cuif, L. (2001). neural patterning: upstream and downstream of the isthmic organizer. *Nat. Rev. Neurosci.* **2**, 99-108.

Xu, P.-X., Adams, J., Peters, H., Brown, M. C., Heaney, S. and Maas, R. (1999). *Eya1*-deficient mice lack ears and kidneys and show abnormal apoptosis of organ primordia. *Nat. Genet.* **23**, 113-117.

Yamamoto, T. S., Takagi, C. and Ueno, N. (2000). Requirement of Xmsx-1 in the BMP-triggered ventralization of *Xenopus* embryos. *Mech. Dev.* **91,** 131-141.

Yntema, C. L. (1933). Experiments on the determination of the ear ectoderm in the embryo of *Ablystoma punctatum*. *J. Exp. Zool.* **65**, 317-352.

Yntema, C. L. (1950). An analysis of induction of the ear from foreign ectoderm in the salamander embryo. *J. Exp. Zool.* **113**, 211-240.

Zhang, H., Catron, K. M., and Abate-Shen, C. (1996). A role for the Msx-1 homeodomain in transcriptional regulation: residues in the N-terminal arm mediate TATA binding protein interaction and transcriptional repression. *Proc. Natl. Acad. Sci.* **93,** 1764-1769.

Zhang, H., Hu, G., Wang, H., Sciavolino, P., Iler, N., Shen, M. M., Abate-Shen, C. (1997). Heterodimerization of Msx and Dlx homeoproteins results in functional antagonism. *Mol. Cell. Biol*. **17,** 2920-2932.

Zhang, J., Talbot, W. S., and Schier, A. F. (1998). Positional cloning identifies zebrafish *one-eyed pinhead* as a permissive EGF-related ligand required during gastrulation. *Cell* **92**, 241-251.

Zheng, W., Huang, L., Wei, Z.-B., Silvius, D., Tang, B., and Xu, P.-X. (2003). The role of *Six1* in mammalian auditory system development. *Development* **130**, 3989-4000.

APPENDIX

AN EXPANDED DOMAIN OF *FGF3* EXPRESSION IN THE HINDBRAIN OF ZEBRAFISH VALENTINO MUTANTS RESULTS IN MIS-PATTERNING OF THE OTIC VESICLE*

OVERVIEW

This appendix is a published account (Kwak et al., 2002) of the role of Fgf3 signaling after otic induction. It is primarily the work of my colleague, S.J. Kwak. However, since I contributed portions of Figures 28 and 30, include it here as a record of my work.

SUMMARY

The *valentino* (*val*) mutation in zebrafish perturbs hindbrain patterning and, as a secondary consequence, also alters development of the inner ear. We have examined the relationship between these defects and expression of *fgf3* and *fgf8* in the hindbrain. The otic vesicle in *val/val* mutants is smaller than normal, yet produces nearly twice the normal number of hair cells, and some hair cells are produced ectopically between the anterior and posterior maculae. Anterior markers *pax5* and *nkx5.1* are expressed in expanded domains that include the entire otic epithelium juxtaposed to the hindbrain, and the posterior marker *zp23* is not expressed. In the mutant hindbrain, expression of *fgf8* is normal, whereas the domain of *fgf3* expression expands to include rhombomere 4

---

*Reprinted from *Development,* Vol. 129, Kwak et al., An expanded domain of *fgf3* expression in the hindbrain of zebrafish *valentino* mutants results in mis-patterning of the otic vesicle, pp 5279-5287, copyright (2002), with permission from the Company of Biologists Ltd.

through rhombomere X (an aberrant segment that forms in lieu of rhombomeres 5 and 6). Depletion of *fgf3* by injection of antisense morpholino (fgf3-MO) suppresses the ear patterning defects in *val/val* embryos: Excess and ectopic hair cells are eliminated, expression of anterior otic markers is reduced or ablated, and *zp23* is expressed throughout the medial wall of the otic vesicle. In contrast, disruption of *fgf8* does not suppress the *val/val* phenotype but instead interacts additively, indicating that these genes affect distinct developmental pathways. Thus, the inner ear defects observed in *val/val* mutants appear to result from ectopic expression of *fgf3* in the hindbrain. These data also indicate that *val* normally represses *fgf3* expression in r5 and r6, an interpretation further supported by the effects of misexpressing *val* in wild-type embryos. This is in sharp contrast to the mouse, in which fgf3 is normally expressed in r5 and r6 due to positive regulation by *kreisler*, the mouse ortholog of *val*. Implications for co-evolution of the hindbrain and inner ear are discussed.

INTRODUCTION

Development of the inner ear requires interactions with adjacent hindbrain tissue. Many studies have shown that the hindbrain can induce otic placodes in adjacent ectoderm (Stone, 1931; Yntema, 1933; Harrison, 1935; Waddington, 1937; Jacobsen, 1963; Gallagher et al., 1996; Woo and Fraser, 1998; Groves and Bronner-Fraser, 2000). A number of the relevant hindbrain signals have recently been identified (reviewed by Whitfield et al., 2002). In zebrafish, two members of the FGF family of signaling molecules, Fgf3 and Fgf8, are expressed in the anlagen of rhombomere-4 (r4) during late gastrulation when induction of the otic placode begins (Reifers et al., 1998; Phillips et al.,

2001; Maroon et al., 2002). At this time, *pax8* is induced in the adjacent otic anlagen. Disruption of both *fgf3* and *fgf8* prevents induction of the otic placode, and conditions that expand the expression domains of these genes lead to production of supernumerary or ectopic otic vesicles (Phillips et al., 2001; Raible and Brand, 2001; Vendrell et al., 2001; Maroon et al., 2002). In addition, disruption or depletion of *Fgf3* perturbs inner ear development in chick and mouse (Represa et al., 1991; Mansour et al, 1993) and misexpression of *Fgf3* in chick is sufficient to induce ectopic otic vesicles (Vendrell et al., 2000). It has also been shown that chick Fgf19, which is expressed in a pattern similar to that of Fgf3 (Mahmood et al., 1995), cooperates with the hindbrain factor Wnt8c to induce a range of otic placode markers in tissue culture (Ladher et al., 2000a). Thus, multiple hindbrain factors are involved in otic placode induction, and FGF signaling plays an especially prominent role.

Much less is known about the role played by hindbrain signals in later stages of inner ear development. Experiments in chick embryos show that rotation of the early otic vesicle about the anteroposterior axis reorients gene expression patterns in a manner suggesting that proximity to the hindbrain influences differentiation of cells within the otic vesicle (Wu et al., 1998; Hutson et al., 1999). In zebrafish, *Xenopus*, chick, and mouse embryos, *Fgf3* continues to be expressed in the hindbrain after otic placode induction (Mahmood et al., 1995, 1996; McKay et al., 1996; Lombardo et al. 1998; Phillips et al., 2001). This raises the question of whether this factor also helps regulate subsequent development of the otic placode or otic vesicle.

Analysis of the *valentino* (*val*) mutant in zebrafish provides indirect evidence that hindbrain signals are necessary for normal development of the otic vesicle (Moens et al., 1996, 1998). *val* encodes a bZip transcription factor that is normally expressed in r5 and r6. *val/val* mutants produce an abnormal hindbrain in which the r5/6 anlagen fails to differentiate properly and gives rise to a single abnormal segment, rX, which shows confused segmental identity. Although the *val* gene is not expressed in the inner ear, *val/val* mutants produce otic vesicles that are small and malformed. Since otic induction appears to occur normally in *val/val* mutants (Mendonsa and Riley, 1999), we infer that altered hindbrain patterning perturbs signals required for later aspects of otic development. Mice homozygous for a mutation in the ortholologous gene, *kreisler*, also show later defects in development of the otic vesicle (Deol, 1964; Cordes and Barsh, 1994). The inner ear defects in *kreisler* mutants are thought to result from insufficient expression of *Fgf3* in the hindbrain (McKay et al, 1996). In contrast to zebrafish, mouse *Fgf3* is initially expressed at moderate levels in the hindbrain from r1 through r6. As development proceeds, expression downregulates in the anterior hindbrain but upregulates in r4 (Mahmood et al., 1996). After formation of the otic placodes, *Fgf3* expression also upregulates in r5 and r6. This upregulation fails to occur in *kreisler* mutants, possibly accounting for subsequent patterning defects in the inner ear (McKay et al. 1996).

To examine the relationship between hindbrain and otic vesicle development in zebrafish, we have examined patterning of these tissues in wild-type and *val/val* mutant embryos. We find that *val/val* mutants produce excess and ectopic hair cells at virtually

any position in the epithelium juxtaposed to the hindbrain. Expression of the anterior otic markers *nkx5.1* and *pax5* is also seen ectopically throughout this region of the otic vesicle. Conversely, expression of the posterior marker *zp23* is ablated in *val/val* embryos. Analysis of hindbrain patterning shows that *fgf3* is misexpressed in the rX region of *val/val* mutants. Disruption of *fgf3* function by injection of an antisense morpholino oligomer blocks formation of ectopic hair cells and suppresses AP patterning defects in the otic vesicle of *val/val* mutants. In contrast, *fgf8* is expressed normally in *val/val* embryos, and loss of *fgf8* does not suppress the inner ear defects caused by the *val* mutation. These data indicate that the expanded domain of *fgf3* plays a crucial role in the etiology of inner ear defects in *val/val* mutants and suggest that Fgf3 secreted by r4 normally specifies anterior fates, suppresses posterior fates, and stimulates hair cell formation in the anterior of the otic vesicle.

MATERIALS AND METHODS

Strains

Wild-type embryos were derived from the AB line (Eugene, OR). Mutations used in this study were *valentino* (*val*^{b337}) and *acerebellar* (*ace*^{ti282a}). Both of mutations were induced with ENU and are thought to be functional null alleles (Moens *et al*. 1996, 1998; Brand *et al*., 1998). Embryos were developed at 28.5ºC in water containing 0.008% Instant Ocean salts. Embryonic ages are expressed as hours post-fertilization (h).

Identification of mutant embryos

Live *val/val* homozygotes were reliably identified after 19 h by the small size and round shape of the otic vesicle. In addition, fixed val/val embryos stained for *pax2.1*,

pax5, or *zp23* showed characteristic changes in posterior hindbrain patterning. At earlier stages, *val/val* mutants were identified by loss of *krox20* staining in rhombomere 5 (Moens et al., 1996). Live *ace/ace* mutants were readily identified after 24 h by the absence of a midbrain-hindbrain border and enlarged optic tectum (Brand et al., 1996). In addition, *ace/ace* specimens that were fixed and stained for *pax2.1* or *pax5* showed no staining in the midbrain-hindbrain border. At earlier stages (14 h), *ace/ace* mutants were identified by loss of *fgf3* expression in the midbrain-hindbrain border.

Whole-mount immunofluorescent staining

Embryos were fixed in MEMFA (0.1 M MOPS at 7.4, 2 mM EGTA, 1 mM $MgSO_4$, 3.7% formaldehyde) and stained as previously described (Riley et al, 1999). Primary antibodies used in this study were: Polyclonal antibody directed against mouse Pax2 (Berkeley Antibody Company, 1:100 dilution), which also recognizes zebrafish pax2.1 (Riley et al. 1999); Monoclonal antibody directed against acetylated tubulin (Sigma T-6793, 1:100), which binds hair cell kinocilia (Haddon and Lewis, 1996). Secondary antibodies were Alexa 546 goat anti-rabbit IgG (Molecular Probes A-11010, 1:50) or Alexa 488 goat anti-mouse IgG (Molecular Probes A-11001, 1:50).

Whole-mount in situ hybridization

Whole-mount in situ hybridization was performed as described (Stachel *et al*., 1993) using riboprobes for *fgf*3 (Keifer *et al*., 1996), *fgf8* (Reifers *et al*., 1998), *dlA* (Appel and Eisen, 1998; Haddon et al., 1998b), *pax5* (Pfeffer et al., 1998), *dlx3* and *msxC* (Ekker et al., 1992), *nkx5.1* (Adamska et al., 2000), *otx1* (Li et al., 1994), and *zp23*

(Hauptmann and Gerster, 2000). Two color in situ hybridization was performed essentially as described by Jowett (1996) with minor modifications (Phillips et al, 2001).

Morpholino oligomer injection

fgf3-specific morpholino oligomer obtained from Gene Tools Inc. was diluted in Danieaux solution (58 mM NaCl, 0.7 mM KCl, 0.4 mM $MgSO_4$, 0.6 mM $Ca(NO_3)_2$, 5.0 mM HEPES, pH 7.6) to a concentration of 5 µg/µl as previously described (Nasevicius and Ekker, 2000; Phillips et al., 2001). Approximately 1 nl (5 ng fgf3-MO) was injected into the yolk cell at the 1- to 2-cell stage.

Mis-expression of *val*

Wild-type *val* was ligated into pCS2 expression vector by Andrew Waskiewicz (Cecilia Moens' lab) and was kindly provided as a gift. RNA was synthesized in vitro and approximately 1 ng of RNA was injected into the yolk of cleaving embryos at the 1- to 4-cell stage.

RESULTS

Altered patterns of hair cells in *val/val* mutants

val/val mutants produce small otic vesicles with shortened anteroposterior axes but relatively normal dorsoventral axes. This gives the mutant ear a characteristic circular shape that is quite distinct from the ovoid shape of the wild-type ear. This is thought to arise secondarily from abnormal development of the hindbrain (Moens et al., 1998), signals from which are required for normal ear development. To test this idea directly, we characterized early patterning of the otic vesicle and hindbrain in *val/val* mutants. In *val/val* mutants, the size, number, and distribution of otoliths in the inner ear

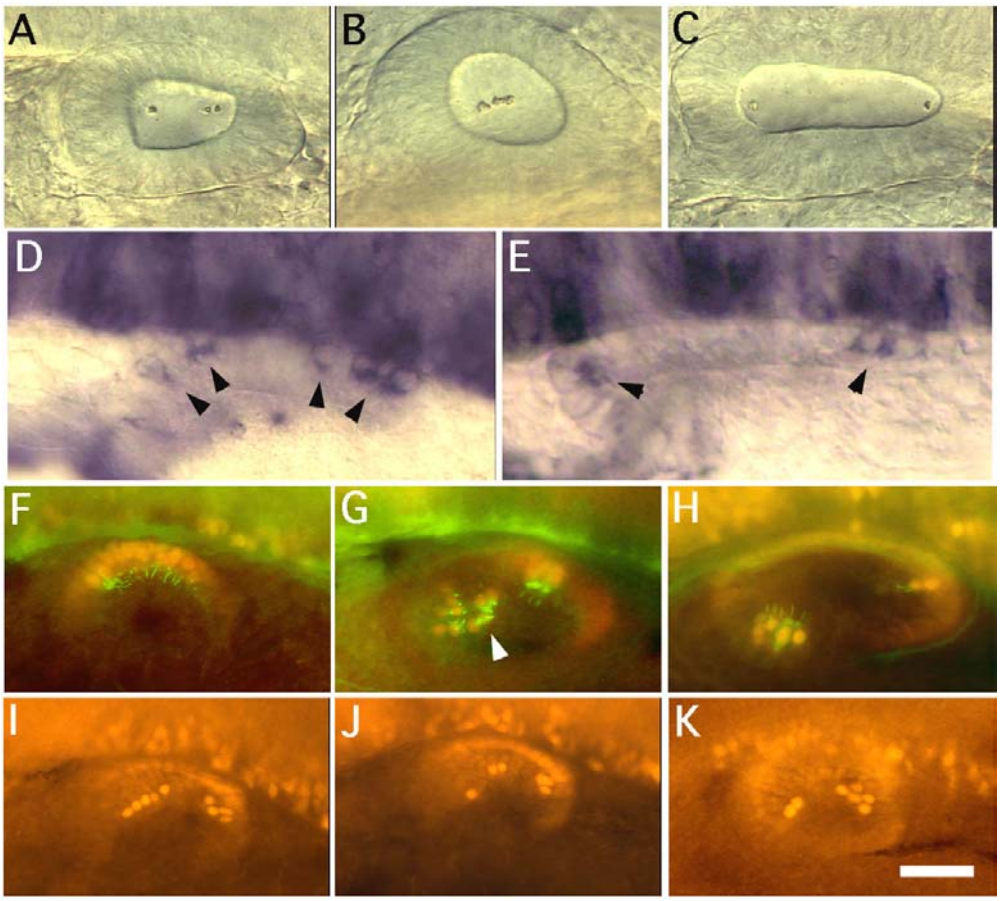

Figure 28. Patterns of hair cells in the otic vesicle. Lateral view of otic vesicles of live *val/val* (A, B) and wild-type (C) embryos viewed under DIC optics at 21h. *val/val* mutants have small, round otic vesicles, and otoliths vary in number and position. (D, E) Dorsolateral view of *deltaA* expression in the otic vesicle at 19 h in *val/val* (D) and wild-type (E) embryos. Arrowheads indicate nascent tether cells. (F-H) Dorsolateral view of otic vesicles showing hair cells stained with anti-Pax2 (red) and anti-acetylated tubulin (green) antibodies. (F) *val/val* mutant at 24 h. Seven hair cells are distributed along the length of the anteroposterior axis of the otic vesicle. (G) *val/val* mutant at 30 h. An ectopic patch of hair cells (arrowhead) is evident between the anterior and posterior maculae. (H) wild-type embryo at 30 h. (I-K) Dorsolateral view of *val/val* mutants at 27 h stained with anti-Pax2 to visualize hair cell nuclei. The number and distribution of hair cells are variable. Anterior is to the left in all specimens. Scale bar, 20 µm (A-C), 15 µm (D, E), 30 µm (F-H), or 40 µm (I-K).

vary considerably (Fig. 28A, B). In wild-type embryos, otoliths form only at the anterior and posterior ends of the otic vesicle where they attach to the kinocilia of tether cells (Fig. 28C; Riley et al., 1997). Tether cells are the first hair cells to form and occur in pairs at both ends of the nascent otic vesicle where they facilitate localized accretion of otolith material. The supernumerary and ectopic otoliths observed in *val/val* embryos were each associated with pairs of tether cells, as seen in live embryos under DIC optics (not shown). Visualizing tether cells by their expression of *deltaA* (Haddon et al., 1998a; Riley et al. 1999) confirms that *val/val* mutants produce excess and ectopic tether cells (Fig. 28D). In both wild-type and *val/val* embryos, tether cells acquire the morphology of mature hair cells by 22 h (Riley et al, 1997, and data not shown) and can be visualized by nuclear staining with anti-Pax2 antibody. This antibody was originally directed against mouse Pax2 but also binds zebrafish Pax2.1, which is preferentially expressed in maturing hair cells (Riley et al., 1999). Because of the unusual positions of some hair cells in *val/val* mutants, their cell type identity was confirmed in some specimens by staining with anti-acetylated tubulin, which labels hair cell kinocilia (Haddon and Lewis, 1996). This confirmed the presence of excess and ectopic hair cells at 24 h in *val/val* mutants (Figs. 28F). *val/val* mutants continue to show greater numbers of hair cells than wild-type embryos through at least 33 h (Fig. 29; Table 3). In addition, ectopic patches of hair cells continue to develop between the anterior and posterior maculae in most *val/val* mutants (Fig. 28G). However, the spatial distribution of hair cells varies widely from one specimen to the next (Figs. 28G, I-K). In general, hair cells can emerge at any position along the ventromedial surface of the otic vesicle in *val/val*

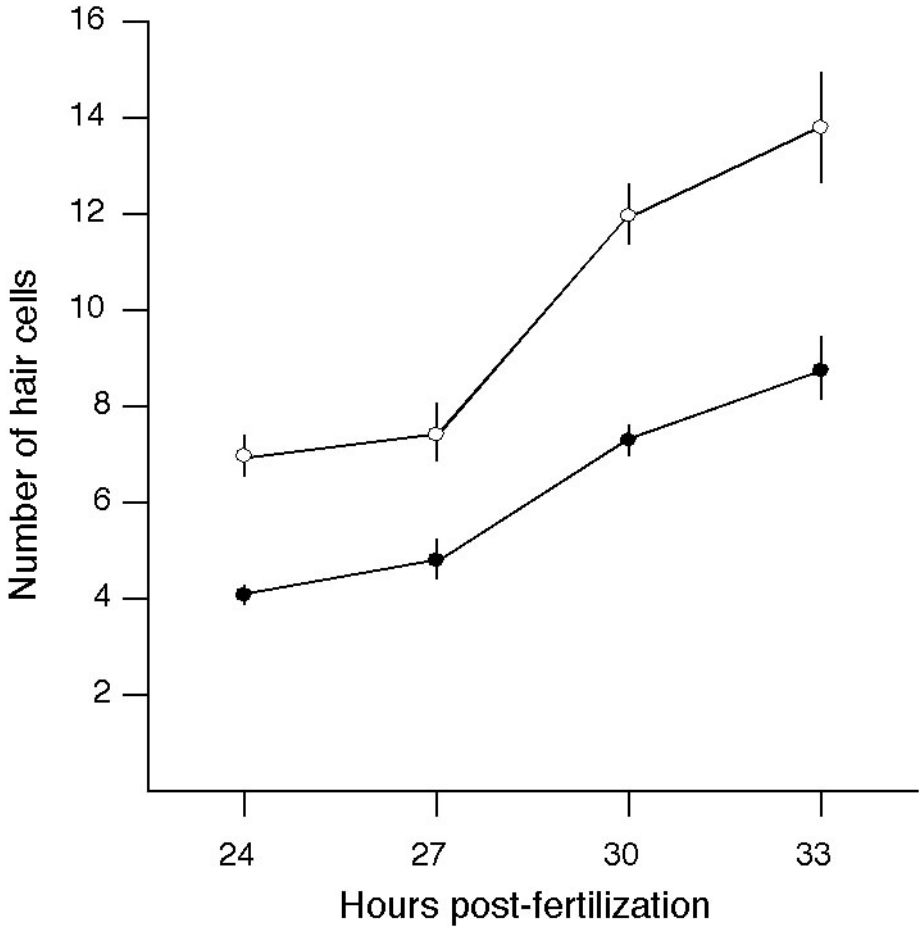

Figure 29. Time course of hair cell formation in the otic vesicle. Embryos were fixed at the indicated times and hair cells were visualized by Pax2 staining. Each datum is the mean number of hair cells per ear (± standard deviation) of 10 or more specimens. *val/val* mutants produce excess hair cells throughout the time course. Symbols: (●) wild-type and (○) *val/val* embryos.

Table 3. Hair cell specification defects resulting from Fgf dysfunction

	number hair cells/ear at 30h		
Genotype	mean ± s.d.	range	number
+/+	6.9 ± 1.1	6-9	28
val/val	12 ± 1.3	10-14	32
fgf3 kd	5.3 ± 1.7	2-8	21
fgf3 kd in val/val	5.7 ± 2.4	2-11	33
ace/ace	2.9 ± 1.0	2-5	19
ace/ace;val/val	2.5 ± 0.7	1-4	28

mutants, unlike wild-type embryos in which hair cells are restricted to the anterior (utricular) and posterior (saccular) maculae. These data suggest that the signal(s) that normally regulate the location and number of hair cells are misregulated in *val/val* mutants, an interpretation further supported by analysis of FGF expression in the hindbrain (see below).

Altered antero-posterior patterning in *val/val* mutants

We next examined Expression of various otic markers to further characterize altered patterning in *val/val* embryos. Expression of *pax5* is first detectable in the inner ear at 17.5-18 h (Pfeffer et al., 1998). This expression domain is normally restricted to the anterior part of the otic vesicle adjacent to r4 and is maintained through at least 30 h (Fig. 30A, C). In *val/val* embryos, *pax5* expression extends along the entire length of the medial wall of the otic vesicle (Fig. 30B, D). Another anterior marker, *nkx5.1*, is also expressed throughout the medial wall of the otic vesicle in *val/val* mutants (Fig. 30F). In

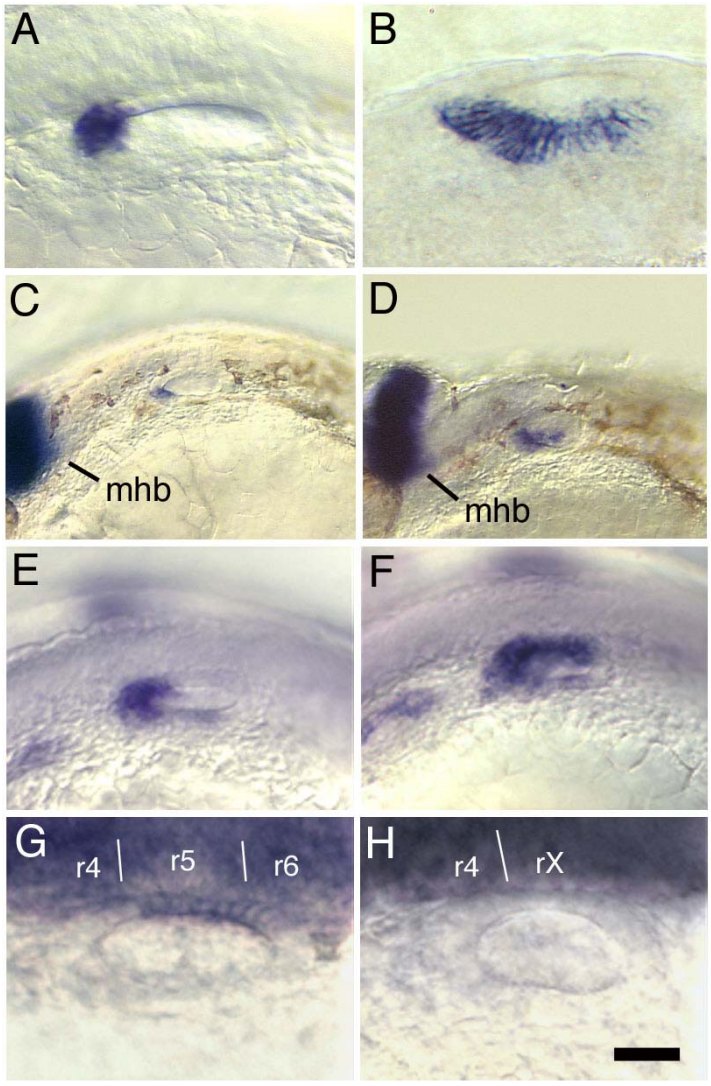

Figure 30. Expression of AP markers in the inner ear. Lateral or dorsolateral views of the otic vesicle (anterior to the left). (A-D) *pax5* expression at 24 h (A, B) and 30 h (C, D). Staining is limited to the anterior end of the otic vesicle in wild-type embryos (A, C) but is greatly expanded in *val/val* mutants (B and D). The midbrain-hindbrain border (mhb) is indicated. (E, F) Expression of *nkx5.1* at 24 h in wild-type (E) and *val/val* (F) embryos. Expression is expanded posteriorly in *val/val* mutants. (G, H) Expression of *zp23* at 24 h in wild-type (G) and *val/val* (H) embryos. No expression is detectable in the ear in *val/val* mutants. Relative positions of rhombomeres are indicated. Scale bar, 25 μm (A, B, G, H), 75 μm (C, D), or 50 μm (E, F).

contrast, *zp23* is normally expressed in posterior medial cells adjacent to r5 and r6 in the wild type but is not detectably expressed in *val/val* embryos (Fig. 30G, H). Otic patterning is not globally perturbed, however. Mutant embryos show a normal pattern of *dlx3* expression in the dorso-medial epithelium (Fig. 31F). Similarly, *otx1* is expressed normally in ventral and lateral cells of *val/val* mutants (Fig. 31A-D). Based on studies in mouse, the dorsal and lateral domains of *dlx3* and *otx1* probably help regulate development of the semicircular canals and sensory cristae (Depew at al., 1999; Krauss and Lufkin, 1999; Morsli et al., 1999; Mazan et al., 2001). It was previously reported that formation of semicircular canals is totally disrupted in *val/val* mutants (Moens et al., 1998). However, we find that this is a highly variable phenotype, ranging from grossly abnormal morphogenesis to nearly normal patterning at day 3 (Fig. 31G-I). Morphology typically becomes increasingly aberrant with time, possibly resulting from improper regulation of endolymph, as seen in *kreisler* mutant mice (Deol, 1964; Brigande et al., 2000; see Discussion). Regardless of whether semicircular canals develop properly, all three sensory cristae are produced and express *msxC* (data not shown). Thus, some aspects of axial patterning are relatively normal in *val/val* embryos at early stages, and the only consistent defect is that medial cells abutting the hindbrain all show anterior character. This is consistent with the hypothesis that factors locally expressed in the hindbrain regulate anterior-posterior fates in the medial wall of the otic vesicle, and that such factors are mis-regulated in the rX region of *val/val* mutants. Such mis-expression could also explain the abnormal pattern of hair cells produced in *val/val* mutants.

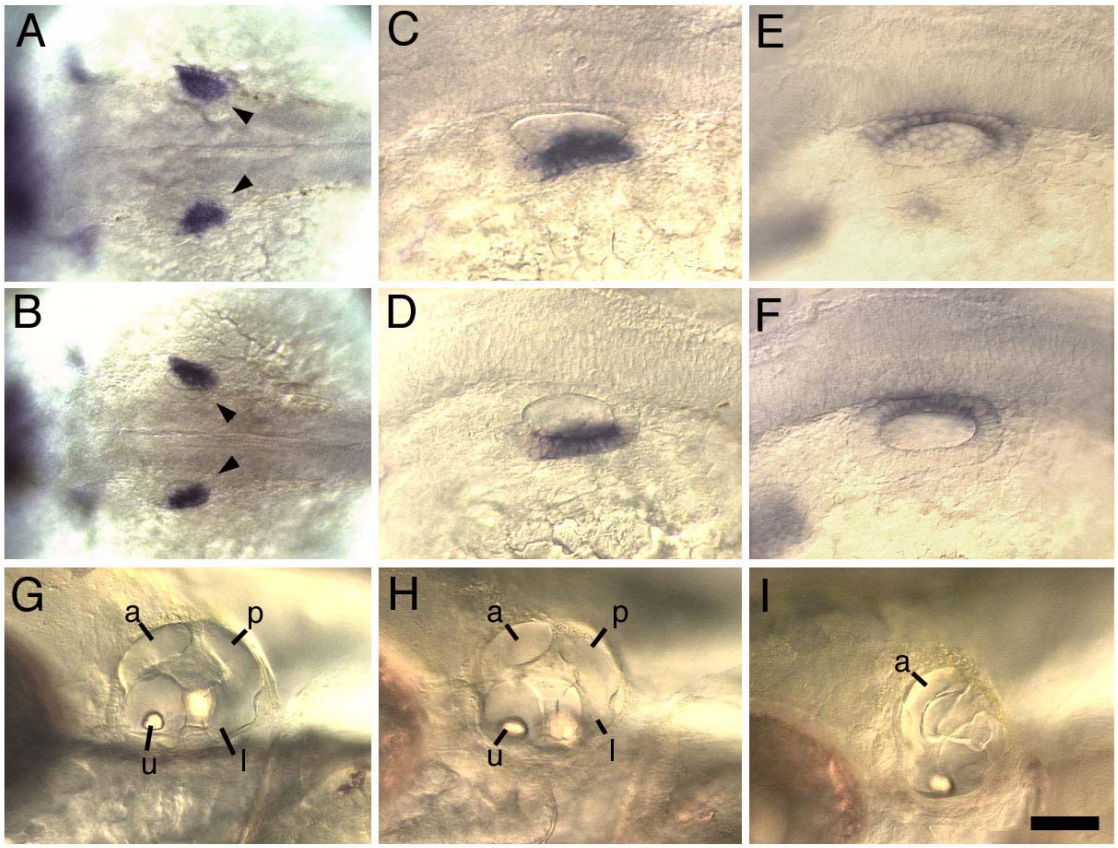

Figure 31. DV and ML patterning in the inner ear. (A-D) Expression of *otx1* at 24 h in wild-type (A, C) and *val/val* (B, D) embryos. Dorsal views (A, B) show expression in the lateral epithelium of the otic vesicle (arrow heads), and lateral views (C, D) show expression in the ventral epithelium. (E, F) Dorsolateral views showing expression of *dlx3* at 24 h in wild-type (E) and *val/val* (F) embryos. Gene expression patterns are normal. (G-I) Lateral views of the inner ear at 72 h in wild-type (G) and val/val (H, I) embryos. Morphology ranges from nearly normal to highly aberrant. Anterior is to the left in all specimens. Abbreviations: a, anterior semicircular canal; l, lateral semicircular canal; p, posterior semicircular canal; u, utricle. Scale bar, 100 μm (A, B, G-I) or 50 μm (C-F).

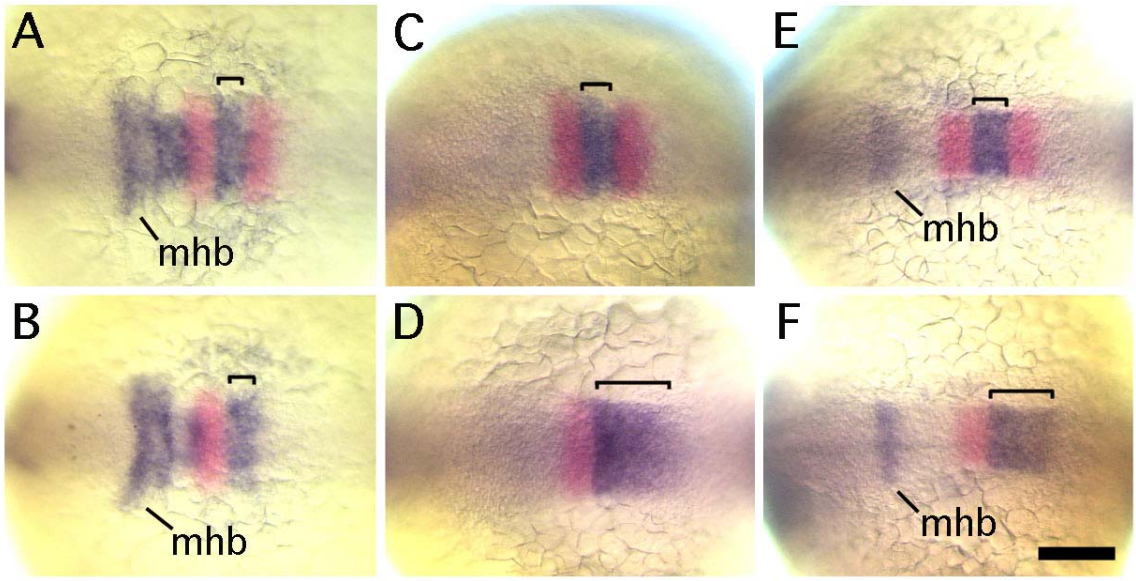

Figure 32. Expression of *fgf8* and *fgf3* in the hindbrain. Dorsal view (anterior to the left) of specimens double stained for *fgf* gene expression (blue) and *krox-20* (red). Loss of *krox20* staining in r5 identifies *val/val* mutants. (A, B) *fgf8* expression at 12 h in wild-type (A) and *val/val* (B) embryos. Brackets indicate the r4 domain of *fgf8*. No change is detected in the mutant. (C, D) *fgf3* expression at 12 h in wild-type (C) and *val/val* (D) embryos. (E, F) *fgf3* expression at 14 h in wild-type (E) and *val/val* (F) embryo. Brackets indicate the domain of *fgf3* corresponding to either r4 (C, E) or r4 though rX (D, F). *fgf3* is ectopically expressed in the rX region in *val/val* embryos. Scale bar, 80 µm.

Expression of *fgf3* and *fgf8* in the *val/val* hindbrain

Fgf3 and Fgf8 are both expressed in the r4 anlagen during late gastrulation and cooperate to induce the otic placode (Phillips et al., 2001). We hypothesized that persistent expression of one or both of these factors in r4 plays a later role in patterning the otic placode and vesicle. In both wild-type and *val/val* embryos, *fgf8* is expressed at high levels in r4 at 12 h (Fig. 32A, B) but is downregulated by 14 h (not shown). This argues against a role for Fgf8 in the etiology of the inner ear phenotype in *val/val* embryos. In contrast, *fgf3* expression shows a consistent difference between *val/val* and wild-type embryos. In the wild type, hindbrain expression of *fgf3* is restricted to r4 and is maintained through at least 18 h when the otic vesicle forms (Fig. 32C, E, and data not shown). In *val/val* mutants, *fgf3* shows similar developmental timing but is expressed in an expanded domain extending from r4 through rX (Fig. 32D, F). Within rX, the level of expression falls off gradually towards the posterior such that there is no clear posterior limit of expression. Ectopic expression of *fgf3* in *val/val* embryos is first detectable at 10h, corresponding to the time when *val* normally begins to function in the r5/6 anlagen (data not shown). Initially, ectopic expression of *fgf3* in rX is much weaker than in r4. Expression in rX subsequently increases to a level similar to that seen in r4 by 12 h (Fig 32D). These data suggest that expansion of the domain of *fgf3* in the hindbrain could play a role in misexpression of AP markers and production of ectopic hair cells in the inner ear.

The above data also suggest that *val* normally functions, directly or indirectly, to exclude *fgf3* expression from r5/6. To explore this more fully, we examined the effects

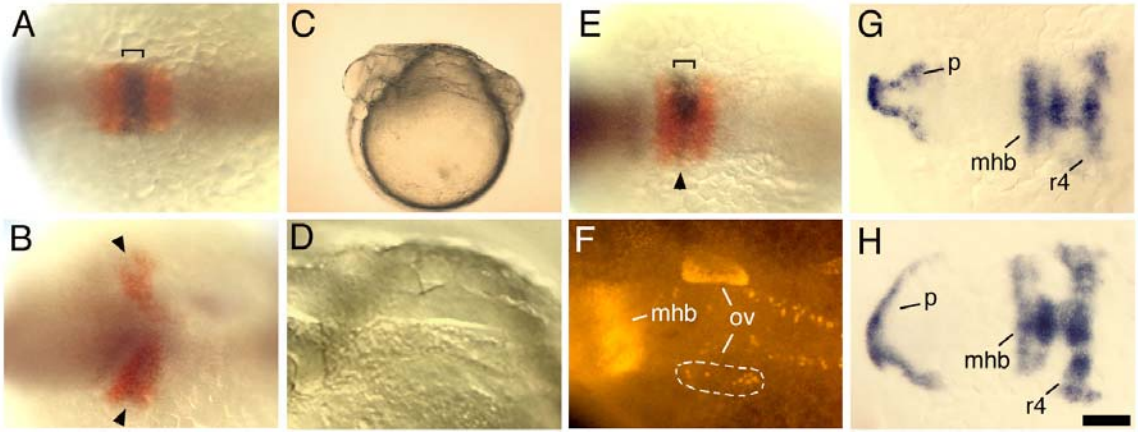

Figure 33. Effects of mis-expressing *val*. (A, B) Dorsal views showing expression of *fgf3* (blue) and *krox20* (red) at 14 h in a normal embryo (A) and an embryo injected with *val* RNA (B). The val-injected embryo shows little or no *fgf3* expression in the r4 domain (arrowheads) and has undergone less convergence than normal. (C, D) Lateral view of a *val*-injected embryo at 24 h. Trunk and tail tissues are ablated (C) and no otic vesicle is visible (D). (E, F) Dorsal views of *val*-injected embryos with relatively normal axial development. (E) Expression of *fgf3* (blue) and *krox20* (red) at 14 h. The left side of r4 shows little *fgf3* expression (arrowhead) whereas the right side is nearly normal (bracket). (F) Expression of *pax2.1* at 24 h in the midbrain-hindbrain border (mhb) and otic vesicles (ov). The left otic vesicle (dashed circle) is severely disrupted. (G, H) Expression of *fgf8* at 12 h in a normal wild-type embryo (G) and a *val*-injected embryo (H). The *val*-injected embryo has a truncated axis (not shown) and has undergone less convergence than normal. Nevertheless, *fgf8* is expressed relatively normally in the prechordal plate (p), midbrain-hindbrain border (mhb), and rhombomere 4 (r4). Anterior is to the left in all panels. Scale bar, 100 μm (A, B, D-H) or 250 μm (C).

of *val* mis-expression by injecting *val* RNA into wild-type embryos. In more than half (55/98) of *val*-injected embryos, hindbrain expression of *fgf3* was dramatically reduced or ablated (Fig. 33A,B). Similar effects were seen at 10, 12, and 14 h (data not shown). At 24 h, otic vesicles were usually small (15/64) or totally ablated (36/64) (Fig. 33C, D). Disrupting *fgf3* by itself impairs, but does not ablate, otic tissue (Phillips et al., 2001; Vendrell et al., 2001; Maroon et al., 2002). This indicates that *val* mis-expression affects other processes in addition to *fgf3* expression. Indeed, ubiquitous mis-expression of *val* frequently caused truncation of the trunk and tail (46/64, Fig. 33C) and could therefore impair mesendodermal signals on which otic development relies (reviewed by Whitfield et al., 2002). However, even amongst embryos with normal axial development, about half showed partial loss of fgf3 expression (5/10) and impaired otic development (18/34). In many of these cases, these defects were limited to one side of the embryo (Fig. 33E, F), possibly resulting from variation in the amount of RNA inherited by early cleavage stage blastomeres. In contrast to *fgf3*, expression of *fgf8* was relatively normal in most (82/85) *val*-injected embryos, even those with axial truncations (Fig. 33H). These data support the hypothesis that *val* specifically represses *fgf3* expression in the hindbrain. This is in sharp contrast to the function of the mouse homolog *kreisler*, which is required to activate high level expression of *Fgf3* in r5 and r6 (McKay et al., 1996). Such species differences may have been important for evolutionary changes in inner ear structure and function (see Discussion).

Dependence of inner ear patterning on Fgf3

To test the role of Fgf3 in otic vesicle patterning, embryos were injected with fgf3-MO, an antisense oligomer that specifically inhibits translation of *fgf3* mRNA (Nasevicius and Ekker, 2000; Phillips et al., 2001; Maroon et al., 2002). Injection of fgf3-MO into wild type embryos results in a range of defects with varying degrees of severity (Phillips et al., 2001). The size of otic vesicle is usually reduced, and about half (42/86) of Fgf3-depleted wild-type embryos show little or no *pax5* expression in the inner ear (Fig. 34A). Expression of *nkx5.1* is also reduced or ablated in the otic vesicle and vestibulo-acoustic ganglion in about half (30/62) of injected wild-type embryos (data not shown). In contrast, expression of *zp23* often expands anteriorly in the otic vesicle to include medial cells adjacent to r4 (21/32 embryos, Fig. 34D). Hair cell production is reduced by up to 70% in severely affected embryos (Fig. 34G; Table 3, note range of data). Injection of fgf3-MO into *val/val* mutants leads to further reduction in the size of otic vesicle. Expression of *pax5* is strongly reduced in most cases: In one experiment, 37% (26/71) showed *pax5* expression limited to the anterior of the otic vesicle (Fig. 34B), and 38% (27/71) showed no detectable expression (Fig. 34C). Similarly, *nkx5.1* is strongly reduced or ablated in about half (16/30) of injected *val/val* embryos (Fig. 34F). Most (12/15) *val/val* embryos injected with fgf3-MO express *zp23* in the otic vesicle, including tissue adjacent to r4 (Fig. 34E). Hair cell production is reduced to a level comparable to that seen in Fgf3-depleted wild-type embryos (Table 3). In addition, depletion of Fgf3 prevents formation of ectopic hair cells in the majority (19/25) of *val/val* embryos (Fig. 34H, I). Thus, Fgf3-depletion prevents formation of

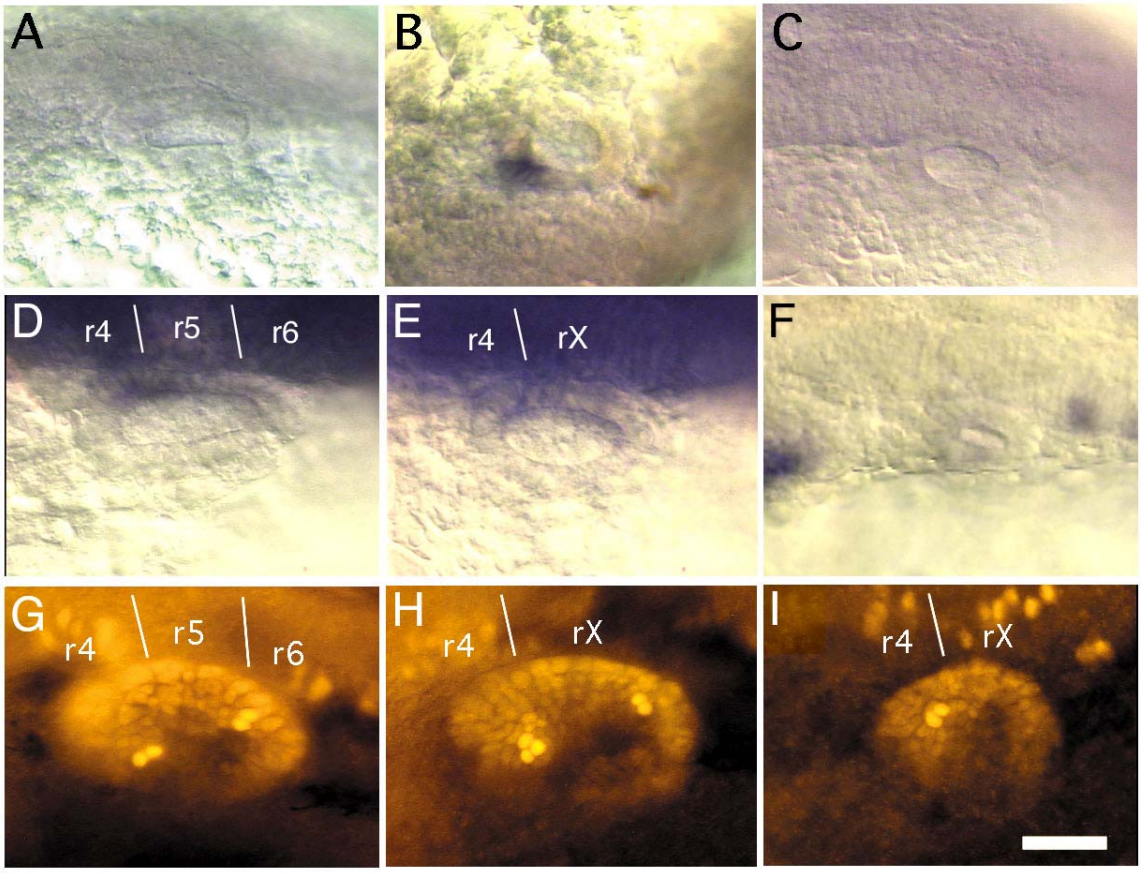

Figure 34. Effects of *fgf3* knockdown on inner ear development. Dorsolateral view (anterior to the left) of otic vesicles in embryos injected with fgf3-MO. (A-C) in situ hybridization of *pax5* at 24 h in injected wild-type (A) and injected *val/val* (B, C) embryos. Expression levels are greatly reduced in 1/2 to 2/3 of embryos (see text for details). (D, E) Expression of *zp23* at 24 h in injected wild-type (D) and injected *val/val* (E) embryos. Expression is detected throughout the medial wall of the otic vesicle, including cells adjacent to r4. (F) in situ hybridization of *nkx5.1* at 24 h in an injected *val/val* embryo. No expression is detected in the otic vesicle. (G-I) Anti-Pax2 staining at 30 h in injected wild-type (G) and injected *val/val* (H, I) embryos. The number of hair cells is reduced relative to uninjected controls, and the majority (19/25) of *val/val* embryos do not produce ectopic hair cells. Fgf3-depleted *val/val* embryos with extremely small otic vesicles (I) produced anterior hair cells only. Relative positions of rhombomeres are indicated. Scale bar, 70 µm (A-C, F), 50 µm (D, E), or 30 µm (G-I).

excess and ectopic hair cells as well as misexpression of AP markers in *val/val* mutants. Since the hindbrain is the only periotic tissue known to express *fgf3* at this time, we infer that the expanded domain of *fgf3* in *val/val* mutants is critical for generation of the above inner ear defects.

Dependence of inner ear patterning on Fgf8

Although expression of *fgf8* did not appear to correlate with changes in inner ear patterning in *val/val* mutants, we sought to characterize patterning defects in *ace/ace* mutants and examine genetic interactions between *ace* and *val*. Defects in *ace/ace* embryos are less variable than in embryos injected with fgf3-MO (Phillips et al., 2001). The otic vesicle in *ace/ace* mutants is reduced in size but usually retains an ovoid shape at 24h. Hair cell production is reduced by more than half in the majority of *ace/ace* mutants (Table 3), and more than a third (7/19) of specimens produce no posterior hair cells at all (Fig. 35E). In *ace/ac*e; *val/val* double mutants, the size of otic vesicle is further reduced and the number of hair cells is comparable to that in *ace/ace* single mutants (Fig. 35F; Table 3). Hair cells often form adjacent to r4 and/or rX in *ace/ace; val/val* double mutants and are usually located in a more medial position than are hair cells in *ace/ace* mutants (Fig. 35F). In addition, *pax5* is expressed along the full length of the anteroposterior axis of the ear (Fig. 35D). Expression of *nkx5.1* is also expanded in ace/ace-val/val double mutants, while *zp23* is not expressed (data not shown). Thus, the *ace* mutation strongly perturbs inner ear patterning, but loss of *fgf8* function does not suppress the patterning defects associated with the *val* mutation. This is probably because expression of *fgf3* is expanded in the hindbrain of *ace/ace; val/val* double

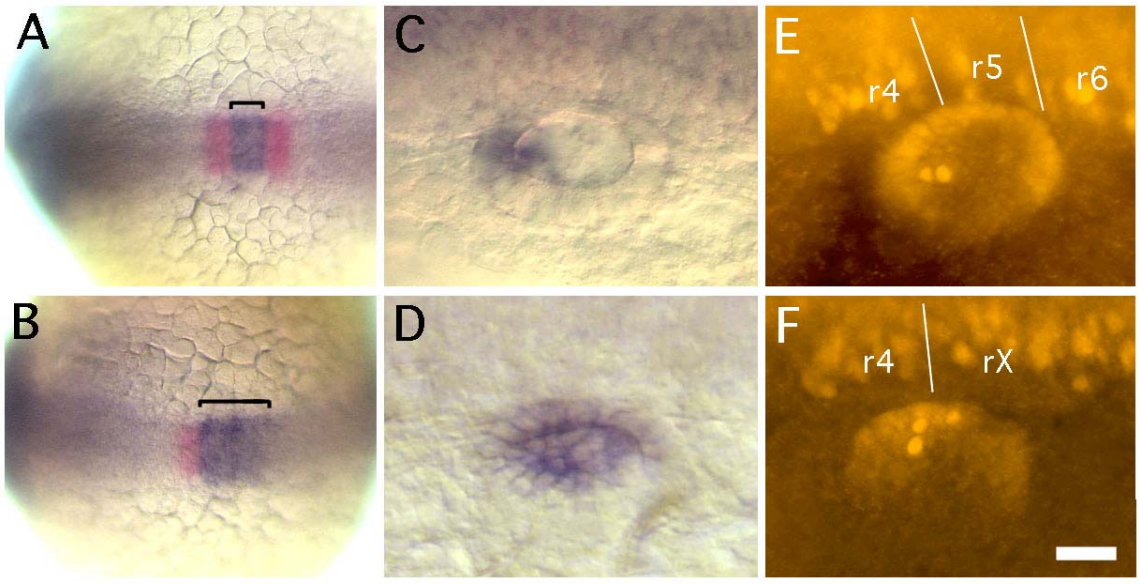

Figure 35. Effects of *fgf8* dysfunction on inner ear development. (A, B) Dorsal view of the hindbrain at 14h showing expression of *fgf3* (blue, with brackets) and *krox20* (red) in *ace/ace* (A) and *ace/ace; val/val* (B) embryos. (C, D) Dorsolateral view showing *pax5* expression in the otic vesicle at 24 h in *ace/ace* (C) and *ace/ace; val/val* (D) embryos. (E, F) Dorsolateral view showing anti-Pax2 staining in the otic vesicle at 30 h in *ace/ace* (E) and *ace/ace; val/val* (F) embryos. Relative positions of rhombomeres are indicated. Double mutants show ectopic expression of *fgf3* in rX (B), ectopic expression of *pax5* (D) and ectopic hair cells in the otic vesicle (F). Anterior is to the left in all specimens. Scale bar, 80 µm (A, B), or 30 µm (C-F).

mutants as in *val/val* mutants (Fig. 35B). Together, these data indicate that *val* and *ace* affect different developmental pathways, and that the early patterning defects seen in the *val/val* mutant ear are not caused by mis-regulation of *fgf8* expression.

DISCUSSION

Fgf3, Fgf8, and hindbrain signaling

Development of the first hair cells is normally restricted to regions of the otic placode directly adjacent to r4 and r6 (Fig. 28), suggesting that signals emitted by those rhombomeres specify the equivalence groups from which hair cells emerge. Data presented here suggest that Fgf3 is an important r4-derived factor that regulates formation of anterior hair cells, as well as expression of various AP markers in the ear. In *val/val* embryos, *fgf3* is expressed ectopically in rX (Fig. 32), and ectopic hair cells form within the adjacent otic vesicle (Fig. 28). Expression of *nkx5.1* and *pax5*, which are normally restricted to the anterior portion of the placode next to r4, expand posteriorly in *val/val* mutants to include all cells abutting the hindbrain (Fig. 30). The posterior marker *zp23* is not expressed in the otic vesicle in *val*/*val* mutants. Depletion of Fgf3 suppresses all of the above patterning defects in the *val*/*val* mutant ear. Moreover, in many Fgf3-depleted embryos, anterior otic markers are totally ablated and *zp23* expression expands anteriorly to include cells adjacent to r4.

The fact that any hair cells are produced at all in Fgf3-depleted embryos indicates that additional hair cell-inducing factors must be present. *fgf8* is clearly required for normal hair cell formation and could partially compensate for loss of *fgf3* (Reifers et al., 1998; Phillips et al., 2001). However, several observations indicate that the role of *fgf8*

is distinct from that of *fgf3*. First, periotic expression of *fgf8* declines sharply just before the placode forms at 14 h, thereby limiting its ability to influence later otic patterning. Second, expression patterns of *nkx5.1*, *pax5*, and *zp23* are not altered in *ace/ace* embryos (Fig. 35C, and data not shown), indicating that AP patterning is relatively normal. Third, loss of *fgf8* inhibits hair cell formation but does not prevent formation of ectopic hair cells in *val*/*val* mutants. The latter are dependent on *fgf3* instead. Thus, in contrast to *fgf3*, there is little evidence to suggest that the r4 domain of *fgf8* regulates regional patterning in the otic placode. Instead, *fgf8* may play a more general role in stimulating hair cell competence during the process of placode induction.

Paradoxically, anterior hair cells are not as severely impaired in *ace/ace* mutants as are posterior hair cells. Posterior hair cells are totally ablated in about 1/3 of *ace/ace* mutants. This is difficult to explain based solely on the expression domain of *fgf8*, but may reflect changes in the dimensions of the otic placode. In *ace/ace* mutants, the otic placode is often reduced to a domain juxtaposed to r4 and r5 only. Thus, secretion of Fgf3 from r4 may be sufficient to induce some anterior hair cells in the absence of Fgf8, whereas cells in the posterior otic placode may lie too far from r6 to benefit from inductive factors possibly secreted from there. No clear candidates for r6-specifc inducers are known, but the Fgf-inducible genes *erm*, *pea3*, and *sprouty4* are expressed in r6 (Fürthauer et al., 2001; Raible and Brand, 2001; Roehl and Nüsslein-Volhard, 2001; and our unpublished observations), suggesting that at least one as yet unidentified Fgf homolog is expressed there.

The reason for expanded expression of *fgf3* in *val/val* mutants is not clear, but there are several possibilities. First, this could result from mis-specification of segment identity in the rX territory. Several other genes normally expressed in adjacent segments, including *hoxb1* in r4 and *hoxb4* in r7, eventually come to be expressed in rX (Prince et al., 1998). However, these changes do not occur until 20 somites (19 h). In contrast, expression of *fgf3* in rX is first detected at 10 h in *val/val* mutants, corresponding to the time when *val* normally begins to function (Moens et al., 1998). This raises the alternative possibility that Val protein normally acts to transcriptionally repress *fgf3*. In support of this, mis-expression of *val* inhibits r4-expression of *fgf3*, but not *fgf8* (Fig. 33). Direct support for transcriptional regulation by Val will require analysis of the promoter/enhancer regions of *fgf3*.

Comparison of *val* and *kr*

In sharp contrast to *val* function in zebrafish, mouse Kreisler is required, directly or indirectly, for upregulation of Fgf3 in r5 and r6 (McKay et al., 1996). This difference is notable because so many other aspects of early hindbrain and ear development are conserved between these species. The high degree of sequence-identity leaves little doubt that the zebrafish genes are orthologous to *kr* and *Fgf3*, respectively (Kiefer et al., 1996a; Moens et al, 1998). There are, however, differences in the N- and C-terminal regions of Fgf3 in zebrafish vs. mouse. These regions are thought to be important for mediating the characteristic receptor binding preferences and signaling properties of Fgf3. Nevertheless, these functional properties are actually quite similar between the fish and mouse proteins (Kiefer et al., 1996b). This, combined with the broad

similarities in their expression patterns and involvement in early otic development, strengthen the notion that the fish and mouse *fgf3* genes are indeed orthologs. Because zebrafish often has multiple homologs of specific tetrapod genes, it is possible that a second *fgf3* gene might be present in the zebrafish genome that shows an expression pattern more like the mouse gene. If so, it will be important to address its function as well. However, we have shown that the known *fgf3* ortholog plays an essential role in the etiology of the ear phenotype in *val*/*val* embryos, since key aspects of the phenotype are suppressed by injecting fgf3-MO. Morpholino oligomers are highly gene-specific in their effects, and even though they do not totally eliminate gene function, they generate phenotypes that are indistinguishable from those caused by known null mutations (Nasevicius and Ekker, 2000; Phillips et al., 2001; Raible and Brand, 2001; Maroon et al., 2002). On balance, it appears that the general role of Fgf3 in otic development has been conserved in mouse and fish but that differential regulation in the hindbrain represents a real difference between these species.

Considering the above differences in hindbrain signaling, one might expect the ear phenotypes in *val/val* and *kr/kr* mutants to be quite different. Instead, the phenotypes appear strikingly similar. In *kr/kr* embryos, as in *val/val* embryos, development of the otic vesicle is highly variable and defects can be seen in virtually all regions of the labyrinth (Deol, 1964). In *kr/kr* mutants, formation of the wall of the otic capsule is often incomplete, with large gaps through with membranous epithelia protrude, and morphology of the labyrinth is usually grossly abnormal. Such global disruption may be related to buildup of excess fluid pressure due failure of the endolymphatic duct to form

in many or most *kr/kr* mutants (Deol, 1964; Brigande et al, 2000). Whether a similar problem occurs in *val/val* mutants is not clear. The existence of an endolymphatic duct in zebrafish was only recently documented (Bever and Fekete, 2002), but it does not begin to form until around day 8. Most *val/val* mutants die before this time, and they often begin to show defects in morphogenesis (e.g. of the semicircular canals) by 72 h (Fig. 31, and data not shown). While these early defects cannot be explained by the absence of an endolymphatic duct, mutant ears often appear swollen and distended by day 3, suggesting a buildup of endolymphatic pressure. It is possible that cellular functions normally required to maintain a proper fluid balance in the early vesicle are mis- regulated in *val/val* mutants. Thus, hydrops may be an important contributing factor to the defects in both *kr/kr* and *val/val* mutants.

Another similarity between *kr/kr* and *val/val* mutants is that they both form ectopic patches of hair cells. However, this phenotype has a completely different etiology in the two species. In tetrapod vertebrates, sensory epithelia do not begin to differentiate until after the various chambers of the labyrinth begin to form. Thus, formation of ectopic hair cells in *kr/kr* mutants probably reflects the general disorganization of, and chaotic protrusions from, the labyrinth (Deol, 1964). In contrast, sensory epithelia in zebrafish begin to differentiate much earlier. Macular equivalence groups are already specified at 14 h when the placode first forms (Haddon et al., 1998a; Whitfield et al., 2002), and the first hair cells (visualized by the presence of kinocilia) are evident as soon as the lumen of the vesicle forms at 18.5 h (Riley et al., 1997). Thus, formation of ectopic hair cells in *val/val* mutants reflects an early defect in cell fate

specification rather than a later defect in morphogenesis. It is noteworthy that there have been no detailed molecular studies of otic development in *kr/kr* mutants, so a direct comparison of early pattern formation is not yet possible.

Evolutionary implications

It is interesting to consider that the altered pattern of *fgf3* expression in the *val/val* mutant hindbrain closely resembles the normal pattern of *Fgf3* expression in chick and mouse embryos (Mahmood, 1995, 1996; McKay et al., 1996). Analysis of *val/val* mutants suggests that misexpression of *fgf3* in rX leads to development of excess and ectopic hair cells in the otic vesicle. It is possible that evolutionary changes that led to normal expression of *Fgf3* in r5/6 in amniotes were crucial for evolution of the cochlea, which has no known counterpart in anamniote vertebrates (Lewis et al, 1985). In the mouse, development of the cochlea requires FGF signaling at early otic vesicle stages (Pirvola et al., 2000). The FGF receptor isoform FGFR-2(IIIb) is expressed in the otic epithelium juxtaposed to the hindbrain. Targeted disruption of this isoform leads to severe dysgenesis of the cochlea. Cochlear development is also impaired in *Fgf3*-null and *kr/kr* mutant mice (Deol, 1964; Mansour et al., 1993). In *Xenopus*, *Fgf3* expression shows a pattern intermediate between that of zebrafish and amniotes: The frog gene is initially expressed in r3 through r5 and only later becomes restricted to r4 (Lombardo et al., 1998). Although amphibians do not possess a cochlea, they do show modifications of the posterior otic vesicle that give rise to the basilar and amphibian papillae, auditory organs not found in fishes (reviewed by Lewis et al., 1985). Thus, expression of *fgf3* in

more posterior regions of the hindbrain correlates with elaborations of the inner ear that may have been essential for enhancing auditory function in terrestrial environments.

VITA

Bryan T. Phillips

2517 Badger Ln Madison, WI 53713 Phone (815) 885-3296
E-mail: bphillips@mail.bio.tamu.edu

EDUCATION

1998	B. S. in biology	University of Illinois at Urbana-Champaign
2004	Ph.D. in biology	Texas A&M University

TEACHING EXPERIENCE

Fall	1998	Instructor, Introductory Biology Lab
Spring	1999	Instructor, Introductory Biology Lab
Spring	2003	Instructor, Embryology Lab

PUBLICATIONS

Phillips, B. T., Storch, E. M., Lekven, A. C. and Riley, B. B. (2004) A direct role for Fgf but not Wnt in otic placode induction. *Development*. **131**, 923-931.

Riley, B. B. and **Phillips, B. T.** (2003). Ringing in the new ear: resolutions of cell interactions in otic development. *Dev. Biol*. **261,** 289-312.

Kwak, S. J., **Phillips, B. T.,** Heck, B., and Riley, B.B. (2002). An expanded domain of *fgf3* expression in the hindbrain of zebrafish *valentino* mutants results in mis-patterning of the otic vesicle. *Development*. **129**, 5279-5287.

Whitfield, T. T., Riley, B. B., Chiang, M-Y., and **Phillips, B. T.** (2002). Development of the zebrafish inner ear. *Developmental Dynamics*. **223**, 427-458.

Phillips, B. T., Bolding, K., and Riley, B. B. (2001). Zebrafish *fgf3* and *fgf8* encode redundant functions required for otic placode induction. *Developmental Biology*. **235**, 351-365.